

3D MORPHOLOGICAL AND STRUCTURAL NANOCHARACTERIZATION FOR MICROELECTRONICS: THE POTENTIAL OF RECENT, LONG SYNCHROTRON BEAMLINES

A.Fraczkiewicz¹, E.Capria², G.Chahine², P.Cloetens², J.Da-Silva², A.Jouve¹, F.Lorut³,
S.Lhostis³, M-I. Richard², P.Bleuet¹

1- Univ. Grenoble Alpes, F-38000 Grenoble, France

CEA, LETI, MINATEC Campus, F-38054 Grenoble Cedex 9, France

2- ESRF, CS40220, F-38043 Grenoble Cedex 9

3- ST Microelectronics 850 rue Jean Monnet FR - 38926 Crolles

Abstract

In microelectronics, 3D integration is an innovative strategy to save space on chips: it consists in designing 3D circuits and using vertical copper bonds through and between silicon wafers as electronic connections (see fig.1). The presence and statistical distribution of voids are critical for the performance and mechanical behavior of such structures. To characterize those features, we investigated samples made of Si and Cu layers on two new ESRF phase I upgrade beamlines, as they can provide a 3D, highly resolved information, as well as a statistical one, which is highly relevant in an industrial context.

The ID16A Nano-imaging beamline offers the possibility to image a given sample in 3D with a sub-50 nm resolution. Holotomography based on a four distance scheme [1] has been performed at 33.6 keV, and the phase retrieval step has been optimized to take into account both absorption and phase contrasts for the specific case of microelectronics samples (see fig.2). For large samples, we took advantage of the penetration depth of hard x-rays to perform region of interest tomography; we show that it does not induce significant artifacts.

The scanned areas were also analyzed on the ID01 diffraction beamline. Thanks to the fast kmap technique [2], we were able to perform Bragg diffraction imaging on 100 μm X 100 μm large areas with a typical spatial resolution of 200 nm (see fig.3). The use of a large, 2D detector allowed us to simultaneously map the strain in the top and bottom layers of silicon, with typical values of 10^{-3} . The strain in the copper layer was also measured.

We believe a combination of these two different analysis modes can provide the microelectronics industry with both statistical information on the spatial distribution of the defects in the samples and their structural behavior.

This work has been funded by the IRT Nanoelec program. The authors acknowledge access to the nanocharacterization platform (PFNC) at the Minatec Campus in Grenoble. The experiments were performed on beamlines ID16A and ID01 at the ESRF, Grenoble, France, in the frame of the long-term project ma2240.

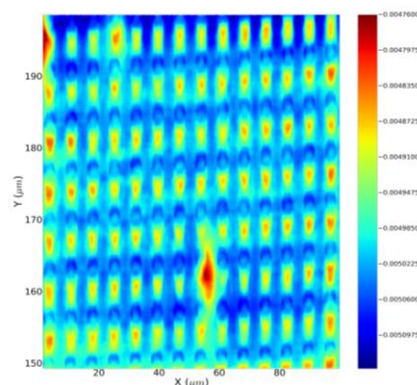
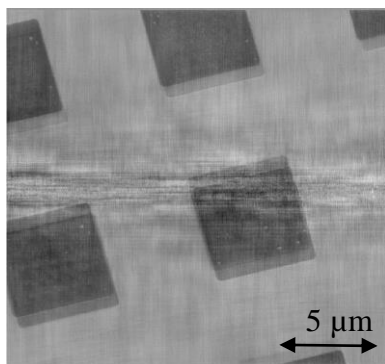
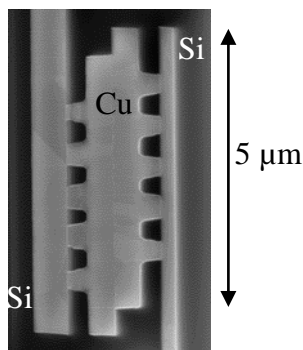


Figure 1: SEM transversal image of a Si-Cu sample.

Figure 2: In-plane tomography slice of Cu pads.

Figure 3: Strain map of the Si layer on top of several Cu pads.

References

- [1] Cloetens, P. et al. (1999). Appl. Phys. Lett., 75(19):2912-2914.
- [2] Chahine, G. et al. (2014). Journal of Applied Crystallography, 47(2) :762-769.

SPECTROMICROSCOPY INSIGHTS OF FERROMAGNETIC RETARDATION IN HYBRID SPIN-VALVE

D. H. Wei^{1,2}, M. R. Chiang^{1,2}, P. Y. Cheng¹, K. T. Lu¹, C. I. Lu¹, T. H. Chuang¹, Y. J. Hsu¹

1National Synchrotron Radiation Research Center, Hsinchu, Taiwan

2Graduate Program for Science and Technology of Synchrotron Light Source, National Tsing Hua University, Hsinchu, Taiwan

Abstract

One unsettled issue in layered organic spin-valve (OSV) is its loss of magneto-resistance (MR) far below room temperature [1]. As organic semiconductor (OSC) spacer is good for spin preservation, and ferromagnetic (FM) electrodes' Curie temperatures are much higher than 300 K, there is no obvious reason, at least from material's point of view, why FM/OSC/FM trilayers cannot exhibit room temperature MR. In this study, we fabricated multiple OSC/FM bilayers to examine possible causes related to the interfaces of multilayers. Employing X-ray photoemission electron microscopy (XPEEM), we recorded the magnetic and chemical images of Cu(100)/pentacene/Co bilayers. According to these images (part of them shown in fig. 1 & 2), we concluded that Co landed on pentacene suffers a retarded development in its room temperature magnetic order [2]. Spectroscopic evidences further suggested that the Co actually hybridizes with pentacene. Recognizing the orbital hybridization at interfacial regions can in principle introduce deviated magnetic transport behavior, we conducted additional studies on three more series of bilayers; Fe, Co, Ni/C₆₀, to clarify if the reacted interface is a scenario universal to all hybrid structures. To our surprise, we found not only there is expected orbital hybridization, but part of the metal deposition would diffuse deep into OSC layer. Insights obtained from X-ray studies and their correlations to transport behavior will be addressed in this presentation.

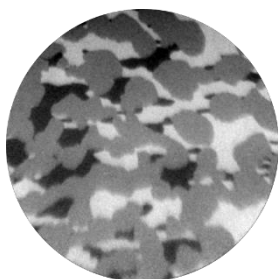


Figure 1: XMCD image of Pn/Co bilayers recorded at Co L-edge.



Figure 2: XMCD image of the same area, but opposite polarization.

References

- [1] D. Sun, E. Ehrenfreund, A. V. Vardeny, Chem. Commun. 50,178 (2014).
- [2] P. Y. Cheng, M. T. Chiang, Y. L. Chan, Y. J. Hsu, P. C. Wang, and D. H. Wei, Appl. Phys. Lett. 104, 043303 (2014).

OBSERVATION OF INTERFACE BETWEEN RESIN AND CARBON FIBER BY SCANNING TRANSMISSION X-RAY MICROSCOPY

Takayuki Harano¹, Reiko Murao¹, Yasuo Takeichi²,
Masao Kimura², Yoshio Takahashi³

¹Nippon Steel & Sumitomo Metal Corporation, Chiba 293-8511, Japan

²Photon Factory, Institute of Materials Structure Science, KEK, Ibaraki 305-0801, Japan

³Department of Earth and Planetary Science, The University of Tokyo, Tokyo 113-0033, Japan

Abstract

It is essential to investigate the interface between materials in order to reveal the origin of physical properties of multi materials. For example, chemical states (e.g. valence, functional group, orbital etc) of interface between resin and carbon fiber (CF) in carbon fiber reinforced plastic (CFRP) are very helpful information to clarify enhancement mechanisms of elastic modulus. Infrared absorption spectroscopy (IR) is a conventional technique for their investigations. However, the spatial resolution of IR is in the order between mm and μm . This makes us difficult to observe the interface structures in detail.

On the other hand, scanning transmission X-ray microscopy (STXM) is a very powerful method based on the XANES (X-ray absorption near edge structure) analysis of interfaces of multi materials. The compact STXM instrument [1] at BL-13A in Photon Factory realizes XANES mappings with the spatial resolution of 40 nm by using the Fresnel zone-plate, and is especially good at measuring XANES spectra around C *K*-edge, which provides us with the information about chemical states around carbon.

In this study, we performed STXM measurement to reveal distributions of chemical states in CFRP. Figure 1 shows an X-ray contrast image of a slice of 80 nm-thick commercial CFRP. XANES (C *K*-edge) mappings of the regions such as (i) the interface structure between resins and a CF, and (ii) inner structure of CF were observed. These results suggested the presence of the third phase at interface between resin and CF. In the presentation, we will discuss the comparison result of the XANES spectra of the third phase with those of resin and the CF.

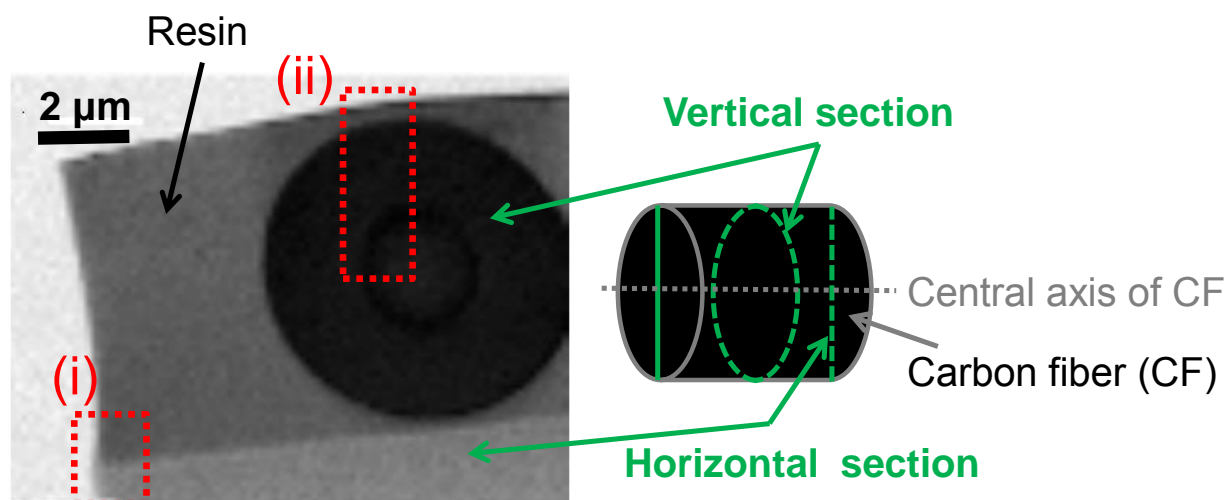


Fig.1: X-ray contrast image of carbon fiber reinforced plastic @ $E = 283.9 \text{ eV}$

References

[1] Y. Takeichi *et al.*, Rev. Sci. Instrum., 87, 013704 (2016)

STUDY OF THE TRANSFORMATION OF CERIA NANOPARTICLES IN PLANTS USING STXM

Y. H. Ma¹, P. Zhang¹, X. He¹, J. Zhang², L. R. Zheng², Z. Guo³, L. J. Zhang³, Y. L. Zhao¹, Z. Y. Zhang¹

¹Key Laboratory for Biomedical Effects of Nanomaterials and Nanosafety, Institute of High Energy Physics, Chinese Academy of Sciences, Beijing 100049, China

²Beijing Synchrotron Radiation Facility, Chinese Academy of Sciences, Beijing 100049, China

³Shanghai Synchrotron Radiation Facility, Shanghai Institute of Applied Physics, Chinese Academy of Sciences, Shanghai 201204, China

Abstract

Transformation is a critical factor that affects the fate and toxicity of manufactured nanoparticles (NPs) in the environment and living organisms. Ceria NPs have been found to be partly biotransformed from Ce(IV) to Ce(III) in plants, yet the transformation process and mechanism are not fully understood [1]. Since synchrotron-based spectroscopic techniques are useful for discerning elemental distributions and chemical speciation of elements *in situ*, STXM was used to elucidate the chemical signatures of the precipitates in cucumber roots that treated with ceria NPs.

Based on the similarity of the NEXAFS spectra, it was corroborated that cerium was deposited as Ce(IV)-containing species on root surfaces and Ce(III)-containing species inside the roots (Fig. 2). This is, for the first time, proof of direct transformation of CeO₂ NPs depending on the different regions in plant roots. It was deduced that root surfaces are the sites, and the physicochemical interaction between the NPs and root exudates at the nanobio interface is the necessary condition for the transformation of ceria NPs in plant systems.

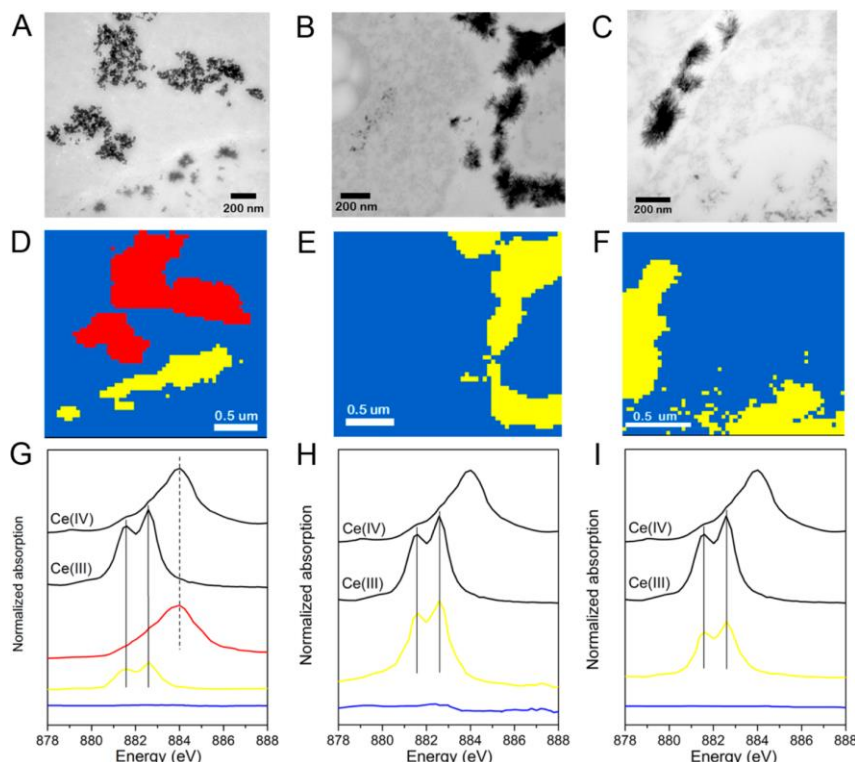


Figure 2: TEM observations of root cross sections at the root surface (A), intercellular space and cytoplasm (B), and vacuole (C). STXM stack images (D–F) of Ce components in the same areas as in panels A–C, and the corresponding XANES spectra (G–I) extracted from the color image sequences in panels D–F.

References

- [1] P. Zhang, Y. H. Ma, Z. Y. Zhang, X. He, J. Zhang, Z. Guo, R. Z. Tai, Y. L. Zhao, Z.F. Chai. ACS Nano, 6, 9943 (2012).

QUICK-XAS USING A MAIA DETECTOR AT P06, PETRA III

U. Boesenberg^{1,2}, C.G. Ryan³, J. Garrevoet¹, R. Kirkham³, K. Spiers¹, A. Madsen², G. Falkenberg¹

¹Deutsches Elektronen Synchrotron DESY, Notkestr. 85, 22607 Hamburg, Germany

²European XFEL GmbH, Albert-Einstein-Ring 19, 22761 Hamburg, Germany

³Commonwealth Scientific and Industrial Research Organisation (CSIRO), Clayton, Victoria, Australia

Abstract

Spatially resolved chemical speciation, i.e. by determination of the oxidation state using X-ray absorption spectroscopy, is a powerful tool to explore and understand ongoing processes in a number of fields such as geology, material science, catalysis or biology. Using the fluorescence signal, speciation at trace element concentrations becomes feasible. Probing the chemical state at distinct spots or regions of interest rapidly and repeatedly using fast X-ray absorption spectroscopy [1] provides an ideal method to study in-situ processes or radiation-sensitive samples.

Such fast scanning X-ray absorption spectroscopy scheme (QXAS) using a Maia fluorescence detector has recently been implemented at the Hard X-ray Micro/Nano-Probe Beamline P06 at the storage ring PETRA III at the Deutsches Elektronen-Synchrotron (DESY) in Hamburg, Germany. One of the key aspects is the direct readout of the sample and monochromator positions during continuous scanning using the Maia system [2] thus embedding position data into the detector data-stream. Figure 1a shows the As-map acquired in QXAS mode of a geological thin-section of arsenic-bearing apatite, which is found in iron-oxide, copper, gold deposits in the Mount Isa inlier [3]. The corresponding chemical phasemap that illustrates the distribution of the As oxidation state measured at the As K-edge and the corresponding XANES spectra are shown in figure 1b and c, respectively.

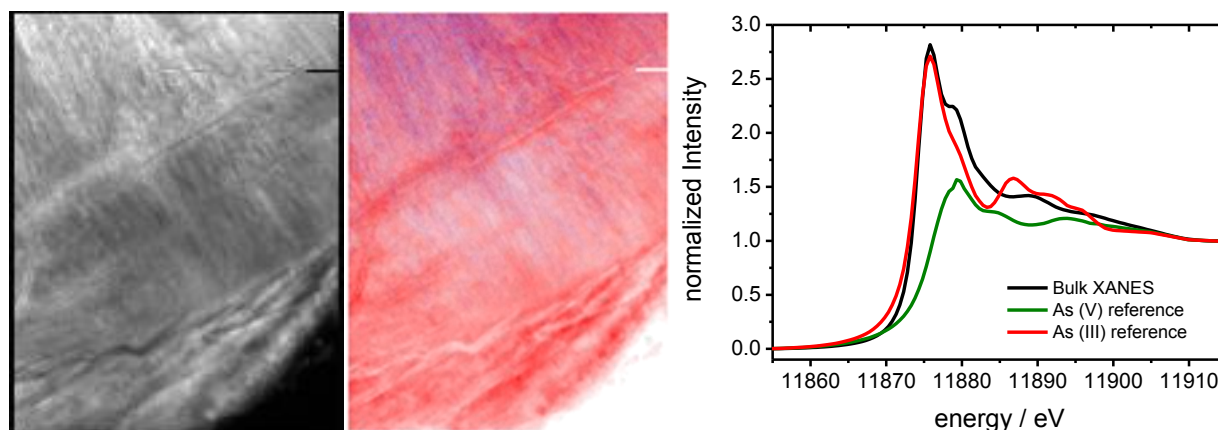


Figure 1a: As distribution in a geological thin-section. **b:** RGB image of the chemical phase map of a) with As (III) red, As (V) green and 50:50 mixture in blue acquired in QXAS. **c:** XANES spectra of the sample and As (V) and As (III) references.

This contribution will include a comparison between standard XAS mapping (acquiring one 2D scan per energy) and the newly implemented QXAS using a Ta-reference sample as well as a geological application. We will discuss the advantages and technical difficulties that accompany with this new scanning scheme.

References

- [1] R. Frahm, Nucl. Instrum. Methods Phys. Res. A, 270, 578–581 (1988).
- [2] C.G. Ryan, et al., Nucl. Instrum. Methods Phys. Res., Sect. A, 619, 37 (2010).
- [3] S. Borg, W. Liu, M. Pearce et al. Geology 42:415–418 (2014).

X-RAY MICROTOMOGRAPHY FOR PAPERBOARD STRUCTURE CHARACTERIZATION USING A LABORATORY SYSTEM

T. Zhou¹, S. Reza^{2,3}, C. Fröjdh², B. Norlin², H. M. Hertz¹, A. Burvall¹

¹Biomedical and X-ray Physics, KTH Royal Institute of Technology, Stockholm, Sweden

²Department of Electronics Design, Mid Sweden University, Sundsvall, Sweden

³FS-DS, Deutsches Elektronen-Synchrotron (DESY), Hamburg, Germany

Abstract

Paperboard is widely used in daily life and its quality can be critical for some industries, such as packaging. The performance of paperboard is closely related to its physical characteristics, in which the structure of cellulose fibres and coating play an important role.

X-ray imaging has been applied in different areas for non-destructive visualization and examination of the objects' inner structures. For traditional x-ray tubes, it is too challenging to resolve cellulose fibres, whose diameters are normally about 10-20 μm [1]. Synchrotrons and microfocus sources are the possible options for the required high spatial coherence. For our study, a liquid-metal-jet source is used [2], which has a spot size with FWHM (full width at half maximum) of $7.6 \times 7.5 \mu\text{m}^2$. As most of the materials in paperboard do not absorb much in the region of hard x-ray, we used the propagation-based phase-contrast method for its advantage in visualizing small structures for low-Z materials [3].

As a result, we have reconstructed a 3D model of a paperboard using laboratory-based x-ray microtomography, from which we can directly analyze cellulose fibre structure regarding orientation, length, etc. After phase-retrieval, we get density maps of the paperboard sample, which can help diagnose, e.g., the homogeneity of coating, and the location of impurities [4].

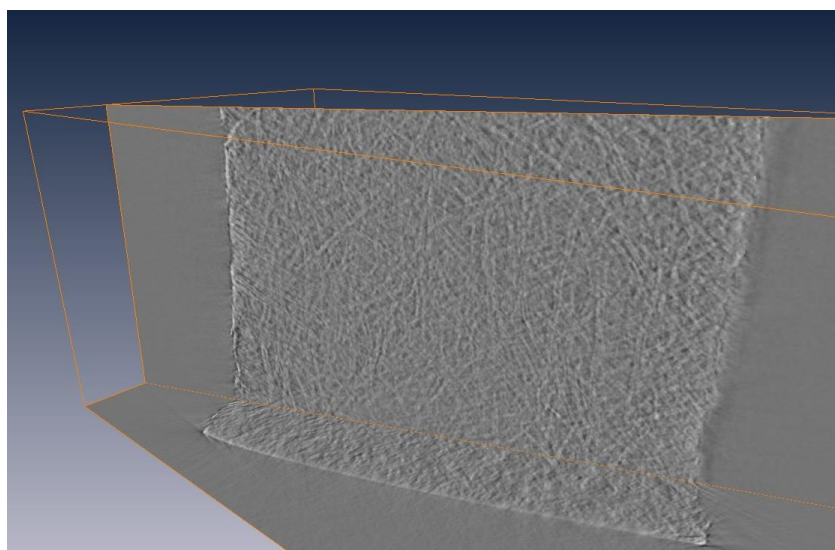


Figure 1: One slice of reconstructed 3D model from x-ray tomography of a paperboard sample showing cellulose fibre structures. The width of the paperboard sample is around 2.5 mm. The sample is placed 0.4 m after the source and 0.8 m before the detector, giving a magnification of 3. The source spot FWHM is $7.6 \times 7.5 \mu\text{m}^2$. The detector has a pixel size of $9 \times 9 \mu\text{m}^2$. The scan is taken every 0.2° over 180° with 40 s exposure time per projection.

References

- [1] C. Ververis, K. Georghiou, N. Christodoulakis, P. Santas, and R. Santas, *Ind. Crops Prod.* 19, 245-254 (2004).
- [2] T. Tuohimaa, M. Otendal, and H. M. Hertz, *Appl. Phys. Lett.* 91, 3 (2007).
- [3] U. Lundström, D. H. Larsson, A. Burvall, P. A. Takman, L. Scott, H. Brismar, and H. M. Hertz, *Phys. Med. Biol.* 57, 2603 (2012).
- [4] S. Reza, T. Zhou, A. Burvall, C. Fröjdh, H. M. Hertz and B. Norlin, *Nordic Pulp & Paper Research Journal* (in preparation).

APPLICATION OF SOFT X-RAY MICROSCOPY TO ENVIRONMENTAL MICROBIOLOGY OF HYDROSPHERE

K.Takemoto¹, M.Yoshimura², T. Ohigashi³, H.Namba², H.Kihara^{2,4}

1Kansai Medical University, 2-5-1 Shin-machi, Hirakata, 573-1010 Japan

2The SR Center, Ritsumeikan University, 1-1-1 Noji-Higashi, Kusatsu, 525-8577 Japan

3Institute for Molecular Science, 38 Nishigonaka, Myodaiji, Okazaki, 444-8585 Japan

4Himeji-Hinomoto College, 890 Koro, Kodera-cho, Himeji, 679-2151 Japan

Abstract

In environmental microbiology of hydrosphere, the needs for observation of microbes and the mucous matter are high. The aim of this study is to observe unprocessed cyanobacteria and estimate mucus composite using a soft X-ray microscopy (XM).

Cyanobacterium is categorized as a prokaryote. It has a prokaryotic organelle with a dedicated biochemical function. Since the difference between prokaryotic organelles is far subtler than the difference between eukaryotic organelles, it is difficult to distinguish a prokaryotic organelle from another by a conventional light microscopy. Many cyanobacteria are surrounded by extracellular polysaccharides (EPS) [1]. It may be a major contributor to the increased organic pollution in a source of drinking water such as lakes and reservoirs. Since EPS is optically transparent and gelatin-like material, it is difficult to estimate the volume and carbon content of each cyanobacterium EPS.

Since a soft XM image strongly reflects chemical compositions of a sample, a soft XM beamline BL-12 has made it possible to observe the prokaryotic organelle and EPS. An optimization of the XM observation method was done. To provide XM images of EPS and polyphosphate granules which play important roles in cellular energy and phosphate (PO₄) storage, the air-drying method has been used. A drop of sample suspension was put onto a thin membrane (e.g. polyimide and SiN membranes). After air-drying, the sample was observed with a wavelength below the oxygen K-edge (2.28 nm). The survey of appearance of polyphosphate granules has succeeded. The estimation of the volume and carbon content of EPS has also succeeded [2]. To provide 3D image of cyanobacteria, the cryo-fixation method has been used. Sample suspension was aspirated by a tip of capillary. Good dispersion stability is obtained by agar solution, when cells go down. Using a cryogenic system which was reported at XRM2014, the high resolution observation of hydrous cyanobacteria in a capillary tube has succeeded. The 3D reconstruction from the images has also succeeded.

References

- [1] R. De Philippis, M. C. Margheri, E. Pelosi, S. Ventura, J. Appl. Phycol. 5, 387 (1993).
- [2] H. Ikegaya, S. Suzuki, S. Ichise, S. Furuta, S. Wakabayashi, T. Ohigashi, D. Bamba, H. Namba, H. Kihara, N. Kishimoto, K. Takemoto, Geomicrobiol. J., 32, 827 (2015).

SOFT X-RAY MICROPROBE AT THE SGM BEAMLINE AT THE CLS

T.Z. Regier, T.D. Boyko, J.J. Dynes, A.W. Gillespie

Canadian Light Source, University of Saskatchewan, 44 Innovation Blvd., Saskatoon, SK Canada, S7N 2V3

Abstract

The X-ray absorption spectroscopy (XAS) endstation on the spherical grating monochromator (SGM) soft X-ray beamline at the Canadian Light Source (CLS) has undergone a major upgrade: (1) XAS endstation's toroidal refocusing mirror replaced with two 150 mm long trapezoidal focusing Kirkpatrick Baez (KB) mirrors, (2) the load lock/transfer arm system was swapped out for a vacuum compatible hexapod sample positioner/holder, and (3) a new detector array was installed. The KB mirror system is 375 mm upstream from the sample, allowing the beam to be focused to a $10 \times 10 \mu\text{m}^2$ spot size. The hexapod's parallel actuator arrangement provides stiffness and accuracy suitable for imaging at the micron scale. In addition, the door mounted hexapod facilitates sample setup and exchange. The detector array consists of four energy resolving silicon drift detectors each positioned 30 mm from the sample with a specific geometry that provides multiple perspectives and optimizes contrast. 3D printed caps are positioned over the detectors to prevent damage, reduce the scattering background and hold thin film filters.

Here we present results that demonstrate the elemental and chemical species mapping capabilities of our new soft X-ray microprobe for materials with structures several microns in size. Moreover, fluorescence detection precludes the need for thin samples and/or sectioning normally required for soft X-ray scanning X-ray transmission microscopy (STXM). The energy range of the SGM beamline is 250 to 2200 eV, allowing for the mapping of biological elements (i.e., C, N, O, P), the alkaline metals (i.e., Na, Mg, K, Ca), all the first row transition metals (e.g., Fe, Mn, Ti), Al and Si. This wide energy range makes the SGM microprobe ideal for correlating the spatial distribution of metals with biological elements in biological and environmental samples. The spatial resolution of the new SGM microprobe is similar to that of synchrotron-based FTIR, making correlative microscopy between these two spectroscopies very attractive. Some of the materials examined to date include a fly wing, banana, a model organic mixture, soils, and plants. The new XAS endstation is now open to general users.

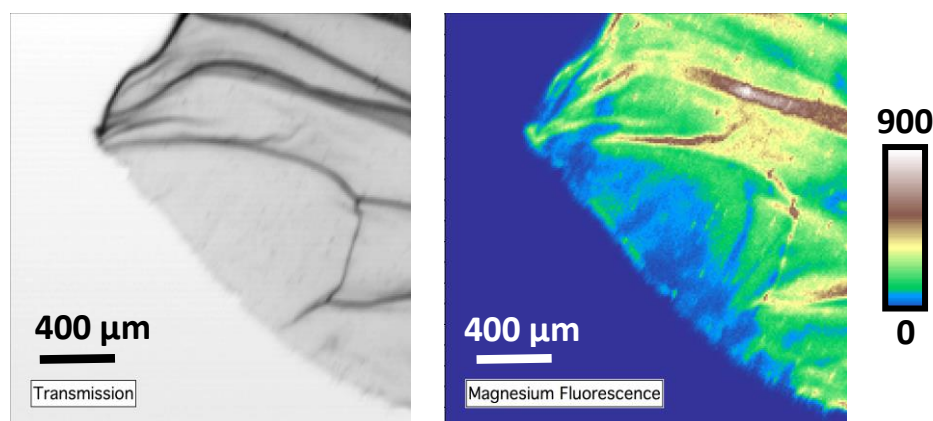


Figure 1: Transmission and Mg fluorescence images of a fly wing collected at a spatial resolution of $20 \mu\text{m}$, 1500 eV and a dwell time of 0.1s. The color scale indicates counts.

QUANTITATIVE MULTI-SCALE ANALYSIS TO A HETEROGENEOUS SHALE BY SYNCHROTRON-BASED X-RAY TOMOGRAPHY

Yudan Wang, Yuqi Ren, Biao Deng, Guangzhao Zhou, Tao Hu¹, Tiqiao Xiao

Shanghai Institute of Applied Physics, Chinese Academy of Sciences, Shanghai, China

Abstract

As a typical kind of heterogeneous and multiphase tight reservoir, multi-scale microstructure is the key to understanding petro-physical and chemical properties of shale. Non-destructively quantifying 3D structures of pore and minerals in shale samples has proven to be challenging, as they are complex, strongly heterogeneous and multi-scale. A combined multi-energy X-ray micro-CT technique and data-constrained modelling (DCM) approach has been used to quantitatively investigate the multi-scale mineral and porosity distributions of a heterogeneous shale from the Junger Basin, northwestern China by sub-sampling. The 3D sub-resolution structures of minerals and pores in the samples are quantitatively obtained as the partial volume fraction distributions. The shale sub-samples from two areas have different physical structures for minerals and pores, with the dominant minerals being feldspar and dolomite, respectively. Significant heterogeneities have been observed in the analysis. The sub-voxel sized pores form large interconnected clusters with fractal structures. The fractal dimensions of the largest clusters for both sub-samples were quantitatively calculated and found to be 2.34 and 2.86, respectively. The results are relevant in quantitative modelling of gas transport in shale reservoirs.

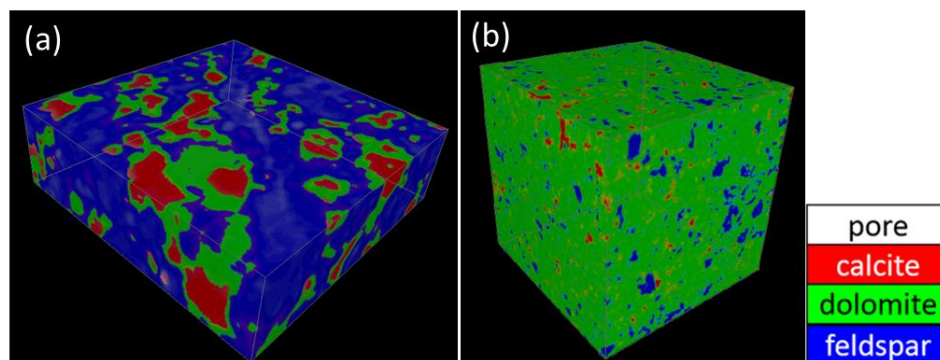


Figure 1: Compositional distributions of two sub-samples. (a) and (b) have the size of $195 \times 195 \times 65 \mu\text{m}^3$ and $650 \times 650 \times 160 \mu\text{m}^3$, respectively.

References

- [1] Wang Y, Liu K, Yang Y, et al., CSIRO Data Collection, (2016), <http://doi.org/10.4225/08/56EA62A09A751>.
- [2] Yudan Wang, Keyu Liu, Yushuang Yang, Yuqi Ren, Tao Hu, Biao Deng, and Tiqiao Xiao, JINST, 2016, accepted.

NANODIFFRACTION MEASUREMENTS WITH MULTILAYER LAUE LENSES AT ESRF BEAMLINE ID13

A. Kubec¹, J. Keckes², S. Niese³, J. Gluch⁴, R. Daniel², S. Braun¹, M. Burghammer⁵,

1Fraunhofer IWS Dresden, Winterbergstr. 28, 01277 Dresden, Germany

2Montanuniversität Leoben, Franz-Josef-Str. 18, 8700 Leoben, Austria

3AXO DRESDEN GmbH, Gasanstaltstr. 8b, 01237 Dresden, Germany

4Fraunhofer IKTS, Maria-Reiche-Str. 2, 01109 Dresden, Germany

5European Synchrotron Radiation Facility, 71, Avenue des Martyrs, Grenoble, France

Abstract

Understanding the behavior of materials and how their properties change after or during deformation or heating is an important part on the way to improve many industrial materials. Thin films are for instance characteristic of their depth-dependent properties, which are related to structural variations across the thickness, worth to be studied in detail. Local characterization of the crystallographic orientation and stress distribution of such nanocrystalline materials can be analyzed with X-ray methods such as wide-angle X-ray scattering (WAXS). In this case, a high-resolution characterization normal to the surface is desired and a line focus improves diffraction statistics.

We have used multilayer Laue lenses (MLL) with a total aperture of 50 μm to focus hard x-rays to a focal spot size of ~ 30 nm in vertical and horizontal directions. 7000 zones made of alternating WSi_2 and Si were deposited starting with zone number 850. The focal length equals 8.2 mm at 13 keV x-ray energy [1]. The working distance from the order sorting aperture to the sample is 2.7 mm. The lenses had been manufactured as flat lenses first. Subsequently an additional SiO_2 layer was deposited on one side of the lens structure. This bends the lens structure and a wedged geometry MLL is obtained [2]. The focal spot size of around 30 nm was determined by ptychography. The geometry of the lens was designed to enable switching between a point and line focus. This was possible by changing the slit position upstream of the lenses only.

A model sample consisting of polycrystalline 3 μm -thick TiN film on Si substrate was characterized (see [3] for a description of the method). The measurements performed using point and line foci revealed abrupt cross-sectional changes in texture, residual stresses and signal FWHM, which are associated with a very specific tilted chevron-like columnar grain microstructure of the film.

References

- [1] A. Kubec, K. Melzer, S. Niese, S. Braun, J. Patommel, ESRF Experimental Report for beam time MI 1177 (2014)
- [2] S. Niese, P. Krüger, A. Kubec, R. Laas, P. Gawlitza, K. Melzer, S. Braun, E. Zschech, Thin Solid Films 571 (2014): 321-324
- [3] J. Keckes, M. Bartosik, R. Daniel, C. Mitterer, G. Maier, W. Ecker, J. Vila-Comamala, C. David, S. Schoeder, M. Burghammer, Scripta Materialia, Vol. 67, Issue 9, November 2012, Pages 748–751

DISTRIBUTION AND CHARACTERIZATION OF CARBON COMPONENTS IN THE ALLENDE METEORITE MATRIX

Hiroki Suga¹, Yasuo Takeichi², Chihiro Miyamoto³, Kazuhiko Mase², Kanta Ono², Masaaki Miyahara¹, Yoshio Takahashi¹⁻³

¹Department of Earth and Planetary Systems Science, Hiroshima University, 1-3-1 Kagamiyama, Higashi-Hiroshima, Japan

²Institute of Materials Structure Science, High Energy Accelerator Research Organization (KEK), 1-1 Oho, Tsukuba, Japan

³Department of Earth and Planetary Science, the University of Tokyo, 7-3-1 Hongo, Bunkyo-ku, Tokyo, Japan

Abstract

Allende meteorite, classed as carbonaceous chondrites, includes many kinds of carbon components in matrix. Their natures and occurrences, however, have not been described in detail by previous studies. In addition, the carbon components might be modified because they were extracted through acid treatments in these studies. In this study, we applied a scanning transmission X-ray microscopy (STXM) combined with a focused ion beam (FIB) technique for *in-situ* carbon functional group analysis, and speciation analysis of minerals.

Figure 1 shows that the distribution of carbon components occurring along with the grain-boundaries of fine-grained olivine crystals (diffusional). Several dense carbon components were also found in the diffusional carbon components (particulate). About half of carbon component was found in particulate portion, and the rest was diffusional portion. Based on C K-edge NEXAFS, as shown in Figure 2, the particulate carbon (aromatic-rich and carboxylic-poor) appears to be insoluble organic matter (IOM) of Allende meteorite [1]. On the other hand, the diffusional carbon portion mainly consists of aromatic-poor and carboxylic-rich components. In addition, submicron-sized chromite and pentlandite crystals are embedded in the particulate carbon, which may become the keystone to clarify origin and history of organic components.

Our FIB-STXM analyses revealed existences of two types of carbon components in the Allende meteorite. Assuming that each carbon components had different origins, the particulate carbon component might had formed on the chromite and pentlandite crystals in the solar nebula, and accreted into the Allende parent-body. In some cases, silicate-minerals are surrounded by the nano-globules in carbonaceous chondrites [2]. On the other hand, diffusional carbon component might have been formed from particulate when the aqueous alteration on the Allende parent-body.

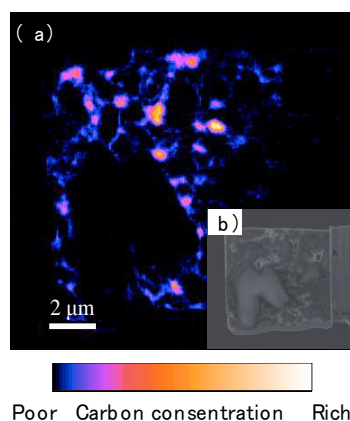


Figure 1: (a) Distribution of the carbon component in the matrix of Allende meteorite. (b) Secondary electron image of thin foil.

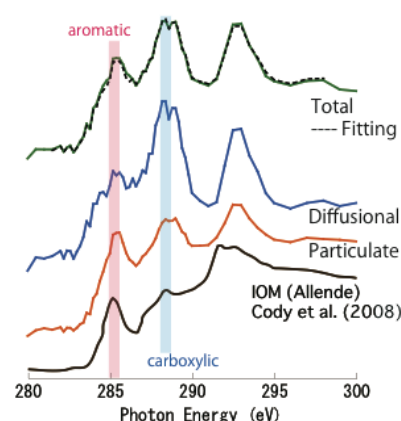


Figure 2: Carbon NEXAFS of particulate, diffusional, and total carbon component with reference spectra of Allende's IOM.

References

- [1] G. Cody et al., *Meteorit Planet Sci* **43**, 353–365. (2008).
- [2] K. Nakamura-Messenger et al., *43rd Lunar and Planetary Science Conference*, #2551. (2012).

MICROSCALE X-RAY SPECTROSCOPIC IMAGING AS A TOOL TO EXAMINE COMPLEX DIAGENETIC PROCESSES

S.M. Webb, C.M. Krest (Roach)

Stanford Synchrotron Radiation Lightsource, Menlo Park, California, USA

Abstract

The sedimentary rock record documents the history of Earth's redox and chemical evolution through time. As geochemists, we rely on these strata to record information in a discernable manner; for example, the measurement of sulfur isotope ratios of sulfide and sulfate phases to reconstruct the history of oxygen in the atmosphere and oceans and the measurement of iron and manganese mineralogy and speciation to determine ancient redox budgets. This geochemical record, however, is rarely pristine as many millions of years of post-depositional processes contribute to a complex assemblage of diagenetic relationships.

A common limitation of virtually all proxy measurements employed to date is that they operate on "bulk" samples, typically grams of powder. As such, these measurements lose the ability to relate the geochemistry to the petrography at the scale of the mineral grains that actually contain the paleo-environmental data. Petrography on a micro-scale contains a rich history that can often be overlooked from bulk measurements.

X-ray spectroscopic imaging provides an important glimpse in the chemical heterogeneity that can exist on the micro-scale. The underlying chemical phase information that can be obtained on this spatial scale, including a wide range of mineralogy, elemental coordination environments and/or redox states, can provide an important context of the depositional and diagenetic histories that is critical for the interpretation by other micro- or nano-scale methods, such as scanning electron microscopy (SEM) and secondary ion mass spectrometry (SIMS). The coupling of these fine-scale tools allows in essence "images" of the proxy data at the micrometer scale, giving a wide array of textural and mineralogical information designed to inform and untangle the complicated histories of ancient sedimentary rocks.

PHANTOM CREATION AND ANALYSIS: IMPROVING X-RAY MICROTOMOGRAPHY SCANNING OF SOFT SEDIMENT CORES CONTAINING VOLCANIC ASH

E. E. Evans^{1,2,3}, S. M. Davies¹, R. E. Johnston^{2,3}

¹Department of Geography, Swansea University, Singleton Campus, Swansea, Wales, UK

²Materials Research Centre, College of Engineering, Swansea University, Bay Campus, Swansea, Wales, UK

³Advanced Imaging of Materials (AIM), College of Engineering, Swansea University, Bay Campus, Swansea, Wales, UK

Abstract

We present a series of soft sediment geological phantoms constructed to simulate structures in volcanic ash horizons found in marine cores. Previous work [1] laid the groundwork for this study by producing several horizontally layered samples in standard drinking straws with the aim of detecting contrast differences between the sediment and two broad classifications of volcanic ash; basaltic and rhyolitic.

The new phantoms were constructed as a series of samples aiming to test a particular aspect of the technique, such as the limits of ash concentration detection. The method of production involved the adding of sediment and volcanic ash to water-filled straws in layers. The resulting sediment pile was then left to settle to prevent additional movement from occurring in the straws during microtomography (microCT) scanning.

This work is currently on going; however preliminary results can be seen in Fig. 1. This study aims to systematically discern which types of natural core samples best respond to X-ray microCT analysis, thus leading to more efficient use of machine time and resources. Suitability is quantified by measuring the grayscale contrast and ease of segmentation using semi-automated processes and consistent colour maps. Because geological samples mainly consist of complex silicates, another variable to optimise is the scan parameters so as to produce histograms either with distinct peaks in the grayscale histogram or with enough dilation in the histogram to assist in segmentation.

We hope this work will have broader applications than the above example, such as assisting other geologists and quaternary scientists in their selection of samples for XRCT analysis.

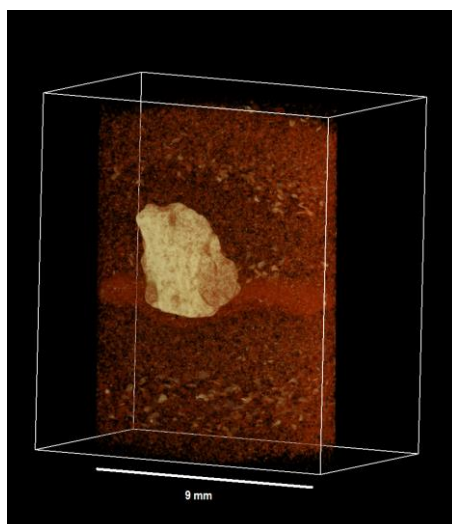


Figure 1: Deformation structure caused by the impact of the large clast (yellow) in the dense red band below the clast. Image generated with Drishti.

References

- [1] A. J. Griggs, S. M. Davies, P. M. Abbott, M. Coleman, A. P. Palmer, T. L. Rasmussen, R. Johnston, *Geochem., Geophys., Geosyst.*, 16, 4329-4343 (2015)

I08-SXM: A multimodal scanning X-ray microscopy facility at the Diamond Light Source

Tohru Araki, Majid Kazemian Abyaneh, Leo Cahill, Silvia da Graca Ramos, Eva Gimenez-Navarro, Jon Kelly, Pete Leicester, Hongchang Wang, Burkhard Kaulich

Diamond Light Source Ltd, Harwell Science & Innovation Campus, Didcot, OX11 0DE, Oxfordshire, United Kingdom

Abstract

Scanning X-ray microscopes find applications in all major research fields, in many cases approaching ultimate diffraction-limited lateral resolutions and with unprecedented performance limited in the past by X-ray source properties, optics and detectors schemes. Missing in the general portfolio of scanning X-ray microscopes worldwide, and addressed by I08-SXM is an instrument that covers a broader photon energy range providing access to all major K- and L-absorption edges for SXM elemental and chemical analysis, combined with complementary imaging and spectro-microscopic techniques as well as versatile specimen environments including cryogenic cooling. The central theme of the beamline is the ability to obtain morphological and chemically-specific information on a full range of materials (inorganic/organic) under real conditions, providing a facility that will be new not only to the UK. I08 will use radiation in the 250 to 4400 eV photon energy range, generated by an Apple II type insertion device. This X-ray source is optimised to enable studies exploiting linearly or circularly polarised radiation. The operating energy range encompasses a significant number of important K and L absorption edges for low- and medium-Z elements, and relatively thick (~10 - 20 μm) samples will be able to be studied with both absorption and phase contrast techniques, with lateral resolutions down to ~20 nm depending on the imaging mode. I08-SXM entered user operation in July 2014 after three years of construction. The potential of the facility will be described and underlined with examples from different scientific research fields.

DEVELOPMENT OF IN-SITU SAMPLE ENVIRONMENTS AT THE 2-ID-D X-RAY FLUORESCENCE MICROPROBE

B. Lai¹, C. Roehrig¹, S. Chen¹, J. Maser¹, M. Stuckelberger², B. West², M.I. Berton², R. Chakraborty³, J. Serdy³, M.L. Culpepper³, T. Buonassisi³

¹Advanced Photon Source, Argonne National Laboratory, Argonne, IL 60439

²Arizona State University, Tempe, Arizona, 85287, USA

³Massachusetts Institute of Technology, Cambridge, MA, 02139, USA

Abstract

With a spatial resolution of 200 nm in the 5-30 keV energy regime, the APS 2-ID-D X-ray fluorescence microprobe had been serving diverse user communities for more than a decade. Typically, samples are mounted inside a helium enclosure to minimize the air absorption and to eliminate fluorescence from atmospheric argon. Recently two other special sample environments had been developed. The first one uses a cryojet to maintain the sample temperature at ~ 100 K, enabling frozen biological samples to be examined at their native hydrated state [1]. This has demonstrated to provide better retention of diffusible ions and reduce drying artifacts. In the second case, we have developed an *in-situ* temperature stage that can quickly heat up a centimeter-size sample to 600 °C, with ramp rate up to 300 °C/min [2]. By careful selection of stage construction materials and the installation of a hazardous gas exhaust system, the sample can be annealed in processing gases such as H₂S or H₂Se. This stage has been applied to *in-situ* characterization of thin-film growth and evolution during photovoltaic device fabrication. In the future these controlled sample environments may be coupled with the use of a double multilayer monochromator, which increases the focus intensity by more than an order of magnitude, thus enabling even faster scanning rates. These and other instrumentation developments, such as stacking six zone plates in intermediate field to increase efficiency above 20 keV [3], have markedly improved the capabilities of the microprobe. Novel applications in life, materials, and energy sciences will be briefly discussed.

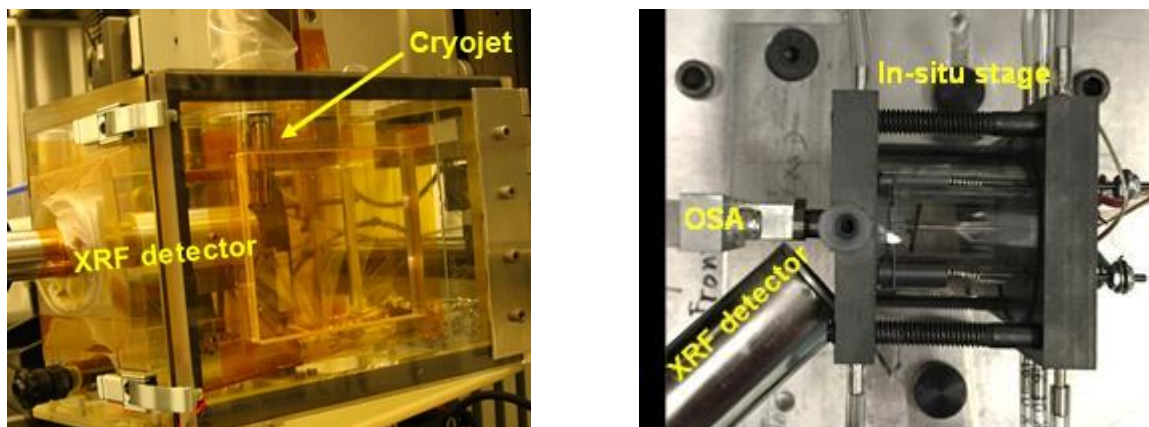


Figure 1 Left: frozen sample cooled by a cryojet within an enclosure. Right: top view of the in situ sample stage. Incident x-ray beam from the left.

References

- [1] Q. Jin, S. Vogt, B. Lai, S. Chen, L. Finney, S-C. Gleber, J. Ward, J. Deng, R. Mak, N. Moonier, C. Ja-cobsen. PLoS One 10 (2), e0117437-1-e0117437-14 (2015).
- [2] R. Chakraborty, J. Serdy, B. West, M. Stuckelberger, B. Lai, J. Maser, M.I. Berton, M.L. Culpepper, T. Buonassisi. Rev. Sci. Instrum. 86 (11), 113705-1-113705-6 (2015).
- [3] S-C. Gleber, M. Wojcik, J. Liu, C. Roehrig, M. Cummings, J. Vila-Comamala, K. Li, B. Lai, D. Shu, S. Vogt. Opt. Express 22 (23), 28142-28153 (2014).

MULTI-SCALE IMAGING AND MODELLING OF A HETEROGENEOUS SANDSTONE

Matthew Andrew¹, Renata Chica-Szot², Sven Liden³, Piotr Such², Grzegorz Lesniak²,
Andreas Wiegmann³, Andy Steinbach¹

¹Carl Zeiss X-ray Microscopy, Pleasanton, CA, USA

²INIG, National Research Institute, ul. Lubicz 25A, 31-503 Kraków, Poland

³Math2Market, Stiftsplatz 5, 67655 Kaiserslautern, Germany

Abstract

Over the last 10-15 years 3 dimensional x-ray microscopy (XRM) has emerged as the leading technology for the non-invasive imaging of materials ranging from the multi-cm to the sub-micron scales. One of the principal challenges when implementing such technology is how to deal with multi-scale heterogeneity [1], for which multi-scale techniques are required (e.g. [2]). X-ray microscopy offers unique advantages when used with such techniques, as the variety of detectors integrated into a single imaging system allows for multiple scales to be proscriptively imaged with minimal user interaction. In this paper we present a novel methodology for integrating multi-scale, non-invasive 3D acquisition and analysis, applied to a heterogenous subsurface sandstone sample.

First the entire 1" (25mm) core-plug sample was imaged across its entire volume with a resolution of around 19 μ m. While the pore structure was not resolvable at this resolution, the macroscopic heterogeneity was. This image was then classified using advanced rock typing techniques (figure 1a). Locations were then defined for interior tomography with a positional accuracy of around 1 μ m. This allows for proscriptive multi-scale 3D image sampling with unprecedented accuracy at arbitrary positions within the macroscopic volume (figure 1b).

Permeability tensors were calculated on each of the high resolution interior tomographies [3] (figure 1C). A macroscopic core-plug scale model based on the low resolution classified image was constructed, such that each voxel from the high porosity lithology and the low porosity lithology was assigned the associated permeability tensor derived from their associated high resolution images. A multi-scale simulation was then performed where stokes flow was computed through the macroscopically pore-resolved fracture and Darcy flow was calculated through the high and low porosity lithologies. The resulting permeability tensor was highly anisotropic, with a high permeability (30-50 mD) in directions parallel to layering and low permeabilities (1.8 mD) perpendicular to it. This result was only possible because the cm scale heterogeneity associated with primary sedimentary layering was maintained, through the use of the macroscopic model.

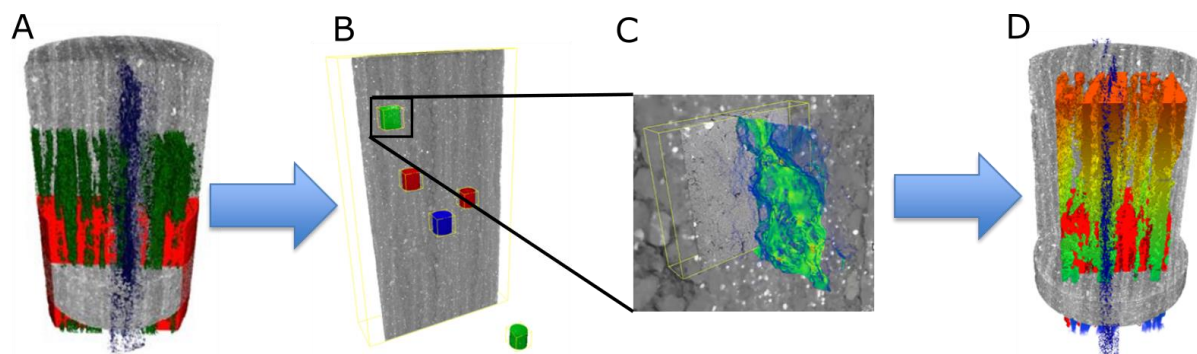


Figure 1: Multi-scale workflow. First the sample was imaged at low resolution, creating a macroscopic map of sample heterogeneity. The

References

- [1] P. S. Ringrose, a. W. Martinius, and J. Alvestad, "Multiscale geological reservoir modelling in practice," *Geol. Soc. London, Spec. Publ.*, vol. 309, no. 1, pp. 123–134, 2008.
- [2] A. Merkle, L. L. Lavery, J. Gelb, and N. Piché, "Fusing Multi-scale and Multi-modal 3D imaging and characterization," *Microsc. Microanal.*, vol. 20, no. Supplement S3, pp. 820–821, 2014.
- [3] S. Linden, A. Wiegmann, and H. Hagen, "The LIR space partitioning system applied to the Stokes equations," *Graph. Models*, vol. 82, pp. 58–66, 2015.

FULL-FIELD XANES TOMOGRAPHY FOR INDUSTRIAL APPLICATION

S. Lee¹, J. Lim¹, I. H. Kwon²

*1Pohang Accelerator Laboratory, POSTECH, 80 Jigokro-127-beongil, Pohang, Korea
2Pohang University of Science and Technology, 77 Cheongam-Ro, Pohang, Korea*

Abstract

The newly modified transmission X-ray microscopy (TXM) of 7C-XNI beamline, Pohang Light Source-II at Pohang Accelerator Laboratory (PAL) has offered great opportunities to image the interior nanostructures of variable industrial materials in 2D and 3D. The newest function of improved beamline is elemental information mapping using X-ray absorption near edge structure (XANES) imaging.

Recently focusing mirror system is adapted to deliver high flux X-rays to transmission X-ray microscopy beamline for high speed elemental mapping. The absorption imaging mode at XNI beamline covers 6 to 11 keV that is interesting energy range of absorption edge of trace metal in the earth (e.g. Zn, Cu, Fe, Co, Ni, Mn etc).

In this presentation, we show some research examples to demonstrate the unique capabilities of hard X-ray nanoscopy beamline for industrial research field. In addition, we present upcoming upgrade plan at 7C-XNI beamline for high speed X-ray fluorescence mapping using new detector system.

A VIRTUAL STRATEGY FOR FAST ITERATIVE RECONSTRUCTION IN INTERIOR TOMOGRAPHY WITHOUT A PRIORI KNOWLEDGE

F. Arcadu^{1,2}, G. Lovric^{2,3}, M. Stampanoni^{1,2}, F. Marone²

*1*Institut for Biomedical Engineering, ETH Zurich, Zurich 8092, Switzerland

*2*Swiss Light Source, Paul Scherrer Institut, Villigen 5232, Switzerland

*3*Centre d'Imagerie BioMédicale, EPFL Lausanne, Lausanne 1015, Switzerland

Abstract

Interior tomography (INT) enables 3D high resolution investigations of a sample in a small region of interest. Achieving high-quality reconstructions of underconstrained (i.e., undersampled and noisy) INT datasets is a challenge that cannot be addressed with analytical methods like filtered backprojection (FBP).

Here we propose a simple and efficient strategy to perform iterative reconstructions of underconstrained INT tomograms without any a priori knowledge of the object support or the attenuation coefficients in specific regions. First, a so-called virtual sinogram is created with the following procedure: (i) reconstruction of the original dataset with edge-padded FBP (FBPE) [1]; (ii) gradient removal [2]; (iii) setting to zero all pixels outside the field of view; (iv) forward projection of the image. This virtual sinogram, simulating a non-INT tomogram, is then reconstructed with the alternate direction method of multipliers plug-and-play [3].

The virtual strategy, tested on INT underconstrained simulated and real datasets, yields reconstructions of higher quality with respect to FBPE (4 times higher contrast-to-noise ratio). Furthermore, it is 3 orders of magnitude faster compared to standard iterative methods, due to the usage of the forward regridding projectors with minimal oversampling [4,5]. We show that reconstructions computed by the proposed algorithm can be more easily segmented with standard methods.

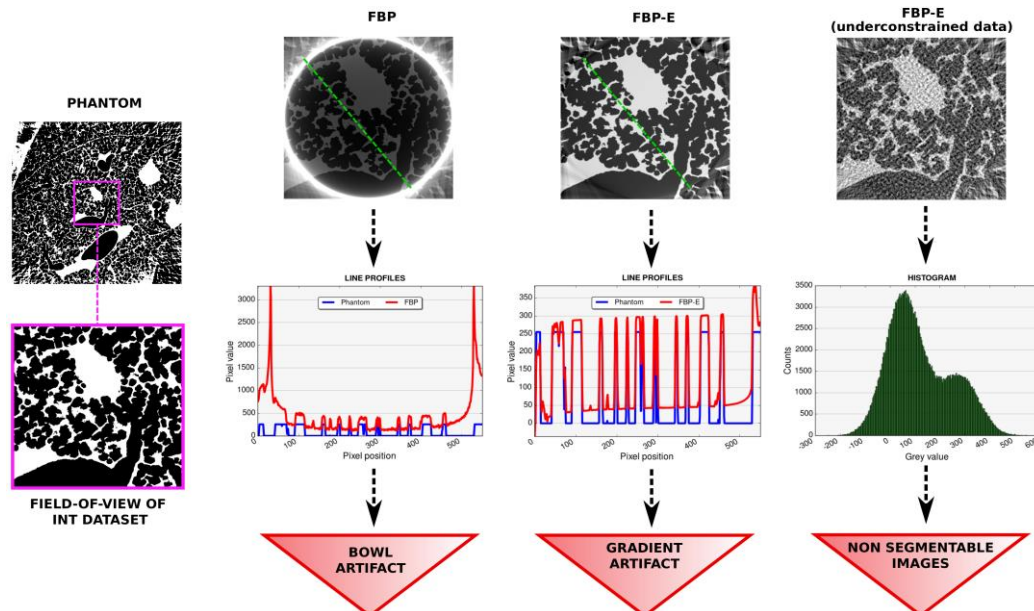


Figure 1: Simulation of the problems (bowl-artifact, gradient artifact, non-segmentability of low-quality analytical reconstructions) arising when dealing with INT datasets.

References

- [1] M. Magnusson Seger, Proc. SSAB02, Symposium on Image Analysis, Sweden, 2002.
- [2] G. Lovric, I. Vogiatzis Oikonomidis, J.C. Schittny, et al, Phys. Med. Biol., Submitted.
- [3] S.V. Venkatakrisnan, C.A. Bouman, B. Wohlberg, IEEE Proc. In GlobalSIP, 945-948, 2011.
- [4] F. Arcadu, M. Stampanoni, F. Marone, IEEE Trans. On Imag. Process., 25(3), 2016.
- [5] F. Arcadu, M. Stampanoni, F. Marone, Optics Express, Submitted.

HIGH THROUGHPUT QUANTITATIVE PER PIXEL XFM ELEMENT IMAGING USING MAIA FOR COMPLEX NATURAL SAMPLES

C.G. Ryan¹, L.A. Fisher², M. Le Vaillant², A. Pagès², D.P. Siddons³, R. Kirkham¹, D.J. Paterson⁴, M.D. de Jonge⁴, D.L. Howard⁴, S.J. Barnes², G.F. Moorhead¹, J.S. Laird¹

¹CSIRO Mineral Resources, Normanby Road, Clayton VIC 3168, Australia

²CSIRO Mineral Resources, ARRC building, Dick Perry Avenue, Kensington WA 6151, Australia

³Brookhaven National Laboratory, Brookhaven, Upton NY, USA

⁴Australian Synchrotron, Blackburn Road, Clayton VIC 3168, Australia

Abstract

Projecting quantitative images from full spectral X-ray fluorescence microscopy (XFM) data from the Maia detector [1,2], for element images up to a billion pixels in size, poses a particular challenge for processing. The GeoPIXE software uses the Dynamic Analysis (DA) linear matrix method [3,4] to process around 10^8 events per second using a single 12-core processor. However it assumes a uniform composition and background shape. Our present approach is to then apply a fast iterative matrix (composition) correction; but this does not account for the variation of background shape, scattering and X-ray relative intensities that evolve spatially with composition.

A new two-pass multiphase (MPDA) method uses an end-member phase decomposition obtained from the first pass and DA matrices determined for each end-member component. These DA matrices are then used to re-process the event data with each pixel treated as an admixture of end-member terms. While still benefitting from the speed of DA (typically $\sim 10^5$ pixels per second), this approach yields quantitative per-pixel concentrations, X-ray line relative intensities and background shapes in spatially-complex images as encountered in geological and environmental research (e.g. Fig. 1 [6]). This paper describes the new method and illustrates how the enhanced accuracy of MPDA spectral deconvolution improves imaging of challenging geological materials at the XFM beamline [5]. Direct spot comparisons with electron probe analysis are used to illustrate the accuracy of the method.

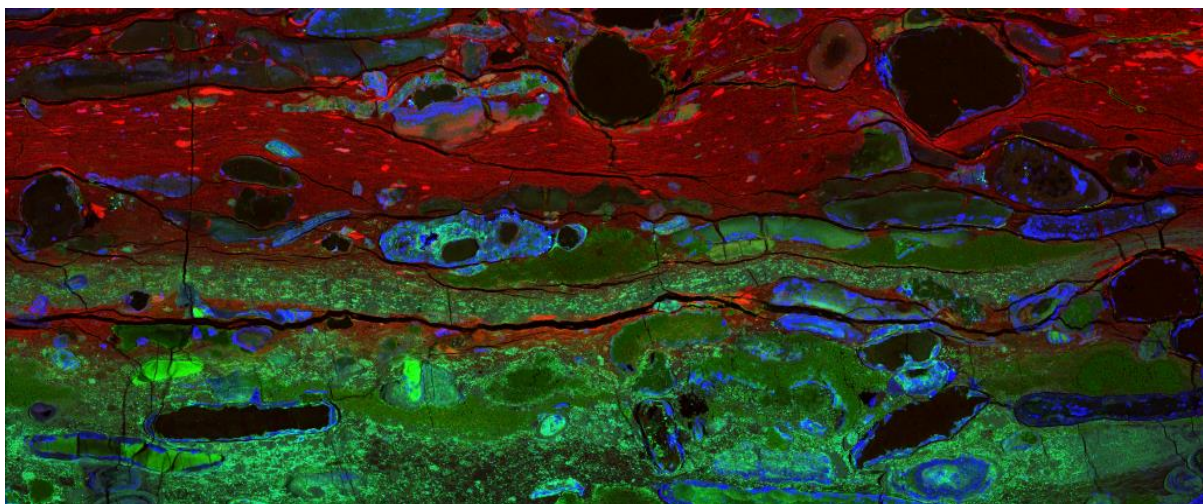


Figure 1: Maia RGB image (V As Ni) of a metalliferous shale [6] (8276 x 4526 pixels, 37 M pixels @ 0.67 ms, 33.1 x 18.1 mm², 18.5 keV, XFM beamline) illustrating multiscale compositional complexity.

References

- [1] R. Kirkham *et al.*, AIP Conf. Proc. 1234 (2010) 240-243.
- [2] D.P. Siddons *et al.*, J. of Physics: Conf. Series 499 (2014) 012001.
- [3] C.G. Ryan, Int. J. of Imaging Systems and Tech. 11 (2000) 219-230.
- [4] C.G. Ryan *et al.*, J. of Physics: Conf. Series 499 (2014) 012002.
- [5] D.J. Paterson *et al.*, AIP Conf. Proc. 1365 (2011) 219-222.
- [6] A. Pagès *et al.*, abstract XRM'16.

ABSORPTION CORRECTION IN X-RAY FLUORESCENCE TOMOGRAPHY

G. Ruben^{1,2}, M. D. de Jonge², S. C. Mayo¹, C. Ryan¹

1 CSIRO, Clayton, VIC 3168, Australia

2 Australian Synchrotron, Clayton, VIC 3168, Australia

Abstract

The X-ray Fluorescence Microscopy (XFM) beamline at the Australian Synchrotron is host to a Maia detector array, jointly developed by CSIRO and BNL [1]. The Maia's large collection area and optimised photon event processing combine to achieve high sensitivity, allowing scanning of bigger imaging regions at higher rates and higher resolution than current alternatives [2]. This makes the beamline well-suited to performing X-ray Fluorescence Computed Tomography (XFCT) of large specimens at high resolution, producing chemical-elemental maps of 2d slices and 3d volumes.

When acquiring XFCT data, many samples are strongly absorbing at the fluorescence assumptions of conventional tomographic approaches leading to errors in naive reconstructions [3]. We are developing software to perform absorption-corrected XFCT at the XFM beamline combining a computational physical model with an iterative tomography reconstruction scheme. We report on progress toward this goal.

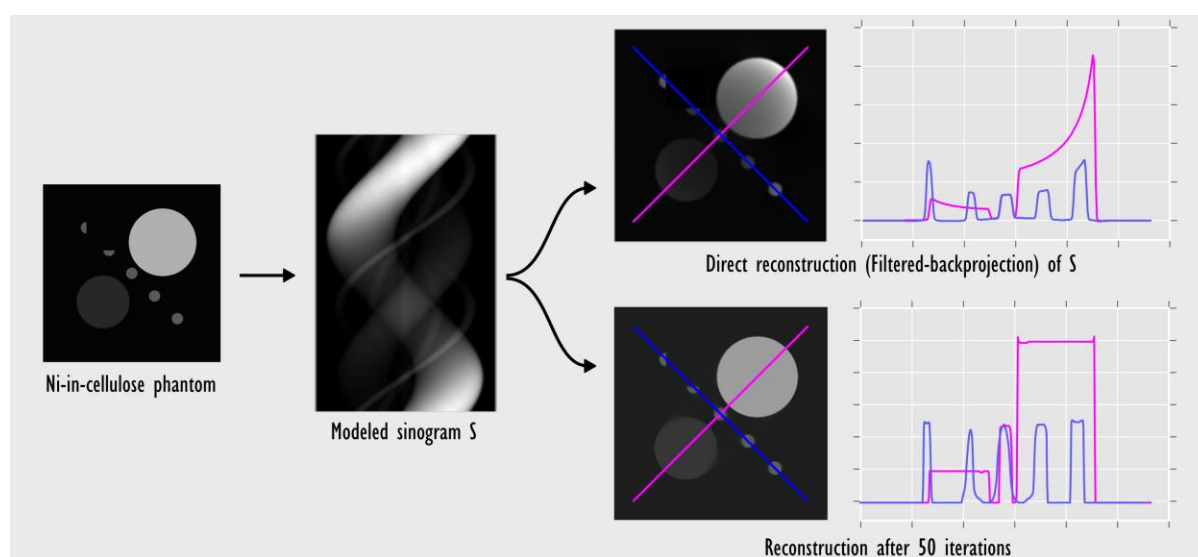


Figure 1: Reconstruction of Ni in a cellulose matrix with and without absorption correction.

References

- [1] R. Kirkham et al. AIP Conf. Proc. 1234, 240 (2010)
- [2] C.G. Ryan et al., J. Phys.: Conf. Ser. 499, 012002 (2014)
- [3] M.D. de Jonge, S. Vogt., Curr. Op. in Struct. Biol. 20/5, 606 (2010)

FAST XRF CT RECONSTRUCTION WITH ABSORPTION CORRECTION ON DIAMOND BEAMLINE I18

Abstract

By now the X-ray absorption MicroCT (computed tomography) is a well-established experimental technique that is applied in a wide range of scientific areas to provide non-destructive information, both static and dynamic, about the 3D structure of the objects of interest with high spatial resolution. Due to advances in the brilliance of photon sources and increased efficiencies in data collection (especially high-speed detector signal processing) that reduced the data collection time significantly, the application of other CT modalities such as XRF, XANES and XRD CT is now becoming practical and is performed on a significant number of beamlines around the world.

The interest in the application of these modalities has grown significantly among the microspectroscopy beamline I18 user community as well, with a large proportion of beamtime allocated for the microprobe CT experiments in the areas such as chemistry, materials science and biology. While the experimental setup and data collection in these types of measurements is mostly straightforward, there are still challenges on the data analysis side.

One of the main problems for quantitative reconstruction in XRF CT is the correction for the absorption of low energy fluorescence signal in thick samples during reconstruction. Here we describe the application of iterative CT reconstruction with absorption correction for multiple chemical elements developed on I18 based on the algebraic reconstruction techniques.

This general algorithm corrects for the attenuation of both incident and fluorescence radiation in the sample that can be comprised of a number of different elements. As iterative reconstruction can be quite slow, especially with absorption correction thrown in, vectorisation with correction matrices is applied during the reconstruction to significantly improve the reconstruction speed. In addition there is an option for geometric corrections if using multi-element energy-dispersive detectors. Several examples of the reconstructions in the area of plant biology and catalysis are shown.

DADA – A WEB-BASED 2D-DETECTOR ANALYSIS TOOL

M. Osterhoff¹

¹Institut für Röntgenphysik, Friedrich-Hund-Platz 1, 37077 Göttingen, Germany

Abstract

Many x-ray experiments utilise 2D pixelated detectors for e.g. imaging applications in full-field and scanning set-ups or for data acquisition in large sections of reciprocal space. University research groups collect data at different beamlines, all with their individual detectors, file formats and file name specifications. Students have only a limited time for their research project, and cannot spend too much of it to answer (again) the question: how can I access my data?

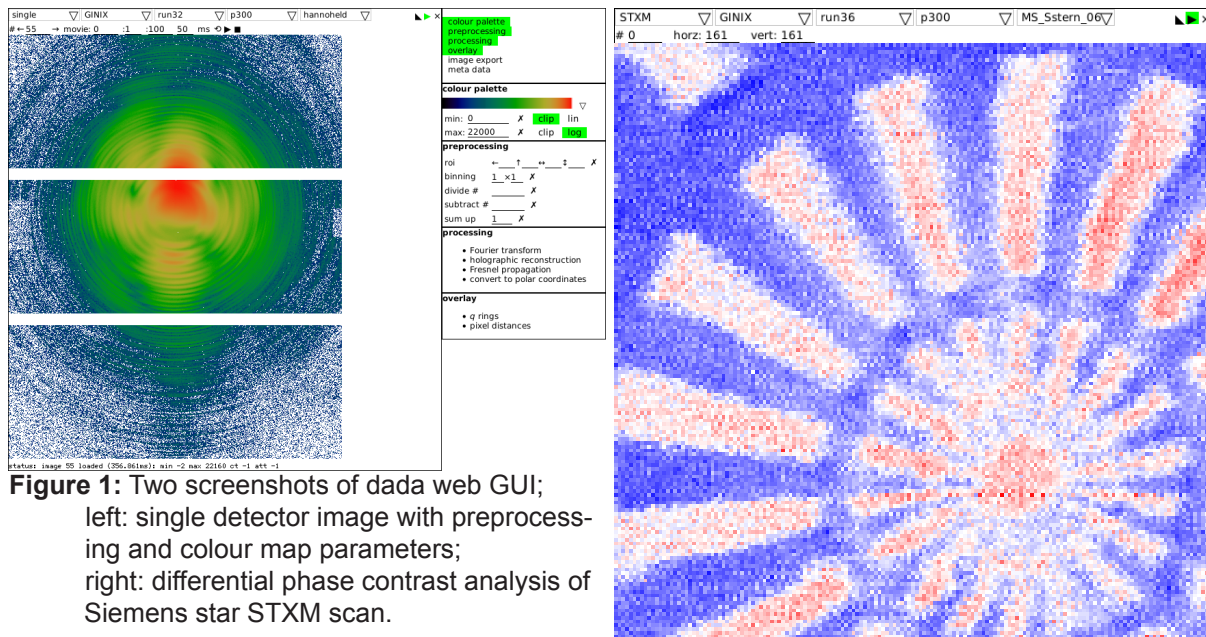


Figure 1: Two screenshots of dada web GUI; left: single detector image with preprocessing and colour map parameters; right: differential phase contrast analysis of Siemens star STXM scan.

We are developing a web-based tool that allows for fast visual inspection of 2D detector images, incorporating basic pre-processing such as empty beam correction and phase retrieval, plus intermediate processing to analyse e.g. scanning transmission x-ray microscopy (STXM) data sets for differential phase contrast. Apart from visualisation, a data export to third-party software is possible – with a unified data format independent from raw data.

In our research groups, currently about 64 TB of data can be browsed and pre-analysed using our dada software. Where applicable, pixel detector data is enriched by meta data such as motor positions. This can be implemented independently from the actual meta data format. A live module of dada allows for fast visualisation during the beam time, to accelerate sample inspection and alignment, and in the end increase throughput of the measurements.

With our contribution we show the current status, implemented algorithms and future plans of dada and are open for users' suggestions. A beta version will be made available in time.

THE *XRAYLIB* LIBRARY FOR INTERACTIONS OF X-RAYS WITH MATTER

T. Schoonjans¹, A. Brunetti², B. Golosio²,
M. Sanchez del Rio³, V.A. Solé³, C.Ferrero³ and L. Vincze⁴

¹ Diamond Light Source Ltd, Diamond House, Harwell Science and Innovation Campus, Didcot, UK

² Università degli Studi di Sassari, Via Piandanna 4, 07100 Sassari, Italy

³ European Synchrotron Radiation Facility, rue Jules Horowitz 6, 38043 Grenoble, France

⁴ X-ray Microspectroscopy and Research group, Ghent University, Krijgslaan 281, B-9000, Gent, Belgium

Abstract

X-ray based analytical techniques have seen a surge in popularity over the last decades. This had led to an increased interest in interaction cross sections and other atomic parameters, which are of fundamental importance in both quantitative and qualitative analysis. In X-ray fluorescence (XRF), for example, quantification using either the fundamental parameter method or Monte Carlo simulations is only possible if accurate data of X-ray interactions with matter are available. Such data can be obtained in two ways: experimental and computational through quantum mechanical calculations. Several authors have published databases and tabulations in the literature, but none of them are presented in the form of freely available library functions, which can be easily included in software applications for X-ray techniques.

In an effort to solve the problem of interfacing the data to the user, Brunetti *et al.*[1] designed a software package called *xraylib* based on a shared ANSI C language library. The physical data included in the package is a compilation of several popular datasets including for example photoionization-, Rayleigh-, and Compton cross sections as well as absorption edge energies, fluorescence line energies and fluorescence yields.

In this work we will present the features offered by the most recent release of the *xraylib* package (version 3.2.0), such as partial photoelectric effect cross sections, cascade effect corrected X-ray fluorescence production cross sections, atomic level widths, Compton broadening profiles, diffraction related functions etc. Furthermore, in order to increase the library's usability, we have added bindings to several popular programming languages such as IDL, Java, Fortran, Python, Perl, Ruby, Lua, PHP and .NET, and have created versions compatible with all major operating systems and architectures [2].

We have constructed a website, hosted at <http://lvserv.ugent.be/xraylib-web>, that relies on *xraylib*'s newly added PHP bindings in order to provide convenient access to all of its databases while simultaneously also giving developers assistance on how to extend their software with the *xraylib* API.

xraylib was recently added to DAWN, Diamond's data analysis Eclipse based workbench. We will demonstrate some of the new data processing features that were made possible due to this addition.

The *xraylib* development occurs at <http://www.github.com/tschoonj/xraylib> where the source code, prebuilt binaries as well as comprehensive documentation can be found.

xraylib is released under the BSD license.

References

- [1] A. Brunetti et al. Spectrochimica Acta B, 59(10-11), 2004, 1725-1731.
- [2] T. Schoonjans et al. Spectrochimica Acta B, 66(11-12), 2011, 776-784.

REGISTRATION OF FRESNEL DIFFRACTION PATTERNS FOR X-RAY PHASE NANOTOMOGRAPHY

A. Hänsch¹, L. Weber^{1,2}, S. Rit¹, A. Pacureanu², P. Cloetens², F. Peyrin^{1,2},
M. Langer^{1,2}

1 Univ Lyon, INSA-Lyon, CNRS, Inserm, CREATIS UMR 5220, U1206, F-69621, LYON, France

2 European Synchrotron Radiation Facility (ESRF), F-38043, GRENOBLE, France

Abstract

X-ray phase contrast imaging is a relatively new imaging modality which offers several orders of magnitude higher sensitivity compared to attenuation imaging [1] [2]. This is especially interesting for the imaging of soft tissue [3]. The X-ray phase cannot be measured directly, however. A simple way of achieving phase contrast is to let the beam propagate in free space after the sample. Several phase retrieval algorithms from such images have been developed [4]. Most of these rely on linearisation of the Fresnel diffraction formula to yield linear filtering based algorithms. The phase maps can be fed to a tomographic reconstruction algorithm to yield a 3D reconstruction of the refractive index decrement distribution [5].

Information transfer from phase shift to contrast in the low spatial frequency range is weak, which makes phase retrieval from Fresnel diffraction patterns sensitive to low frequency noise [6]. Several approaches to overcome this limitation have been proposed [6-9]. One particularity of the CTF-based methods [6, 8, 9] is that they allow the use of several phase contrast images taken at different sample-to-detector distances, yielding a better coverage of the phase information in the frequency domain. Indeed, using several distances seems necessary to achieve good image quality in high-resolution imaging [10].

The images at different distances will be out of alignment due to instrumental imprecisions, drift and vibrations. This problem has only been mentioned in passing in literature, despite being non-trivial. It is a registration problem where at lower resolution the contrast is reasonably similar, and at higher resolution the contrast can be very different, between the different distances. To our knowledge, this problem has so far been handled using correlation based methods. In our experience, correlation works well at relatively low resolutions and in the absence of strong artifacts, but fail more often as resolutions become higher.

Therefore, the aim of this work is to investigate the use of different registration algorithms for the alignment of Fresnel diffraction patterns acquired at different distances. The influence of misalignments on the retrieved phase maps and 3D reconstructions is investigated using simulated data. Then, different registration algorithms are evaluated using experimental phase nano-CT data from the new Nano-Imaging beamline ID16A at the ESRF, Grenoble, France, and compared to the previously used correlation-based method. This work was supported by the ANR grant ANR-14-CE35-0030-01, the Région Rhône-Alpes, and LabEx PRIMES (ANR-11-LABX-006"). We thank the ESRF for support through the LTP MD830.

References

- [1] R. Boistel et al., Plos one 6, e22080 (2011).
- [2] I. Zanette et al., Physica Status Solidi A 208, 2526 (2011).
- [3] J. P. Guigay et al., Opt. Lett. 32, 1617 (2007).
- [4] M. Langer et al., Med. Phys. 35, 4556 (2008).
- [5] P. Cloetens et al., Appl. Phys. Lett. 75, 2912 (1999).
- [6] M. Langer, P. Cloetens, F. Peyrin, IEEE Trans. Imag. Process. 19, 2428 (2010).
- [7] D. Paganin et al., J. Microsc. 206, 33 (2002).
- [8] M. Langer et al., Opt. Lett. 37, 2151 (2012).
- [9] M. Langer et al., Phil. Trans. R. Soc. A 372, 20130129 (2014).
- [10] M. Langer et al., Plos one 7, e35691 (2012).

MOUSE BRAIN NETWORK VISUALIZED WITH X-RAY MICROTOMOGRAPHY

Rino Saiga¹, Masato Ohtsuka², Masato Hoshino³, Akihisa Takeuchi³, Kentaro Uesugi³, and Ryuta Mizutani¹

1Department of Applied Biochemistry, Tokai University, Hiratsuka, Kanagawa 259-1292, Japan

2Tokai University School of Medicine, Isehara, Kanagawa 259-1193, Japan

3Japan Synchrotron Radiation Research Institute (JASRI/SPring-8), Sayo, Hyogo 679-5198, Japan

Abstract

The brain is composed of a large number of neurons, which constitute a 3D network. The first step to understanding brain function is to determine the network structure. We report here a 3D analysis of a murine brain network by x-ray microtomography.

Soft tissues are composed of light elements, which produce little contrast in a hard x-ray image. Therefore, contrast should be enhanced to visualize cellular structures. We have reported a number of methods for labeling cellular structures with high-Z elements [1,2]. Another way to visualize cellular structure is lowering the intensity of the surrounding extracellular matrix, giving a contrast between the target structure and its background. This can be achieved by removing water from the tissue. In this study, murine brain hemispheres were immersed in t-butyl alcohol and then subjected to lyophilization so as to reduce the intensity of the background matrix. The resultant brain was visualized with x-ray microtomography at the BL20B2 beamline of SPring-8.

A cutaway section of the obtained 3D structure is shown in Figure 1. Fibrous structures were clearly observed in the striatum (Figure 2), indicating that axonal tracts can be visualized with this method. The tracts were traced to build a network model of the brain. Further analysis of this network should be able to delineate the functional mechanisms of the murine brain.



Figure 1: A coronal cutaway rendering of murine brain hemisphere. X-ray attenuation coefficients were gray-scaled from 0.9 cm^{-1} (black) to 3.4 cm^{-1} (white). Anterior view.

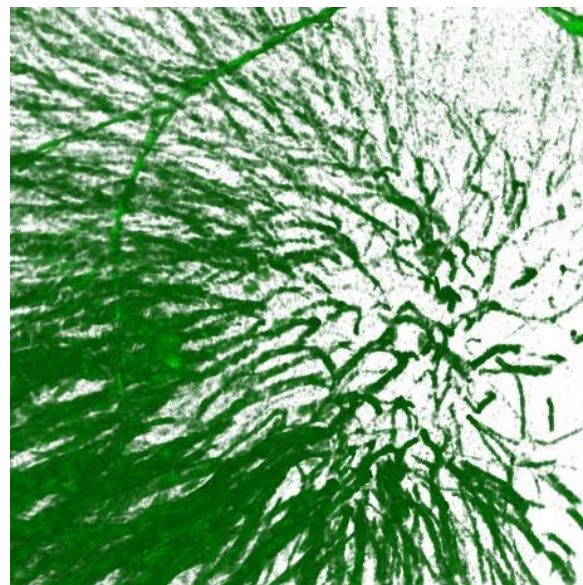


Figure 2: Axonal tracts observed in the striatum. X-ray attenuation coefficients in a $1.0 \times 1.0 \times 0.4 \text{ mm}$ volume were rendered from 1.6 cm^{-1} to 3.4 cm^{-1} . Posterior view.

References

- [1] R. Mizutani et al., J. Synchrotron Radiat. 15, 374-377. (2008).
- [2] R. Mizutani et al., Cerebral Cortex 20, 1739-1748 (2010).

DEVELOPEMENT OF SOFT X-RAY TOMOGRAPHIC MICROSCOPY FOR BIOMEDICAL RESEARCHES AT TAIWAN PHOTON SOURCE

L.J. Lai, Y. J. Su, G. C. Yin, D. J. Wang, S.Y. Chiang, L. J. Huang, Z.J. Lin, C. C. Hsieh, M. T. Tang, D. J. Huang.

National Synchrotron Radiation Research Center, 101 Hsin-Ann Road, Hsinchu 30076, Taiwan

Abstract

The construction of the full-field transmission soft X-ray tomography (SXT) beamline at the Taiwan Photon Source (Figure 1) has been conducted with intense strength. The beamline, adapting the design of varied-lines-spacing plane grating monochromator (VLS PGM), will be operational in the energy range of 260 ~ 2,600 eV [1]. The microscope is a generic design, namely, an association of a high demagnification condenser and an objective Fresnel zone plate [2]. With nominal spatial resolution of 15~30 nm for 2D imaging and 50 nm for 3D tomography, the beamline and associated facility is dedicated to image frozen-hydrated biological specimen for bio-medical researches.

The schematic of the endstation is shown in Figure 2. Crucial optical components as well as associated sample environment are tested parallel to the beamline construction. These include, the measurement of the focal spot and divergence from the capillary condenser, the assembly and test of the on-line cryo-fluorescence structure illumination microscope (SIM), the effectiveness of the cryo-environment for sample transfer and measurement. User-supporting equipment for off-line sample preparation, such like the P2 level biological laboratory and a plunge freezer is consequently constructed. The beamline is planned to be in the phase of pilot commissioning by the end of 2016.

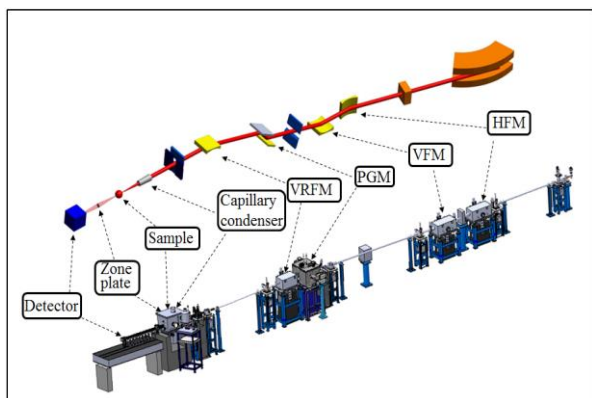


Figure 1: The layout of SXT beamline and endstation.

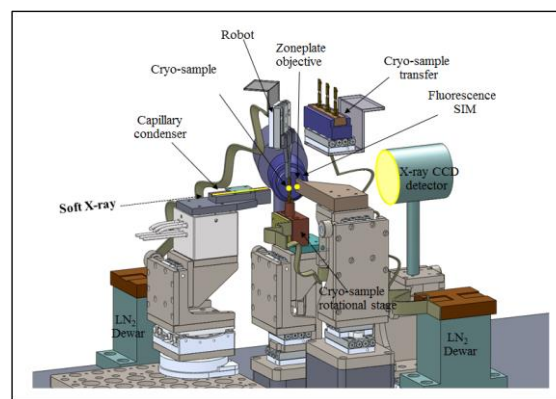


Figure 2: Schematic of the SXT microscope endstation.

References

- [1] E. Pereiro, J. Nicolás, S. Ferrer, M. R. Howells, J. Synchrotron. Rad. 16, 505 (2009).
- [2] G. Schneider, P. Guttmann, S. Rehbein, S. Werner, R. Follath, J. Struct. Biol. 177, 212 (2012).

COMBINED USE OF X-RAY FLUORESCENCE MICROSCOPY, PHASE CONTRAST IMAGING AND NANOTOMOGRAPHY FOR HIGH RESOLUTION QUANTITATIVE Fe MAPPING IN INFLAMED CELLS

Chiara Gramaccioni^{1,5}, Alessandra Procopio², Alessandra Frioni³, Emil Malucelli², Stefano Iotti², Andrea Notargiacomo⁴, Michela Fratini^{5,6}, Yang Yang⁷, Peter Cloetens⁷, Sylvain Bohic⁷, Piera Valenti³, Luigi Rosa³, Lorenzo Massimi⁵, Francesca Berlutti³ and Stefano Lagomarsino⁵.

1Dept. of Physics, Univ. of Cosenza, Arcavata di Rende, (Cosenza), Italy

2Dept. of Pharmacy and biotechnology, Univ. Bologna, Bologna, Italy

3Dept. of Public Health and Infectious Diseases, Univ. Sapienza, Roma, Italy

4Institute for Photonics and Nanotechnologies - CNR, Roma Italy

5CNR-Nanotec, c/o Dept. of Physics Univ. Sapienza, Roma, Italy

6Fondazione Santa Lucia, Roma, Italy

7ESRF, Grenoble, France

Abstract

Iron is a primary component of fundamental processes which can become toxic when present in excess. In human fluids, free iron is maintained at 10^{-18} M concentration thanks to several proteins as lactoferrin (Lf) in secretions and transferrin in blood. The altered iron balance favors bacterial infection and the related inflammatory response as occurs in cystic fibrosis[1,2]. Therefore, it is of great importance to provide quantitative mapping of iron concentration at high spatial resolution. Here we studied human phagocytic cells unstimulated or stimulated with bacterial lipopolysaccharide (LPS) or/and Lf to map the intracellular density and iron concentration. For this aim, X-ray fluorescence microscopy (XRFM), atomic force microscopy (AFM) and phase contrast imaging were combined, as previously demonstrated [3,4]. To determine the concentration map, we normalized the fluorescence intensity with the volume of the illuminated region (Fig.1). The volume of freeze-dried cells has been obtained by AFM with lateral resolution of 100 nm. The XRFM and phase contrast measurements have been carried out at the beamline ID16A-NI at ESRF, with spatial resolution of 100 nm and 50 nm, respectively. Moreover, we determined the weight fraction distribution map, normalizing the fluorescence intensity with the projected density obtained by phase contrast imaging (Fig.2) [5]. Indeed, we obtained the density distribution (Fig.3) by normalizing phase reconstruction maps with AFM data. Similar evaluations were carried out for LF- and LPS plus LF-treated cells. We also carried out nanotomography measurements, to obtain the three-dimensional density distribution. The nanotomography is of paramount importance to reach the volumetric information in frozen-hydrated cells because AFM cannot be used since frozen hydrated cells are stored in liquid nitrogen.

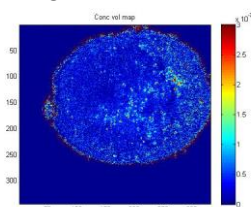


Figure 1: Iron concentration map of cell treated with LPS.

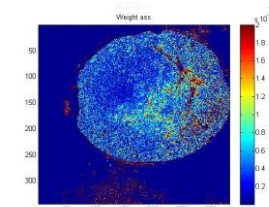


Figure 2: Iron Weight fraction distribution map of cell treated with LPS.

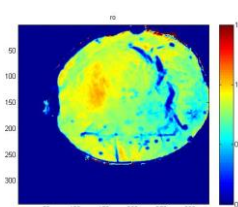


Figure 3: Density distribution map of cell treated with LPS.

Acknowledgements: the research was granted by Sapienza University of Rome to PV and FB and by Cystic Fibrosis Foundation (Italy) (FFC#16/2014 and FFC#12/2015) to FB.

References

- [1] R. Paesano et al. Pathogens and Global Health 2012, 106, 200.
- [2] P. Valenti et al., Lactoferrin and cystic fibrosis airway infection. In: Diet and Exercise in Cystic Fibrosis. 2015, 30, 259
- [3] S. Lagomarsino et al., Spectrochim. Acta B 2011 66, pp767-866
- [4] E. Malucelli et al., Anal. Chem., 2014, 86, pp 5108–5115
- [5] E. Kosior et al., J. Struct. Biol. 2012 177(2):239-47

COMBINED USE OF MICRO COMPUTED TOMOGRAPHY AND HISTOLOGY TO EVALUATE THE BONE INGROWTH IN 3D PRINTED BIOACTIVE GLASS SCAFFOLDS

X. Shi¹, A. Nommeots-Nomm², P.D.Lee², J. R.Jones¹

¹Department of Materials, Imperial College London, Prince Consort Road, London SW7 2BP, UK

²The Manchester X-Ray Imaging Facility, Harwell Oxford, Didcot OX11 0FA, UK

Abstract

Porous melt-derived bioactive ICIE 16 (49.46% SiO₂, 36.27% CaO, 6.6% Na₂O, 1.07% P₂O₅ and 6.6% K₂O, in mol%) glass scaffolds developed by Wu *et al.* showed rapid hydroxycarbonate apatite (HCA) formation after 3 days immersed into simulated body fluid (SBF) [1].

In this study, the three-dimensional (3D) ICIE 16 porous scaffolds fabricated by a 3D printing technique were used to repair subcritical-sized (3 mm) rat femur condyle defects. The 3D print scaffold showed uniform interconnected macropores (~125 μm), suitable porosity (~45.5%) and enhanced compressive strength (18.3 ± 2.2 MPa). Both micro computed tomography (μCT) and histology were performed to analyse the characteristics of the scaffolds and bone ingrowth at different time points. The registration of histological slices with their counterparts in the 3D μCT dataset were performed both visually and automatically in order to identify anatomical features.

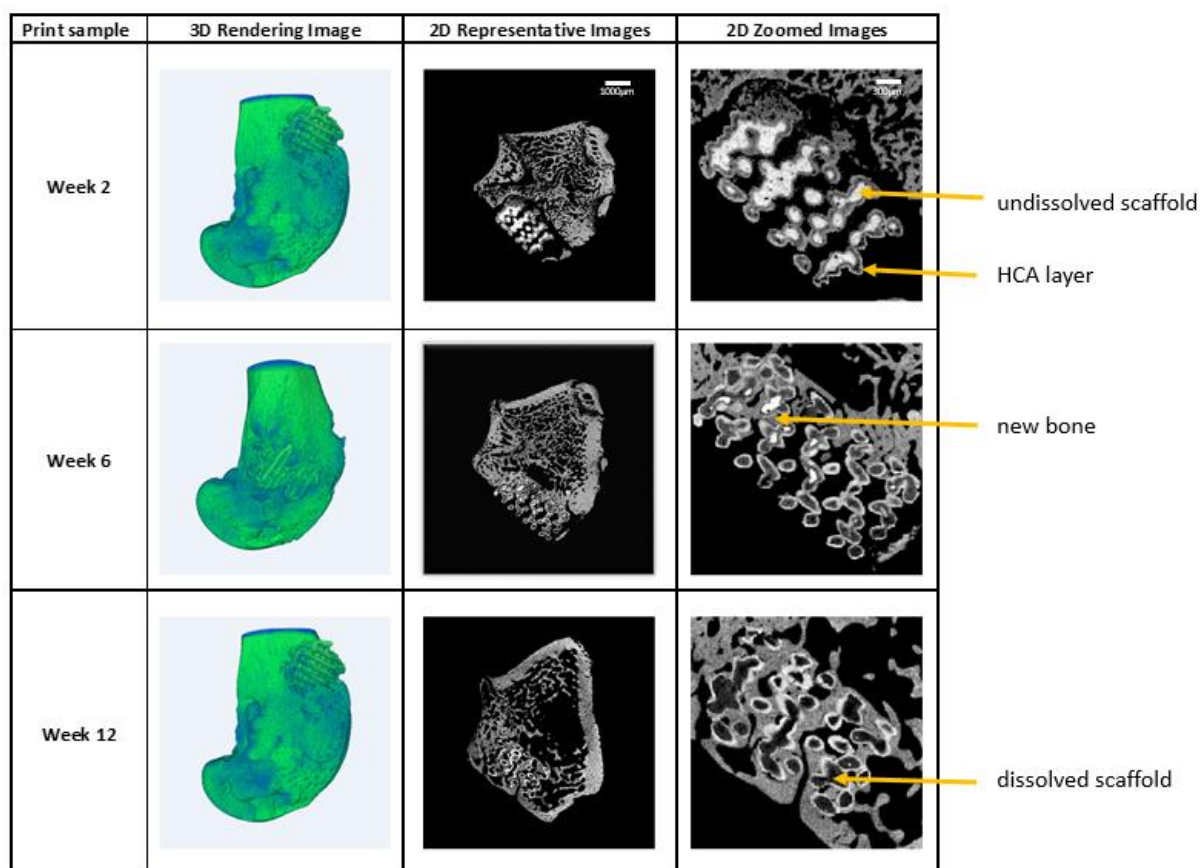


Figure 1: 3D rendering images and 2D representative slices of 3D print samples at week 2, 6, and 12.

References

- [1] Wu ZY, Hill RG, Yue S, Nightingale D, Lee PD, Jones JR. Melt-derived bioactive glass scaffolds produced by a gel-cast foaming technique. *Acta Biomater. Acta Materialia Inc.*; 2011;7(4):1807–16.

DESCRIBING ACINAR MICROSTRUCTURE AND DYNAMICS AT THE MICROMETER SCALE

Ioannis Vogiatzis Oikonomidis^{1,2}, Tiziana P. Cremona¹, Goran Lovric^{2,4}, Filippo Arcadu^{2,3},
Christian M. Schlepütz², Rajmund Mokso², Marco Stampanoni^{2,3}, Johannes Schittny¹

1Institute of Anatomy, University of Bern, 3012 Bern, Switzerland,

2Swiss Light Source, Paul Scherrer Institute, 5234 Villigen, Switzerland,

3Institute for Biomedical Engineering, University and ETH Zurich, 8092 Zurich, Switzerland,

4Center for Biomedical Imaging (CIBM), EPFL, 1015 Lausanne, Switzerland

Abstract

The acinus represents the functional unit of the lung, a life-supporting organ in mammals, however there is still limited knowledge on the acinar 3D microscopic dynamics during breathing and development [1]. Recently we have realized ex-vivo and in-vivo X-ray tomographic microscopy at different pressures with pixel sizes reaching down to a micrometer [2]. However, low CNR and local tomography artifacts mainly characterize such data. In addition, the structures to be resolved are on the resolution limit and represent high structural complexity, i.e. large size variation within a slice, no clear shape descriptor and no clear borders between different acini on 2D sections. In our attempt to extract the acinar skeleton and conduct a detailed deformation analysis with inflating lungs as well as track development, several challenging tasks have to be undertaken.

Here we demonstrate the methodology to acquire datasets of fresh ex-vivo mice with large field-of-view and at high resolution ($3.7 \times 3.7 \text{ mm}^2$ at $1.1 \mu\text{m}$ pixel size) in the order of tens of seconds. We present how to automatically stitch overlapping CT-reconstructed volumes in order to visualize an entire acinus at different pressures. Following that, we propose an automatized algorithm for 3D segmentation of the low CNR reconstructed volume, enabling the extraction of the acinar skeleton. In particular, a combined multilevel filtering approach without any manual input is adopted. The proposed method first applies a connected component analysis, followed by a vesselness filter [3] aimed at generating per slice-automatized seeds for a random walk [4]. Information of adjacent slices is used to classify them as tissue, thus mimicking the way the human eye classifies regions (tissue or air) by scrolling between adjacent slices. Finally, we propose a way to extract acinar skeletons and describe their dynamics.

Our method is the first step for an automated analysis on how the lung breathes and develops at a micrometer and acinar scale. It manages to accurately segment thin septa of an entire acinus and track changes in acinar development and dynamics through the description of extracted skeletons. This approach can be applicable to wide range of other dynamic geometries with large size variations within a single slice like heart vessel walls.

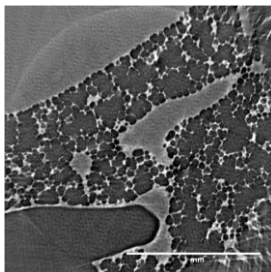


Figure 1. Reconstruction.



Figure 2. Initial segmentation.

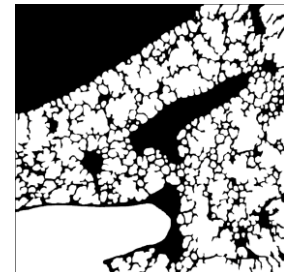


Figure 3. Final segmentation.

References

- [1] Weibel E. R., The American Journal of Physiology, 261, 1991: 361–9.
- [2] Lovric G., ETH PhD thesis, 2015.
- [3] Frangi Z., et al. MICCAI'98. Springer Berlin Heidelberg, 1998: 130–137.
- [4] Grady L., IEEE Transactions on 28.11 2006: 1768–1783.

PROPAGATION-BASED PHASE-CONTRAST TOMOGRAPHY FOR EVALUATION OF HUMAN ATHEROSCLEROTIC PLAQUES

W. Vågberg¹, J. C. Larsson¹, L. Szekely², J. Persson³ and H. M. Hertz¹

1 KTH Royal Institute of Technology, AlbaNova Universitetscentrum, Stockholm, Sweden

2 Karolinska Institutet, Department of Microbiology Tumor and Cell Biology (MTC), KI Solna Campus, Karolinska Institutet, Stockholm, Sweden

3 Division of Cardiovascular Medicine, Department of Clinical Sciences, Karolinska Institutet, Danderyd University Hospital, Stockholm, Sweden

Abstract

Cardiovascular disease is the major causes of death in developed countries. Ischemic stroke and myocardial infarction is caused by thrombus formation in the cerebral or coronary arteries. The thrombus develops within minutes secondary to the rupture of a vulnerable atherosclerotic plaque. The atherosclerotic plaques consist of lipid-rich necrotic core, cellular debris and macrophages. The plaques are separated from the vessel lumen by a fibrous cap. The likelihood of rupture to occur depends on the thickness of the fibrous cap (20 μm to a few 100 μm) and infiltration of macrophages in the fibrous cap.

Atherosclerotic plaques have previously been assessed with grating-based phase-contrast tomography using laboratory sources [1]. Grating-based imaging provides very good density resolution, but suffers from low spatial resolution. To be able to determine which atherosclerotic plaques are to develop into vulnerable plaques higher spatial resolution is required. With higher spatial resolution the thickness of the fibrous cap and macrophage infiltration can be determined.

In this work, we show that propagation-based phase-contrast tomography can be useful to evaluate the vulnerability of atherosclerotic plaques. This was done using a liquid-metal-jet x-ray source [2] and a scintillator-coupled CCD camera. We imaged human coronary arteries, which are only a few millimeters in diameter, and are of high medical interest, since a rupturing lesion can cause myocardial infarction. We were able to achieve enough density resolution to identify lipid-rich plaques, with spatial resolution of around 10 μm allowing for measuring the thickness of the fibrous cap.

References

- [1] H. Hetterich, M. Willner, S. Fill, J. Herzen, F. Bamberg, A. Hipp, U. Schüller, S. Adam-Neumair, S. Wirth, M. Reiser, F. Pfeiffer and T. Saam. *Radiology*. 271, 870-878 (2014).
- [2] D. H. Larsson, U. Lundström, U. K. Westermark, M. A. Henriksson, A. Burvall and H. M. Hertz. *Med. Phys.* 40, 021909 (2013).

VISUALISING THE 3D MICROSCOPIC REMODELLING OF MECHANICALLY LOADED NATIVE TISSUES

Background

The function and mechanical behaviour of biological tissues relies on their 3D microstructure which may undergo profound remodelling as a consequence of age or disease. In the case of the intervertebral disc (IVD) structural remodelling is associated with chronic low back pain. In order to understand the pathological mechanisms and develop new treatments it will be necessary to characterise the 3D microstructure of the IVD under different loading conditions. We have previously shown that microfocus tube 'laboratory' microCT instruments can resolve micron-scale structures in paraffin-embedded skin and arteries. Although this method gives excellent imaging results it does not allow for the sequential compression and imaging of the same tissue sample. The high brilliance and coherence of synchrotron source X-rays has the potential to overcome these difficulties by rapidly resolving the microstructure of weakly absorbing, native (fresh) soft tissue under in situ load.

Aims/Objectives

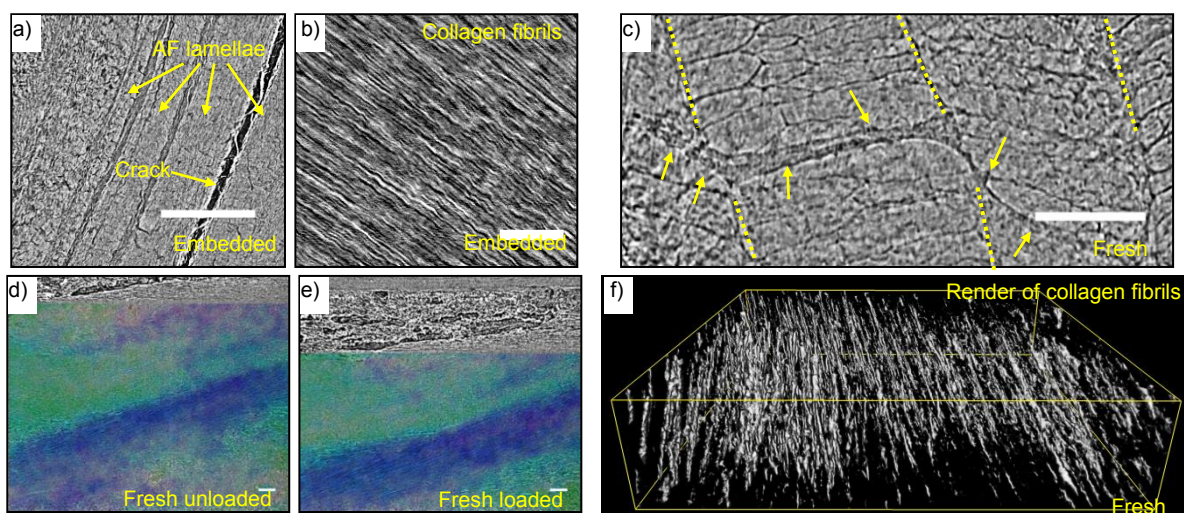
In this study we aimed to resolve the microstructure of both chemically fixed and native bovine IVDs using synchrotron based microCT at the Diamond-Manchester beamline and to image the effects of sequential loading.

Methods

Bovine tail IVDs (aged 18-36 months) were obtained from the local abattoir. Chemically fixed and paraffin embedded samples were prepared using standard histological protocols. In-line phase contrast imaging technique was used for both paraffin embedded and fresh tissue. Fresh tissue segments were also imaged following sequential compression.

Findings and Conclusions

Key IVD structures were resolved in all samples (marked in figures). Reconstructed data from the embedded samples showed the best resolution, resolving collagen fibril orientation, but suffered from crack artefacts in the paraffin. Reconstructed data from fresh tissue had slightly lower resolution which may be due to sample movement during the scan. Loading and allowing 20 minutes relaxation time improved stability of the sample during the scan resulting in a similar resolution as the embedded tissue. Importantly features were able to be tracked in 2D slices and work is ongoing to track these in 3D using digital volume correlation.



MicroCT of paraffin embedded and fresh IVD tissue. a) Transverse slice. b) Magnified radial slice. c) Transverse slice where dashed lines mark lamella boundaries and arrows indicate compartments and bridging structures. d&e) Radial slices with 2D orientation analysis. f) Rendering showing collagen fibrils. a, c, d, e scale bar 500 μm. b scale bar 200 μm.

INTERACTION OF BIOLOGICALLY RELEVANT NANOPARTICLES WITH CELLS STUDIED BY X-RAY TOMOGRAPHY

B. Kepsutlu¹, S. Kapishnikov¹, P. Guttman¹, S. Werner¹, A. Graebert¹, E. Pereiro², T. Ducic², J. Vonnemann³, R. Haag³, M. Breunig⁴, M. Ballauff¹, G. Schneider¹, J. McNally¹

1Helmholtz Zentrum Berlin, Hahn-Meitner-Platz 114109, Berlin, Germany

2ALBA Synchrotron, Carrer de la Llum 2-26 08290 Cerdanyola del Vallès, Barcelona, Spain

3Freie Universität Berlin, Takustrasse 3 14195, Berlin, Germany

4Universität Regensburg, Universitätsstrasse 31 93053 Regensburg, Germany

Abstract

We have analyzed the cellular uptake and processing of two different biologically relevant nanoparticles, namely gold nanoparticles coated with either polyglycerol sulfate dendrons (dPGS-AuNP) or polyethyleneimine (PEI-AuNP). dPGS-AuNP are good candidates for the diagnosis and treatment of inflammation [1]. PEI-AuNP are promising agents for the delivery of DNA or RNA into cells for the treatment of genetic diseases [2]. The success of either of these medical applications is affected by the cellular behavior of the nanoparticles. To analyze the uptake mechanism and cytoplasmic access at the single cell level over time, we used a combination of differential interference contrast (DIC) light microscopy and soft X-ray tomography. We find that dPGS-AuNP and PEI-AuNP are both internalized via endocytosis, and progress into early, then late endosomes and thereafter into multivesicular bodies. At this point the processing paths may diverge, as dPGS-AuNP are found in individual autophagosomes whereas PEI-AuNP are not, and instead are seen in amphisomes which arise from the fusion of multivesicular bodies with autophagosomes. Another potential difference between the two uptake pathways is that dPGS-AuNP appear to escape more readily from the endosomal system into the cytoplasm, whereas cytoplasmic escape appears to be rarer for PEI-AuNP. We also find that nanoparticle interaction with the cells may differ depending on the concentration of nanoparticles applied and also on the cell type. Finally, we observe that both types of nanoparticles induce changes in cellular organelle content. Our results show that the nanoparticles have profound effects on cellular ultrastructure, and they also demonstrate that nanoparticle processing can vary markedly depending on the nanoparticle coating, concentration and cell type. Therefore, it is essential to examine cellular interactions of nanoparticles under the conditions specific to the intended medical application.

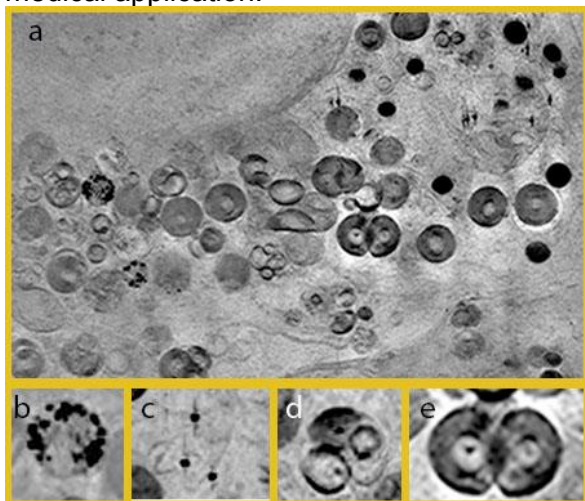


Figure 1: A slice from a whole reconstruction of a cell with dPGS-AuNP (a). dPGS-AuNP are in endosomes (b), free in cytoplasm (c), in MVB (d), in autophagosomes (e).

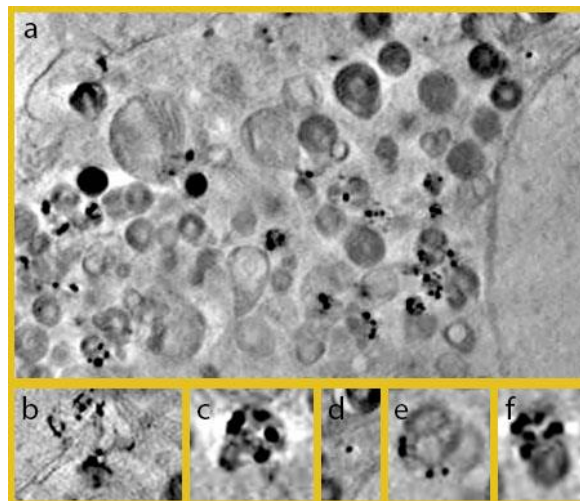


Figure 2: A slice from a whole reconstruction of a cell with PEI-AuNP (a). PEI-AuNP are internalized (b), in endosomes (c), free in cytoplasm (d), in MVB (e), in amphisomes (f).

References

- [1] Vonnemann, J., et al., *Theranostics*, 2014. 4(6): p. 629-641.
 [2] Elbakry, A., *ACS*, 2009. 9(5): p. 2059-2064.

STRAIN AND MICRODAMAGE PROGRESSION IN THE VERTEBRAL BODY FROM DIGITAL VOLUME CORRELATION

G. Tozzi¹, V. Danesi², M. Palanca², L. Cristofolini²

¹School of Engineering, University of Portsmouth, Portsmouth PO1 3DJ, United Kingdom

²Department of Industrial Engineering, University of Bologna, Bologna 40136, Italy

Abstract

Strain distribution in the vertebral body has been extensively carried out in the past, mainly by means of strain gauges [1]. The combination of X-Ray micro-focus computed tomography (micro-CT) in conjunction with *in situ* mechanical testing and digital volume correlation (DVC) has been exploited over the past decade to measure complex deformation fields within biological tissues. In this perspective, digital volume correlation (DVC) is ideal to investigate the internal strain in vertebral bodies and couple this information with microdamage progression during loading. In this study step-wise compression testing of vertebrae in combination with time-lapsed micro-CT imaging was performed. The specimens were compressed axially in a step-wise fashion up to 15% nominal strain (0% with 50N preload, 5%, 10% and 15%). Micro-CT imaging (XTH225, Nikon Metrology, UK) was carried out after each loading step (voxel size: 38.8 μ m; voltage: 88kV; current: 115 μ A; exposure: 2s). Strain was computed using DVC (DaVis-DC v8.3, LaVision, Germany) with a sub-volume of 48voxels, reached after successive (predictor) passes of 128-112-96-80-64voxels (multipass) and a 0% overlap [2, 3]. The axial, antero-posterior and lateral-lateral strain distributions for the three loading steps (5%, 10% and 15%) on the sagittal section of the vertebrae were evaluated (Fig. 1). The results obtained in this study show how DVC has the ability to predict high-strain concentration and therefore damage way before this occurs. This has the potential to be implemented in clinical CT assessment of vertebrae, given controlled loading conditions during imaging.

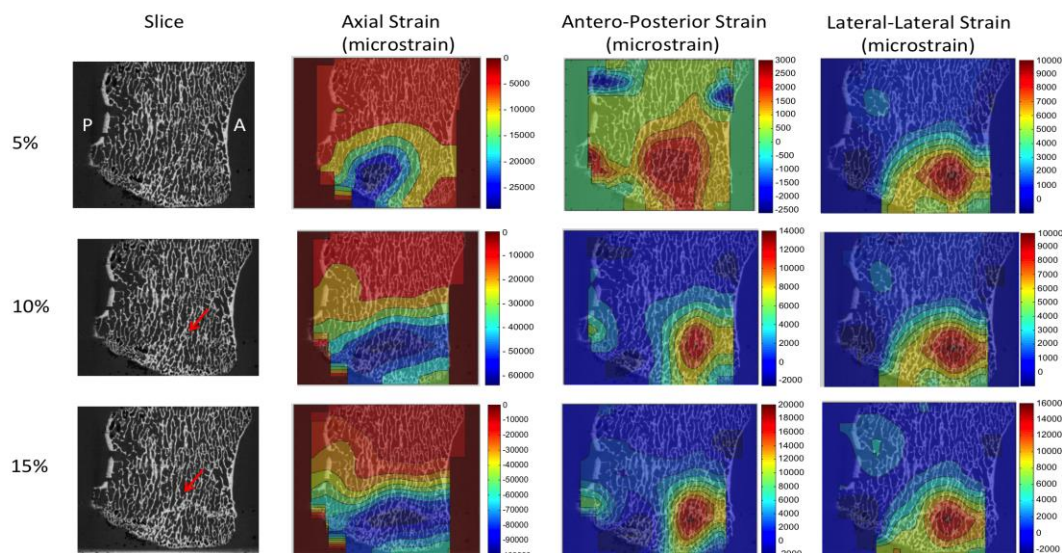


Figure 1. Strain distribution (axial, antero-posterior and lateral-lateral) and microdamage progression for one specimen. A-P indicates the Antero-Posterior direction on the image.

References

- [1] L. Cristofolini, N. Brandolini, V. Danesi, M. Juszczak, P. Erani, M. Viceconti, *Spine*. 13(10), 1281-92 (2013).
- [2] M. Palanca, L. Cristofolini, E. Dall'Ara, M. Curto, F. Innocente, V. Danesi, G. Tozzi (submitted to *J. Mech. Behav. Biom. Mater.*).
- [3] G. Tozzi, E. Dall'Ara, M. Palanca, M. Curto, F. Innocente, L. Cristofolini (submitted to *J. Mech. Behav. Biom. Mater.*).

CALCIUM OXALATE CLUSTER CRYSTALS INVESTIGATION OF WILD GINSENG VIA QUANTITATIVE X-RAY MICRO-TOMOGRAPHY

Y. L. Xue, L. L. Ye, H. Tan, T. Q. Xiao

Shanghai Institute of Applied Physics, Chinese Academy of Sciences, 239 Zhangheng Road, Shanghai, China

Abstract

Identification and quality evaluation of Chinese medicinal materials (CMMs) is the foundation of traditional Chinese medicines. Both the traditional identification methods and modern identification methods are all need chemical extraction, which entails the adding of reagents and other destructive processes. Owing to the high spatial coherence, high flux density and unique penetrating characters of the third generation of synchrotron radiation X-ray beam, synchrotron radiation X-ray imaging can achieve in situ, nondestructive research on CMMs, which are mainly composed of C, H, O, and N elements, with better spatial and density resolutions, and some achievements have been attained at Shanghai Synchrotron Radiation Facility (SSRF) [1-4].

Calcium oxalate cluster crystals (COCCs) is a kind of secondary metabolites in medicinal plants, the different shape, distribution and amount of crystals are important characteristics for microscopic identification of medicinal plants. The accumulation of secondary metabolites in medicinal plant roots is also correlated with plant age and quality. In this presentation, X-ray phase-contrast micro-tomography (XPCMT) quantitative imaging method was used to investigate the COCCs microstructures of wild ginseng. COCCs were extracted successfully by XPCMT combining phase-retrieval method. The shape, size, amount, volume and position distribution of COCCs, which can be used for the identification and quality evaluation of ginseng, were obtained accordingly (shown in Fig.1&2). This study is the first to present different morphologies in different angles of the same crystal (shown in Fig.1). The results showed that this method provides a feasible comprehensive evaluation of the distribution of COCCs accumulation in wild ginseng. This method is also expected to reveal important relationships between COCCs and the occurrence of the effective medicinal components of ginseng. XPCMT quantitative analysis could also be applied to other types of CMMs and even many different kind of plants that contain different microstructures and crystalline types.

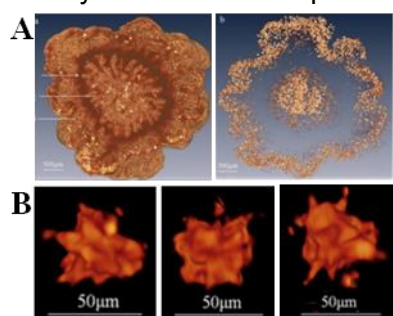


Figure 1: A: Volume renderings of the main root of wild ginseng. (a) 3D planform: 1-cambium, 2-tissues inside of cambium, 3-tissues outside of cambium; (b) 3D planform of COCCs; B: different morphology of the same crystal in different angles.

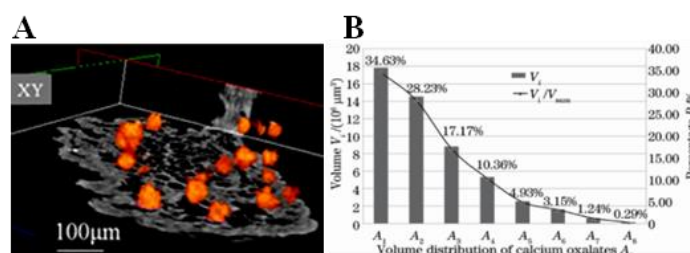


Figure 2: A: Volume renderings of COCCs of wild ginseng fibrous root (H=118.4μm). B: distribution curve of COCCs volumes of main root of wild ginseng across volume ranges of A_i

This work is supported by the National Natural Science Foundation of China grant 11475248 and 11105213.

References

- [1] Y. L. Xue, T. Q. Xiao, L. H. Wu, et al., Acta Phys Sin-Ch Ed 59,5496(2010).
- [2] L. L. Ye, Y. L. Xue, H. Tan, et al., Acta Optica Sinica-Ch Ed 33,1234002(2013).
- [3] L. L. Ye, Y. L. Xue, L. H. Ni, et al., J Instrum 8, 8 C07006 (2013).
- [4] T. Q. Xiao, H. L. Xie, B. Deng, et al., Acta Optica Sinica-Ch Ed 34,0100001(2014).

CHEMISTRY AND MICROSTRUCTURE OF ECO-CEMENT PASTES STUDIED BY PTYCHOGRAPHIC X-RAY COMPUTED TOMOGRAPHY

A. Cuesta¹, J.C. da Silva^{2,§}, P. Trtik², A. Diaz², M. Holler², A.G. De la Torre³, M.A.G. Aranda¹

¹ALBA Synchrotron, Carrer de la Lum, 2-26, 08290 Cerdanyola del Vallès, Barcelona, Spain

²Paul Scherrer Institut, 5232 Villigen PSI, Switzerland

³Departamento de Química Inorgánica, Universidad de Málaga, 29071 Málaga, Spain

§Currently at European Synchrotron Radiation Facility, Grenoble, 3800, France

Abstract

Calcium SulfoAluminate, CSA, eco-cements invariably contain ye'elimite, $\text{Ca}_4\text{Al}_6\text{O}_{12}\text{SO}_4$. The manufacture of CSA cements is more environmentally friendly than that of Portland cements as their production decreases CO_2 footprint by up to 40%. The hydration of ye'elimite leads to hydrated compounds: crystalline ettringite (AFt), crystalline monosulfoaluminate (AFm) and amorphous aluminum hydroxide, $\text{Al}(\text{OH})_3 \cdot n\text{H}_2\text{O}$.

On the other hand, ptychographic X-ray computed tomography (PXCT) is a nondestructive X-ray imaging technique having demonstrated an isotropic 3D resolution better than 20 nm [1]. PXCT provides 3D images of the sample complex-valued X-ray refractive index and it has been recently applied to the hydration of Portland pastes [2, 3].

Here, we present results for the PXCT study of the hydration of ye'elimite. Sample 1 was prepared by hydrating ye'elimite with gypsum and water. Sample 2 was prepared by hydrating ye'elimite with water. The pastes were measured at the cSAXS beamline, at the Swiss Light Source. The main goals were the quantification of the mass densities of the phases, chiefly amorphous $\text{Al}(\text{OH})_3 \cdot n\text{H}_2\text{O}$, and the analysis of the microstructure of the pastes. Figure 1 and 2 display vertical slices of the phase contrast for the two samples. The different phases were identified and their mass densities determined. Bivariate histograms of the refractive index decrement and the absorption index (not shown here) were very helpful for the correct identification of the hydrated phases. Furthermore, the tomograms have been segmented and the volume percentage of each phase determined.

The long-standing problem of the density of amorphous aluminum hydroxide (commonly named as amorphous gibbsite) has been solved. From PXCT and complementary techniques, the water content and mass density of amorphous gibbsite have been determined to be $\text{Al}(\text{OH})_3 \cdot 4\text{H}_2\text{O}$ and 1.46(3) g/cc for sample 1 and $\text{Al}(\text{OH})_3 \cdot 3\text{H}_2\text{O}$ and 1.98(3) g/cc for sample 2, respectively. For the sake of comparison, the mass density of crystalline gibbsite, $\text{Al}(\text{OH})_3$, is 2.40 g/cc. The density values are key to predict the volume stability of the resulting mortars and concretes as well as to estimate the mechanical strength developments.

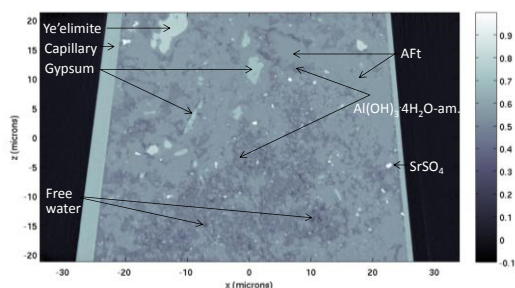


Figure 1: Vertical slice of the phase contrast for sample 1 at 18 days of hydration. The different phases have been labeled. Color scale bar indicates electron density in \AA^{-3} .

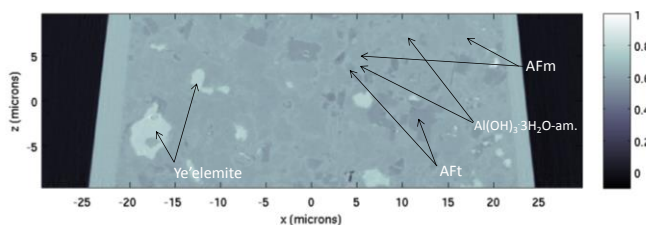


Figure 2: Vertical slice of the phase contrast for sample 2 at 8 days of hydration. The different phases have been labeled. Color scale bar indicates electron density in \AA^{-3} .

References

- [1] M. Holler, A. Diaz, M. Guizar-Sicairos, P. Karvinen, et al., *Sci Rep*, 4, 3857 (2014).
- [2] P. Trtik, A. Diaz, M. Guizar-Sicairos, A. Menzel and O. Bunk, *Cem Concr Res*, 36, 71 (2013).
- [3] J. C. da Silva, P. Trtik, A. Diaz, M. Holler, M. Guizar-Sicairos, et al., *Langmuir*, 31, 3779 (2015).

BRAGG COHERENT X-RAY DIFFRACTIVE IMAGING OF SINGLE NANOWIRES

D. Dzhigaev^{1,2}, A. Shabalin¹, T Stankevič³, U. Lorenz⁴, R. P. Kurta⁵, F Seiboth⁶, J. Wallentin⁷, A. Singer⁸, S. Lazarev¹, O. M. Yefanov⁹, M. Borgstöm¹⁰, M. N. Strikhanov², L. Samuelson¹⁰, G. Falkenberg¹, C. G. Schroer¹, A. Mikkelsen¹⁰, R. Feidenhansl³, I. A. Vartanyants^{1,2}

¹Deutsches Elektronen-Synchrotron DESY, Notkestraße 85, D-22607 Hamburg, Germany

²National Research Nuclear University, "MEPhI", 115409 Moscow, Russia

³Niels Bohr Institute, University of Copenhagen, DK-2100 Copenhagen, Denmark

⁴Institut für Chemie, Universität Potsdam, Karl-Liebknecht-Straße 24-25, D-14476 Potsdam, Germany

⁵European XFEL GmbH, Albert-Einstein-Ring 19, D-22761, Hamburg, Germany

⁶Institute of Structural Physics, Technische Universität Dresden, D-01062 Dresden, Germany

⁷Institute for X-Ray Physics, Friedrich-Hund-Platz 1, 37077 Göttingen, Germany

⁸Department of Physics, University of California, San Diego, La Jolla, CA 92093, USA

⁹Center for Free-Electron Laser Science CFEL, Notkestraße 85, D-22607 Hamburg, Germany

¹⁰Solid State Physics, Lund University, 22100 Lund, Sweden

Abstract

Three-dimensional (3D) Bragg coherent x-ray diffractive imaging (CXDI) with a nanofocused beam was applied to quantitatively map the internal strain field of a single indium phosphide (InP) nanowire [1]. The quantitative values of the strain were obtained by pre-characterization of the beam profile with transmission ptychography on a test sample. Our measurements revealed 3D strain distribution in a region of 150 nm below the catalyst Au particle. We observed a slight gradient of the strain in the range of $\pm 0.6\%$ along the growth direction of the nanowire. We also determined spatial resolution in our measurements to be about 10 nm in the direction perpendicular to the facets of the nanowire. The CXDI measurements were compared with the finite element method simulations and show a good agreement with our results. The proposed approach can become an effective tool for *in operando* studies of the nanowires.

References

[1] D. Dzhigaev et al., J. of Optics (2016) (submitted).

IN OPERANDO SCANNING X-RAY DIFFRACTION MICROSCOPY OF STRAIN AND BENDING IN NANOWIRE DEVICES

J. Wallentin^{1,2*}, M. Osterhoff¹, and T. Salditt¹

¹Institute for X-Ray Physics, University of Göttingen, GERMANY
²Synchrotron Radiation Research, Lund University, SWEDEN

Abstract

We demonstrate how hard X-ray diffraction (XRD) using a nanofocused beam can non-destructively measure both lattice contraction and bending in a single InP nanowire device under electric bias.

Nanowire transistors were fabricated and mounted in a special sample holder which allowed simultaneous X-ray and electrical measurements, and characterized using nanofocused X-rays at the ESRF and PETRA-III synchrotrons. Scanning X-ray Bragg diffraction was performed along the nanowire axis, with 100 nm real-space resolution, also in regions covered by the metal contacts. The 3D shape of the nanowire was reconstructed from the XRD data.

In the as-processed device, we found that the strain was small but that the nanowire was bent in an arch between the contacts. The device was then exposed to increasing bias voltages until breakdown, while simultaneously measuring the current and performing scanning X-ray Bragg diffraction at each bias. We observed small and non-reversible bending at 2V bias. At higher bias voltages the arch gradually disappeared while the lattice constant changed in the contact regions. The structural changes were correlated with a reduction in electrical conductance [1].

Measurements with another nanowire device show that carriers generated by X-ray absorption increased the electrical conductance by five orders of magnitude. By 2D scanning the device at constant electrical bias, and measuring the current at each point, we could create an image of the X-ray nanofocus with submicron resolution [2].

References

- [1] J. Wallentin, M. Osterhoff, and T. Salditt, "In operando X-ray diffraction reveals electrically induced strain and bending in single nanowire device" *Adv. Mater.* 28 (9), 1788 (2016) <http://dx.doi.org/10.1002/adma.201504188>
- [2] J. Wallentin, M. Osterhoff, R. N. Wilke, K.-M. Persson, L.-E. Wernersson, M. Sprung, and T. Salditt, "Hard X-ray detection using a single 100 nm-diameter nanowire" *Nano Lett.* 14 (12), 7071 (2014) <http://dx.doi.org/10.1021/nl5040545>

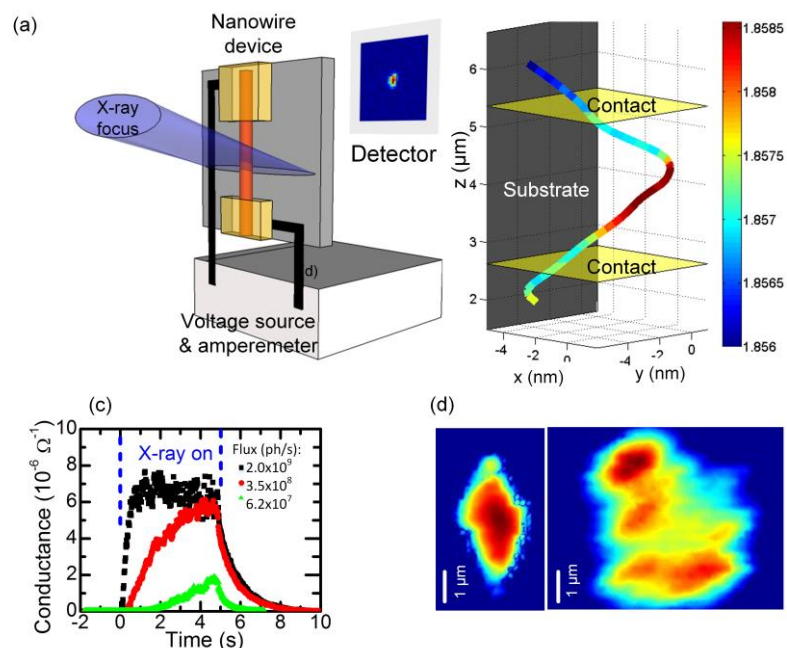


Figure 1: (a) Experimental setup, (b) 3D model of nanowire in the device [1], (c) Conductance of a nanowire device as function of time, for three different X-ray fluxes [2], (d) Imaging of a focused X-ray beam using the nanowire device, at (left) and 24 nm (right) after the nanofocus.

HIGH-RESOLUTION IMAGING OF WEAK-PHASE OBJECTS BY DARK-FIELD X-RAY PTYCHOGRAPHY

Nicolas Burdet¹, Akihiro Suzuki^{1,2}, Kei Shimomura^{1,2}, Makoto Hirose^{1,2}, Yukio Takahashi^{1,2}

1RIKEN SPring-8 Center, 1-1-1 Kouto, Sayo-cho, Sayo, Hyogo, Japan

2Graduate School of Engineering, Osaka University, 2-1 Yamada-oka, Suita, Osaka, Japan

Abstract

Phase shift of light or electrons in objects is now necessary to probe weak-phase objects such as soft biological tissues. Optical microscopy (OM) and transmission electron microscopy (TEM) have been used to observe weak-phase objects such as biological specimens. However, classical OM has low spatial resolution and TEM is limited to thin specimens. While classical X-ray ptychography can accurately retrieve the phase, the large dynamic range of diffraction patterns together with the data missing behind the beamstop still represent a barrier towards further increasing the spatial resolution and sensitivity. Dark-field X-ray ptychography [1], which uses a reference light source to create an inline hologram, has been recently proposed as a means of overcoming these limitations. Figure 1 shows a schematic view of dark-field X-ray ptychography. By combining X-ray ptychography and X-ray in-line holography in an alternating phase retrieval calculation scheme, we were able to observe a test object of 30-nm-thick Ta with a phase sensitivity better than 0.01 rad, a spatial resolution better than 15 nm, and a field of view larger than 5 μm . We have applied this method to the high-resolution observation of both the shape and internal structure of magnetic bacteria MO-1. Figure 2 shows a phase image of MO-1. The ability to observe a thick sample with a high resolution and high sensitivity is expected to have broad applications in not only biology but also materials science.

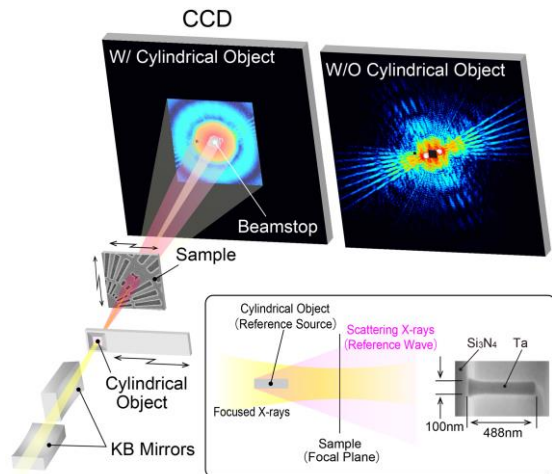


Figure 1: Schematic view of the experimental setup of dark-field X-ray ptychography.

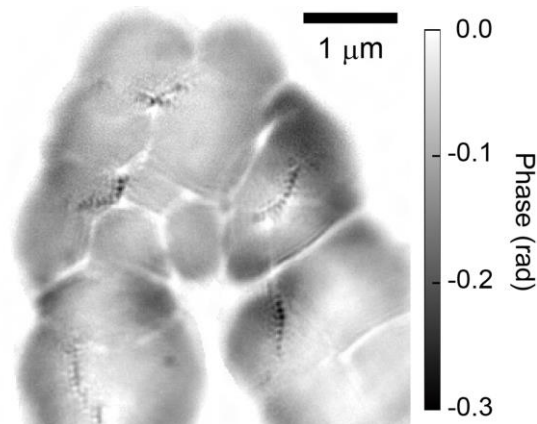


Figure 2: Reconstructed image of the magnetic bacteria MO-1.

Reference

[1] A. Suzuki and Y. Takahashi, *Opt. Express* **23**, 16429-16438 (2015).

X-RAY DIFFRACTION MICROSCOPE ON THE NANODIFFRACTION BEAMLINE ID01/ESRF FOR FAST AND HIGH RESOLUTION STRUCTURAL ANALYSIS

J. Hilhorst¹, G.A. Chahine, T. Zhou, S. J. Leake, P. Boesecke, H. Djazouli, M. Elzo, M-I. Richard, G. Bussone, R. Grifone, T. U.Schüllli

European Synchrotron Radiation Facility, BP 220, F-38043, cedex, Grenoble, France

Abstract

The ID01 beamline at the European Synchrotron Radiation Facility (ESRF) is a long beamline specialized in nano-diffraction imaging using full-field and scanning probe techniques. With the completion of the first phase (2009-2015) of the ESRF upgrade program, the ID01 beamline has successfully returned to user operation, offering full-field x-ray diffraction microscopy using compound refractive lenses[1], scanning diffraction microscopy at 100Hz[2] and coherent beams for coherent diffractive imaging applications [3].

The scanning x-ray diffraction microscope (Fig. 1a) is the most commonly used technique on ID01, which consists of a continuous mapping (K-Map) with a 100nm focused beam on a surface area of up to $200 \times 200 \mu\text{m}^2$. Rocking curves are performed by repeating the scan for slightly different scattering angles, allowing for precise determination of the strain value of down to $\Delta a/a \sim 10^{-5}$.

Using a parallel incident beam, the full field x-ray diffraction microscope (Fig. 1b) offers an intrinsically larger field of view of $100 \times 100 \mu\text{m}^2$. It is theoretically possible to obtain the same level of information as K-map (Fig. 1cd) by performing rocking curves at multiple Bragg peaks, but is rarely practiced. Instead, the instrument usually works at one Bragg angle at a time, thanks to which the imaging speed is increased by a factor of ~ 100 (compared to K-map for the same surface area) while still maintaining a submicron spatial resolution. The latter is achieved by a combination of small detector pixel size ($6.5 \mu\text{m}$, Andor) and long sample detector distance (up to 6.5 m). The instrument is intended for in situ measurements.

Finally, the very long source-sample distance ($\sim 120\text{m}$) produces a highly coherent beam, which is ideal for CDI/ptychography measurements. The resolution in these cases is further increased to sub-beamsize ($\sim 10\text{nm}$), albeit at the cost of a longer data acquisition time and more complex data analysis.

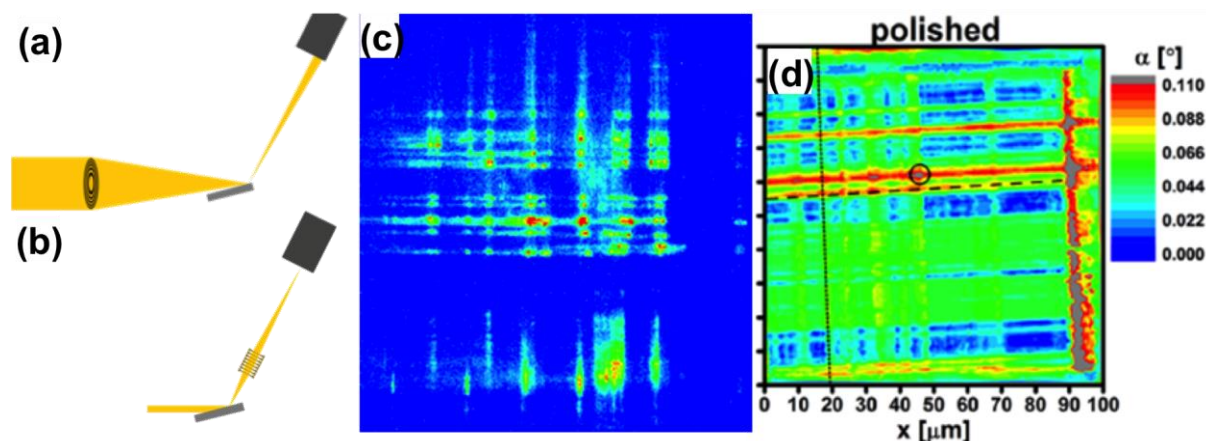


Figure 1: Schematics of (a) the scanning probe and of (b) the full field diffraction microscope at ID01. Comparison between the results of (c) 0.2 sec exposure of dark field image and of (c) K-map.

References

- [1] J. Hilhorst, F. Marschall, T.N. Tran Thi, A. Last and T. U. Schüllli, *J. Appl. Cryst.* 47, 1882-1888. (2014).
- [2] G. A. Chahine, M.H. Zoellner, M-I. Richard, S. Guha, C. Reich, P. Zaumseil, G. Capellini, T. Schroeder and T. U. Schüllli, *Applied Physics Letters*, 106, 071902 (2015)
- [3] S. T. Haag, M-I. Richard, U. Welzel, V. Favre-Nicolin, O. Balmes, G. Richter, E. Mittemeijer and O. Thomas, *Nano Lett.*, 13 (5), 1883-1889 (2013)

3D STUDIES OF MAGNETIC STRIPE DOMAINS IN CoPd MULTILAYER THIN FILMS

S. Flewett¹, L. Nuñez¹, D. Mishra², M. Fohler², C. Günther³, B. Pfau³, S. Eisebitt⁴

1Pontificia Universidad Católica de Valparaíso, Avenida Universidad 330, Valparaíso, Chile

2 Helmholtz Zentrum Berlin, Albert Einstein Strasse 15, 12489 Berlin, Germany

3 Technische Universität Berlin, Strasse des 17 Juni 135, 10623 Berlin, Germany

4 Max-Born-Institut, Max-Born-Str. 2a, 12489 Berlin, Germany

Abstract

The study of perpendicular anisotropy multilayer samples in two dimensions is now a well-established field. Their experimental study in 3D however remains largely unexplored, with only the work of Durr [1] and micromagnetic simulations providing an insight into their predicted structure. New extreme brightness synchrotron sources such as MAX IV and SIRIUS will hopefully however allow tomographic studies of such samples to become a reality.

With existing sources, whilst holographic studies are commonplace when working with perpendicular illumination, the strong absorption prevents such work at the high incidence angles necessary to study the in-plane closure domains which form on the surface between the principal out-of-plane domains. Using partially-coherent but high flux illumination at beamline UE 49 of BESSY II, we performed transmission geometry Resonant Soft X-Ray Scattering (RSXS) measurements on films of different thickness and at different incidence angles, and compared the results with theoretical simulations for diffraction from a disordered stripe domain pattern with triangular closure domains.

Such closure domains are difficult to study, because their diffraction signal is weak compared to the principal domains, even at high incidence angles. However, at a critical incidence angle where the radiation passes on average through exactly two principal domains (the angle depending on the sample geometry), the X-Ray Magnetic Circular Dichroism (XMCD) signal from the principal domains is found to be suppressed, allowing the closure domains to contribute in a relatively greater manner to the total diffraction pattern. In practice, this results in both the 1st and 3rd order diffraction peaks being suppressed at this angle where no closure domains are present, but suppression occurring only in the 1st order peak where closure domains are present.

We found that for the thinner sample with 50 repeats of 5 Angstrom Co and 8 Angstrom Pd layers, closure domains were too small to be detected, with the diffraction behavior found to be comparable to that predicted in the no-closure domain case. However for the thicker sample with 100 repeats of 8 Angstrom Co and 8 Angstrom Pd, the diffraction was consistent with the presence of 40nm triangular in-plane closure domains alongside the observed average 120nm wide out-of-plane domains.

Reference

- [1] H. A. Durr, E. Dudzik, S. S. Dhesi, J. B. Goedkoop, G. van der Laan, M. Belakhovsky, *et al.*, "Chiral magnetic domain structures in ultrathin FePd films," *Science*, vol. 284, pp. 2166-2168, Jun 25 1999.

OPTICAL PTYCHOGRAPHIC MICROSCOPY FOR QUANTITATIVE BIO-MECHANICAL IMAGING

N. Anthony^{1,2}, G. Cadenazzi^{1,2}, K. A. Nugent^{1,2}, B. Abbey^{1,2,3}

1Department of Chemistry and Physics, La Trobe Institute for Molecular Sciences, La Trobe University, Bundoora, VIC 3086, AUSTRALIA

2ARC Centre of Excellence for Advanced Molecular Imaging, Department of Chemistry and Physics, La Trobe Institute for Molecular Sciences, La Trobe University, Bundoora, VIC 3086, AUSTRALIA

3Melbourne Centre for Nanofabrication, Melbourne, 3168, AUSTRALIA

Abstract

Ptychography is a method for quantitatively determining the phase of a samples' complex transmission function. The technique relies upon the collection of multiple overlapping coherent diffraction patterns from laterally displaced points on the sample. The overlap of measurement points provides complementary information that significantly aids in the reconstruction of the complex wavefield exiting the sample. Moreover the method is sufficiently robust to simultaneously recover both the sample and probe functions from a single dataset.

Ptychography was initially realised for applications involving electron microscopy [1] but has been widely adopted by the x-ray lensless imaging community. More recently, it has found application in the optical regime [2] where it can be applied to 2D and 3D quantitative phase contrast imaging of weakly interacting specimens.

Here we describe and demonstrate the realisation of a high-quality optical ptychographic microscope at La Trobe University comprising 'off the shelf' components. Our microscope provides the ability to probe anisotropic samples, including biomechanics of cellular samples, with polarized light resolving the optical birefringence properties. Some recent results using this microscope are showcased here.

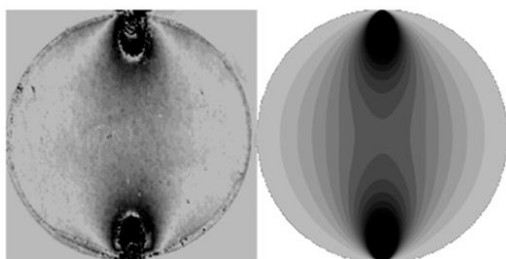


Figure 1: Reconstructed profile of a circular disk under compression for experimental (left) and theoretical (right) stress along the x-direction

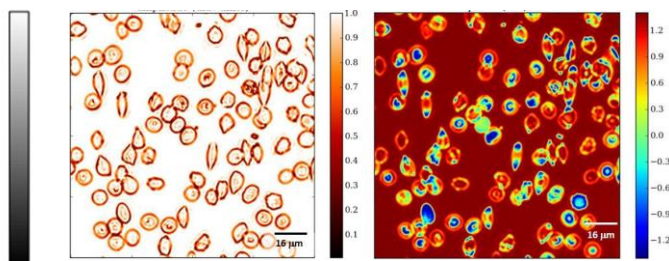


Figure 2: Reconstructed amplitude (left) and phase (right) of malaria infected red blood cells.

References

- [1] Hoppe et al., Acta Cryst. A, 1969
- [2] Godden et al. Optics Express, 2014

HIGH RESOLUTION PTYCHOGRAPHY IMAGING OF HIPPOCAMPAL NEURONS AT 42 eV USING A COHERENT LABORATORY SOURCE

M. Odstrcil¹, P. Baksh¹, J. Bailey², K. Deinhardt², J.E. Chad², J.G. Frey³, W.S. Brocklesby¹

¹Optoelectronics Research Centre, University of Southampton, SO17 1BJ, UK

²Biological Sciences, Faculty of Natural and Environmental Sciences, University of Southampton, UK

³Chemistry, Faculty of Natural and Environmental Sciences, University of Southampton, UK

Abstract

We are developing a high resolution biological imaging technology using ptychography at 42eV. Ptychography allows label-free imaging of neuronal cell structure. We intend to exploit this system to image neuronal morphological changes during their development and degeneration. Morphological analysis of fine neuronal structures, such as synapses, during degenerative conditions, eg. Alzheimer's Disease, will allow greater understanding of disease progression and the molecular mechanisms which control it.

To achieve this, hippocampal neurons from E17 mouse embryos were cultured for 10 days on poly-D-lysine coated 50nm SiN substrates before fixation.

Partially coherent extreme ultraviolet (EUV) radiation was generated from a tabletop laser-based high harmonic generation (HHG) source. EUV light was partially spectrally filtered and focused onto the sample using a single multilayer mirror. Scattered radiation was collected in the far-field regime using an EUV-sensitive CCD camera. Around 400 diffraction patterns from partly-overlapping regions were collected, with an effective dynamic range of up to 17 bits. Ptychographic reconstruction of the complex transmission function of the sample was performed by the ePIE algorithm [1] with additional corrections for partially coherent light [2] and a novel method for variable wavefront correction, needed due to limited pointing stability of the HHG source [3]. Our EUV images provide ~50nm resolution for highly-transmissive regions of the samples, and significantly higher contrast in both phase and amplitude compared to SXR/HXR sources, in combination with lower radiation damage.

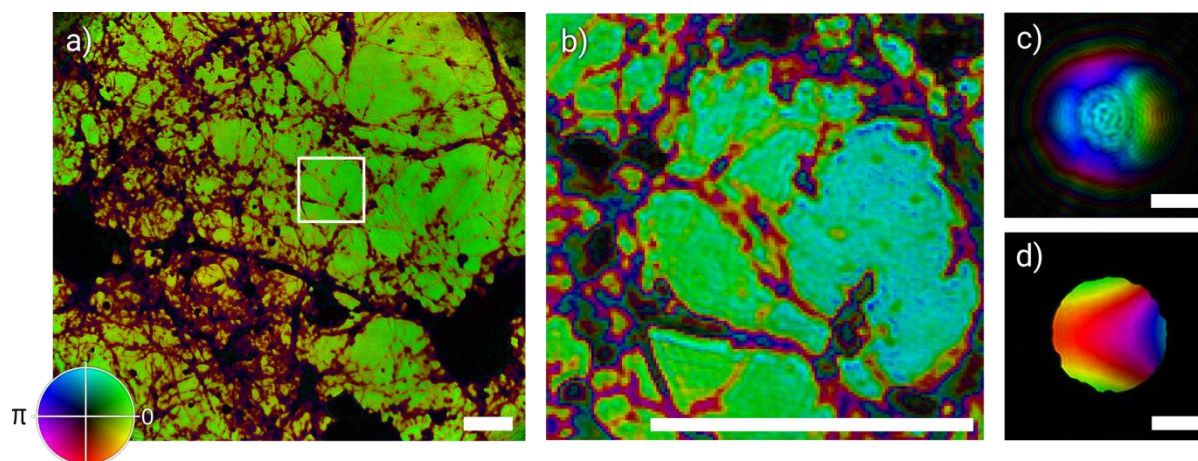


Figure 1: Image (a) shows complex representation of mouse hippocampal neurons. Image (b) is a contrast enhanced magnification of the region marked in (a) showing details of the reconstructed neurites. Image (c) presents the reconstructed illumination probe and (d) shows illumination back-propagated 97 μ m to the pinhole position. Scale bars are 5 μ m.

References

- [1] A. M. Maiden and J. M. Rodenburg, *Ultramicroscopy* 109.10 (2009): 1256-1262.
- [2] P. Baksh, et al., *Opt. Lett.* 41, 1317-1320 (2016)
- [3] M. Odstrcil, P. Baksh, S.A. Boden, R. Card, J.E.Chad, J.G. Frey, and W.S. Brocklesby, (accepted to *Optics Express*)

QUANTITATIVE EVALUATION OF HARD X-RAY DAMAGE TO BIOLOGICAL SAMPLES USING EUV PTYCHOGRAPHY

P. Baksh¹, M. Odstrcil¹, A. Parsons⁴, J. Bailey², K. Deinhardt², J.E. Chad², W.S. Brocklesby¹, J.G. Frey³

¹Optoelectronics Research Centre, University of Southampton, SO17 1BJ, UK

²Biological Sciences, Faculty of Natural and Environmental Sciences, University of Southampton

³Chemistry, Faculty of Natural and Environmental Sciences, University of Southampton

⁴Diamond Light Source, Didcot, OX11 0DE

Abstract

Neuronal cells use calcium and iron ions for intracellular signalling and metabolism. Ca^{++} is a known intracellular signal and in neurons, different Ca^{++} domains (both micro and nano) control different functional aspects of neuronal cell activity and activation of different signalling pathways. Iron is an essential enzymatic co-factor for many redox reactions in neuronal cells. Mitochondria can accumulate iron, utilising it in oxidative phosphorylation. The ability to localise these elements to high resolution (<100nm) in neurons during development and degeneration would provide insight into how cell function and signalling may be altered during these processes.

The high yield offered by K-edge emissions, along with the potential for quantitative XANES, makes hard X-ray (HXR) fluorescence imaging an attractive imaging modality for such samples. Whilst it is known that the resolution of X-ray imaging is limited by the absorbed dose [1], the damage processes for thin samples such as neuronal cultures are not well studied.

We show the results from a multimodal (XRF and ptychography) hard X-ray (7.3keV) imaging experiment for a range of X-rays doses. A correlative ptychograph was then taken using a lab-based source of EUV (42 eV)[2] and the HXR damage to the sample was evaluated. Blurring of the higher resolution detail due to HXR exposure is seen and quantitatively analysed as a function of exposure time, demonstrating a novel way of investigating damage of radiation sensitive samples and providing scope for future correlative experiments.

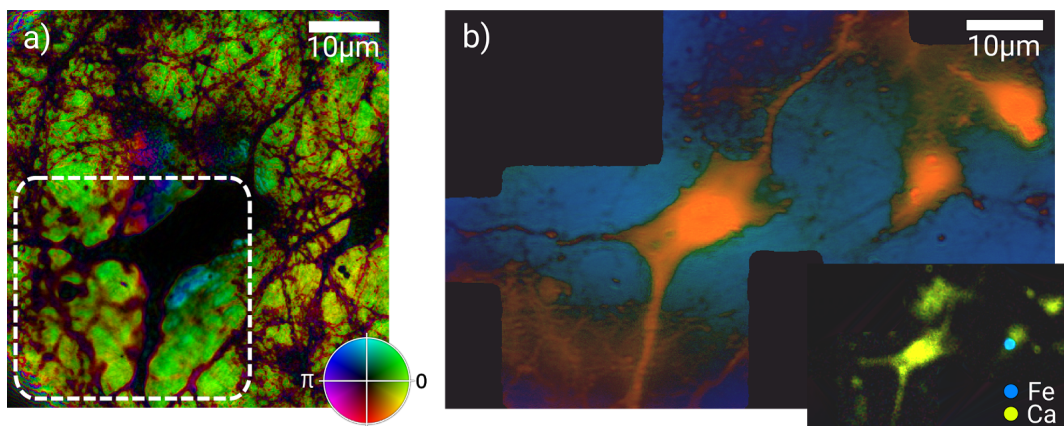


Figure 1: a) EUV ptychograph of an high HXR dose exposed area of the sample. The area inside the white box was exposed for 10s per scan point during HXR imaging, and shows significant loss of smaller features b) Contrast enhanced HXR ptychography (main) and fluorescence (inset) images showing localised Fe and global Ca distributions.

References

[1]Howells, Malcolm et al. J Electron Spectros Relat Phenomena. 2009 Mar 1;170(1-3):4-12.

[2]Baksh, Peter, et al. Opt. Lett. **41**, 1317-1320 (2016)

WATER WINDOW PTYCHOGRAPHIC IMAGING

M. Rose¹, D. Dzhigaev^{1,3}, I. Besedin¹, P. Skopintsev¹, T. Senkbeil², A. von Gundlach², S. Stuhr², C. Rumancev², J. Viefhaus¹, A. Rosenhahn² and I. Vartanyants^{1,3}

¹Deutsches Elektronen-Synchrotron DESY, Hamburg 22607, Germany

²Analytical Chemistry - Biointerfaces, Ruhr-University Bochum, Bochum 44780, Germany

³MEPhI (Moscow Engineering Physics Institute), Moscow 115409, Russia

Abstract

Due to low efficiency and aberrations of X-ray imaging lenses, the field of coherent X-ray diffractive imaging (CXDI) has gained much attention being a candidate for atomic resolution microscopy [1]. X-ray ptychography is the scanning extension of CXDI to obtain tens of micro meter field of view reconstructions of micro- and mesoscale objects with nano meter resolution [2, 3]. The soft X-ray range of the water window (284 eV to 532 eV) offers unique imaging opportunities. Here a maximum of contrast between biological and its aqueous components can be obtained without any additional contrast enhancing sample preparation. Thus a cell stays in its most natural state promising insight into its undisturbed nano-structure [4].

Previously we have published water window ptychographic reconstructions of fossil silicon dioxide skeleton structures [5] and obtained chemical element specific contrast to highlight the unique imaging opportunities in the water window [6]. Together with our experiments we routinely measure coherence with a newly developed X-ray diffraction technique based on non-redundant arrays of apertures [5, 7].

Recently we have collected a high resolution soft X-ray ptychographic diffraction data set of a dried and unstained fibroblast cell. By using a beam stop and two exposures we have effectively extended the dynamical range of the collected diffraction data which gives access to water window imaging of biological objects. Our strategy is applicable for radiation damage limited resolution around 10 nm of hydrated biological specimen. Here we present new results on a large field of view ($25 \times 25 \mu\text{m}^2$) a high resolution (50 nm) X-ray imaging experiment of a fibroblast cell.

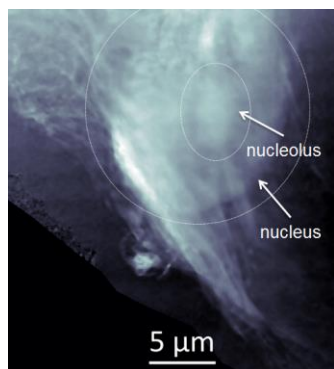


Figure 1: Fibroblast cell ptychographic reconstruction.

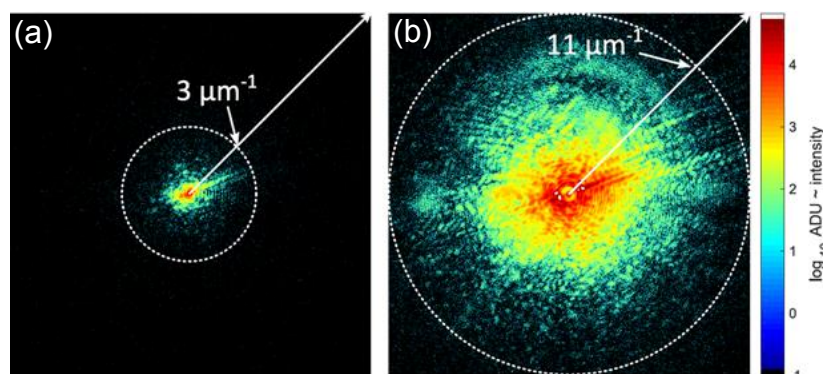


Figure 2: (a) Low dynamic range and (b) extended dynamic range diffraction pattern with central beam stop.

References

- [1] I. A. Vartanyants & O. M. Yefanov, X-ray Diffraction: Modern Experimental Techniques p269, Pan Stanford Publishing (2014)
- [2] J. M. Rodenburg et al., Phys. Rev. Lett. 98, 034801 (2007)
- [3] P. Thibault, M. Guizar-Sicairos, A. Menzel, Journal of Synchrotron Radiation 21, 1011 (2014)
- [4] C. A. Larabell, K. A. Nugent, Curr. Op. Struct. Biology 20, 623 (2010)
- [5] M. Rose et al., Journal of Synchrotron Radiation 22, 819 (2015)
- [6] M. Beckers et al., Phys. Rev. Lett. 107, 208101 (2011)
- [7] P. Skoptinsev et al., Journal of Synchrotron Radiation 21, 722 (2014)

QUANTITATIVE IMAGING OF SINGLE UNSTAINED BACTERIA BY COHERENT X-RAY DIFFRACTION MICROSCOPY

Jiadong Fan¹, Zhibin Sun¹, Shengkun Yao¹, Huaidong Jiang^{1,2}

*1*State Key Laboratory of Crystal Materials, Shandong University, Jinan, Shandong 250100, China
2 iHuman Institute, ShanghaiTech University, Shanghai 201210, China

Abstract

Coherent diffraction microscopy provides a path to high-resolution structural determination of specimens to obtain a better understanding of the microorganism at nanoscale [1]. Because of weak diffraction capability of unstained biological materials, it is usually difficult to obtain experimentally high quality diffraction patterns from bacteria. Here we demonstrated quantitative imaging of intact unstained magnetotactic bacteria using coherent x-ray diffraction microscopy [2]. Although the signal-to-noise ratio of the X-ray diffraction pattern from single magnetotactic bacterium is weak, an 18.6 nm half-period resolution of reconstructed image was achieved by using a hybrid input-output phase retrieval algorithm. Based on the quantitative reconstructed images, the morphology and some intracellular structures, such as nucleoid, granules, and magnetosomes were identified, which were also confirmed by scanning electron microscopy and energy dispersive spectroscopy. Benefit from the quantifiability of coherent diffraction imaging, an average density of magnetotactic bacteria was calculated. This technique has a wide range of applications, especially in imaging of low-scattering biomaterials and multicomponent materials at nanoscale resolution. Combined with cryogenic technique or x-ray free electron lasers, this technique could quantitatively image cells with a higher spacial resolution.

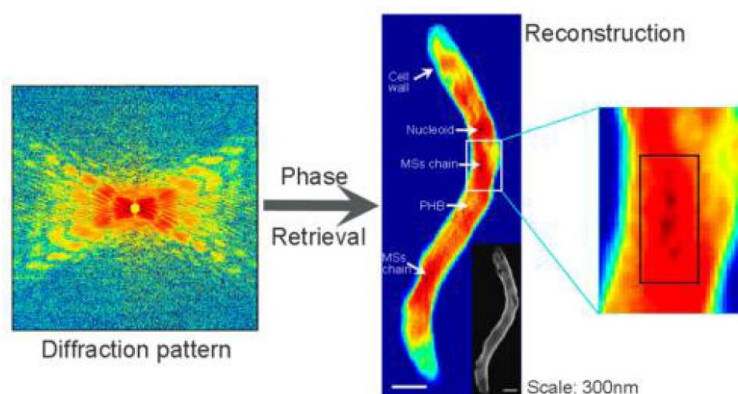


Figure 1: High-resolution image of a single bacterium reconstructed from a coherent diffraction pattern.

References

- [1] J. Miao, P. Charalambous, J. Kirz, D Sayre, *Nature* 400, 342 (1999).
- [2] J. D. Fan et al., *Anal. Chem.* 87, 5849 (2015).

Efficient use of coherent X-rays in ptychography: Towards high-resolution and high-throughput observation of weak-phase objects

K. Shimomura^{1,2}, N. Burdet², M. Hirose^{1,2}, A. Suzuki^{1,2}, Y. Takahashi^{1,2}

¹Graduate School of Engineering, Osaka University, 2-1 Yamada-oka, Suita, Osaka, Japan

²RIKEN SPring-8 Center, 1-1-1 Kouto, Sayo-cho, Sayo, Hyogo, Japan

Abstract

Coherent diffraction imaging is a lensless imaging technique based on the iterative phasing method. Ptychography [1] is a method of coherent diffraction imaging that applies translational diversity, in which the object of interest is scanned in small steps by an overlapping probe, providing redundancy in collected data. The multiplicity in diffraction data provides robustness and accelerates the convergence of the iterative algorithm. X-ray ptychography techniques rely on the realization of a fully coherent beam with high spectral purity. The efficient use of coherent X-rays is a crucial issue for the employment of X-ray techniques in synchrotron experiments. Recently, the mixed-state reconstruction algorithm [2] has been developed, in which blurry diffraction data are described as the sum of the diffraction intensities over multiple mutually incoherent illumination modes. Here we propose a means of efficiently using coherent X-rays in ptychography using the mixed-state reconstruction algorithm [3].

Our numerical simulation showed that a nearly diffraction-limited focusing X-ray beam can be described as an incoherent sum of a few orthogonal modes and that the first-mode flux significantly increases by relaxing the requirement on the degree of coherence. We performed its demonstration experiment at SPring-8. The degree of coherence was controlled by the cross slits positioned ~50 m upstream of the sample. An increase in the first-mode dose improved the spatial resolution of the reconstructed image of a test object as shown in Fig. 1. The present approach enables the high-resolution and high-throughput observation of weak-phase objects in materials science and biology.

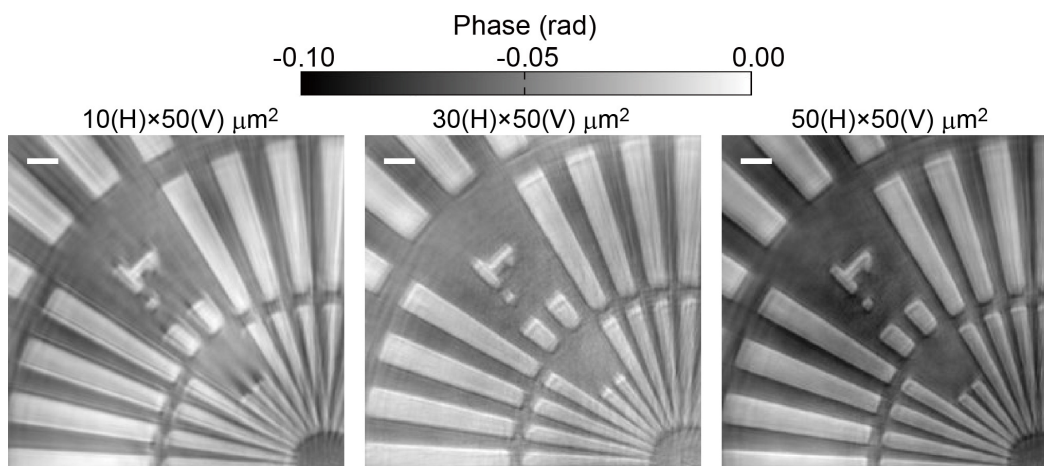


Figure 1: Phase images for the three slit openings reconstructed using the mixed-state reconstruction algorithm. The scale bar is 200 nm.

References

- [1] J. M. Rodenburg, A. C. Hurst, A. G. Cullis, B. R. Dobson, F. Pfeiffer, O. Bunk, C. David, K. Jefimovs, I. Johnson, *Phys. Rev. Lett.* 98, 034801 (2007)
- [2] P. Thibault and A. Menzel, *Nature* 494, 68 (2013)
- [3] N. Burdet, K. Shimomura, M. Hirose, A. Suzuki, and Y. Takahashi, *Appl. Phys. Lett.*, 198, 071103 (2016)

ULTRAFAST X-RAY IMAGING OF RADIATION DAMAGE IN A NANOPLASMA AT THE FLASH FREE-ELECTRON LASER

L. Flückiger^{1,2}, D. Rupp², M. Adolph², T. Gorkhover^{2,3}, M. Krikunova², M. Müller², T. Oelze², Y. Ovcharenko^{2,4}, M. Sauppe², S. Schorb³, C. Bostedt^{3,5}, S. Düsterer⁶, M. Harmand^{6,7}, H. Redlin⁶, R. Treusch⁶, and T. Möller²

¹ARC Centre of Excellence in Advanced Molecular Imaging, Department of Chemistry and Physics, La Trobe University, Melbourne, VIC 3086, Australia

²Institut für Optik und Atomare Physik, Technische Universität Berlin, Hardenbergstrasse 36, 10623 Berlin, Germany

³SLAC National Accelerator Laboratory, 2575 Sand Hill Road, Menlo Park, CA94025, USA

⁴European XFEL GmbH, Notkestraße 85, 22607 Hamburg, Germany

⁵Argonne National Laboratory, 9700 S. Cass Avenue, Argonne, IL 60439, USA

⁶Deutsches Elektronen-Synchrotron DESY, Notkestraße 85, 22607 Hamburg, Germany

⁷Institute of Mineralogy, Materials Physics and Cosmochemistry, 4 Place Jussieu, F-75252 Paris, France

Free-electron lasers (FELs) have triggered a wide range of experiments, especially for studying the geometry of nanoparticles with coherent diffractive imaging technique [1,2]. The femtosecond short pulses facilitate to track ultrafast light-induced transient states and conformational changes. We explored the evolution of individual, large gas-phase xenon clusters, turned into a nanoplasma by a high power infrared (IR) laser pulse [3]. Snapshots of the cluster disintegration were recorded at extreme time regimes from several pico- up to 1.5 ns, using extreme ultraviolet (XUV) pulses at FLASH. We identified two different kinds of scattering images on different time scales (see figure 1): fringe and speckle patterns. The former reveals a softening of the cluster surface due to ion emission from a highly excited nanoplasma. The later mirrors a new stage of cluster expansion where the particle core is recombined to full neutrality and disintegrates with pronounced density fluctuations.

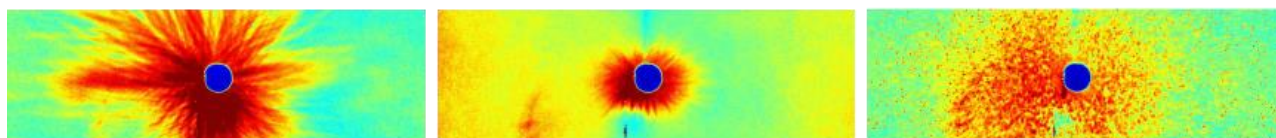


Figure 1: Scattering patterns of xenon clusters recorded with an XUV probe pulse at varying time delays after IR pump pulse impact. Snapshots taken between pico- and nanoseconds reveal different states of radiation damage and nanoplasma evolution.

References

- [1] D. Rupp, M. Adolph, L. Flückiger, T. Gorkhover, J.P. Müller, M. Müller, M. Sauppe, D. Wolter, S. Schorb, R. Treusch, C. Bostedt, and T. Möller, *J. Chem. Phys.*, 141, 044306 (2014).
- [2] I. Barke, H. Hartmann, D. Rupp, L. Flückiger, M. Sauppe, M. Adolph, S. Schorb, C. Bostedt, R. Treusch, C. Peltz, S. Bartling, T. Fennel, K.-H. Meiwes-Broer, and T. Möller, *Nat. Commun.*, 6:6187 (2015).
- [3] L. Flückiger, D. Rupp, M. Adolph, T. Gorkhover, M. Krikunova, M. Müller, M. Sauppe, T. Oelze, Y. Ovcharenko, M. Sauppe, S. Schorb, C. Bostedt, S. Düsterer, M. Harmand, H. Redlin, R. Treusch, and T. Möller, *New Journal of Physics*, in press (2016).

FLAT BEAM BASED X-RAY DIFFRACTION MICRO-CT FOR GRAIN ANALYSIS IN POLYCRYSTALLINE MATERIALS

Yiming Yang^{1,2}, Liang Xu^{1,2}, Yushuang Yang³, Tiqiao Xiao^{1,2,*}

¹Shanghai Institute of Applied Physics, Chinese Academy of Sciences, Shanghai 201800, China

²University of Chinese Academy of Sciences, Beijing 100049, China

³Commonwealth Scientific and Industrial Research Organization, Melbourne VIC 3168, Australia

Abstract

Grain information in polycrystalline materials, including morphology, distribution and orientation, is important to the material properties and X-ray diffraction microscopy[1] could be a practical tool to collect all these information at the same time. As shown in figure 1, an experimental system for X-ray diffraction micro-CT was built at SSRF BL13W beamline, in which flat beam is used to improve the data collection efficiency and meanwhile maintain high enough resolution for crystal grain. A new method for data processing and image reconstruction is developed to identify unknown phases in alloy, based on a figure-of-merit function.

Sphericity of grains in metallic materials is usually an important parameter to evaluate the properties of materials, which can be acquired by full volumetric reconstruction, as shown in figure 2. Second phase in metals, alloys or metal matrix composites play an important role in their mechanical and physical performances[2]. Identification, separation and analysis of extreme fine precipitated phases in alloy is usually not easy. Experiments on 6061 aluminum alloy with unknown phase were carried out to evaluate the developed system. As shown in fig.3(a), (b), a Fe-rich second phase is revealed in the slice of X-ray diffraction micro-CT. From fig.3(c), the absorption CT slice shows also the existence of second phase which has obviously different density to aluminum. SEM image and energy spectrum analysis (EDS) confirmed that the second phase is a Fe-rich phase of the alloy. In addition, the Al₂CuMg phase was also identified by this method in another experiment on sample of 2xxx aluminum alloy. The spatial resolution of about 5 μ m can be achieved, which is practical for the study of high temperature alloy with micron-scale grains.

In conclusion, the developed X-ray diffraction micro-CT system is a practical tool for unknown phase identification in polycrystalline alloys with micron-scale crystal grains.

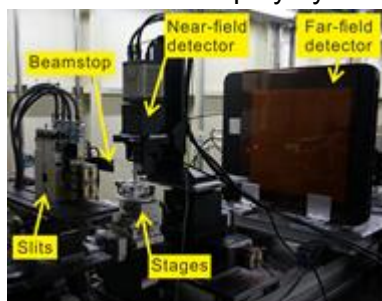


Figure 1: Setup of X-ray diffraction micro-CT. The sample is mounted on the stages and rotated in full 360° with a step of 0.5° during each exposure. The near- and far-field detector are used alternatively to collect the diffraction data.

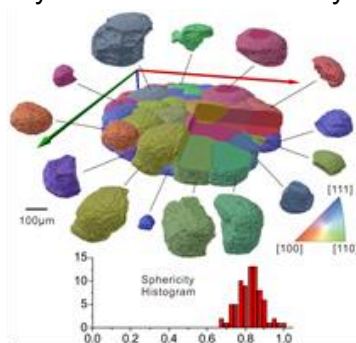


Figure 2: Volumetric reconstruction and sphericity histogram of grains. The different colors here represent different orientations.

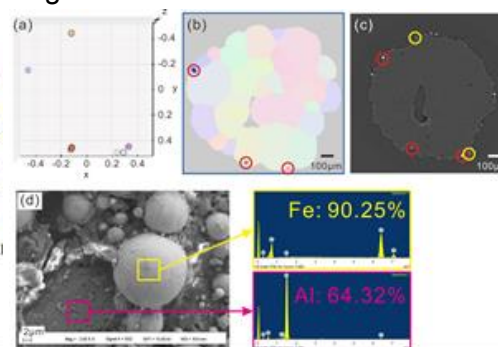


Figure 3: Identification and validation of Fe-rich phase within an Al alloy sample. (a) center-of-mass position of identified Fe-rich particles from the far-field data; (b) volumetric reconstruction of Fe-rich phase superposed on that of Al phase; (c) absorption CT slice of the same layer as (b), where the red and yellow circles represent the identified Fe-rich particles; (d) SEM and EDS of an Fe-rich particle.

References

- [1] H. F. Poulsen, "An introduction to three-dimensional X-ray diffraction microscopy," *Journal of Applied Crystallography*, vol. 45, pp. 1084-1097, Dec 2012.
- [2] G. Requena and H. P. Degischer, "Three-Dimensional Architecture of Engineering Multiphase Metals," *Annual Review of Materials Research*, vol. 42, pp. 145-161, 2012.

COHERENT DIFFRACTIVE IMAGING FOR SOLUTION SAMPLES BY FEMTOSECOND X-RAY LASER

Takashi Kimura¹, Yasumasa Joti², Yasutaka Bessho³, and Yoshinori Nishino¹

¹ Research Institute for Electronic Science, Hokkaido University,
Kita 21 Nishi 10, Kita-ku, Sapporo 001-0021, Japan

² Japan Synchrotron Radiation Research Institute (JASRI)/SPring-8,
1-1-1 Kouto, Sayo-cho, Sayo-gun, Hyogo 679-5198, Japan

³ Institute of Biological Chemistry, Academia Sinica,
128, Academia Road Sec. 2, Nankang, Taipei 115, Taiwan

Abstract

X-ray free-electron lasers (XFELs) with angstrom wavelength and femtosecond pulse duration enable us to reveal high-resolution sample structure before the onset of radiation damage [1,2]. Radiation-damage-free measurement by XFELs is especially effective for biological samples and fragile nanoparticles in solution, which suffer from serious damage from high-energy radiation, such as electron and X-ray beams.

In the measurement of solution samples, it is important to control surrounding environment to maintain their structure and morphology. In this presentation, we describe XFEL diffraction imaging of solution samples in environment close to their natural state by pulsed coherent X-ray solution scattering (PCXSS) we developed [3]. In the method, we use a carefully-designed solution sample holder named micro-liquid enclosure array (MLEA). We performed PCXSS experiments at SPring-8 angstrom compact free-electron laser (SACLA) using the MLEA chips. Each liquid enclosure of the MLEA chip was exposed to a single 4-keV XFEL pulse and diffraction patterns were recorded with the multi-port charge-coupled device (MPCCD) detector. From the recorded diffraction patterns, we successfully retrieved images of living bacteria and self-assembled nanoparticles [4,5] in solution at nanometer resolution. Figure 1 and 2 show a single-shot coherent diffraction pattern of self-assembled gold nanoparticles and its reconstruction image with a spatial resolution of 13 nm.

The images obtained by PCXSS will help us understand the complex dynamics of fragile samples in solution, such as biological activities of nanometer-scale organelles and self-assemble processes of nanoparticles.

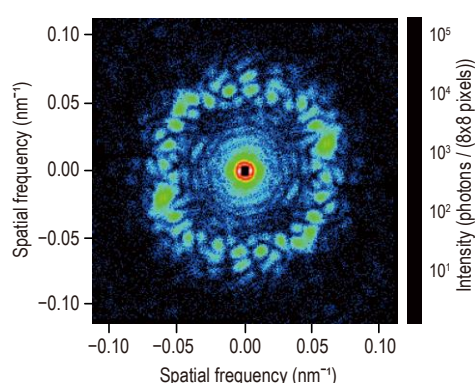


Figure 1: Single-shot coherent diffraction pattern of a self-assembled gold nanoparticles in solution.

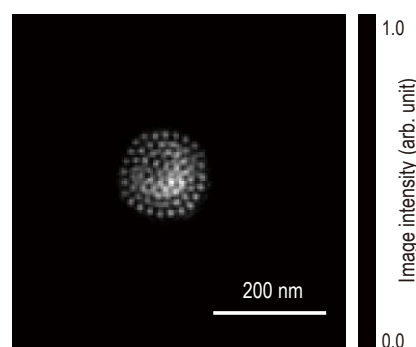


Figure 2: Reconstructed image of a self-assembly of 15-nm gold nanoparticles in solution.

References

- [1] R. Neutze *et al.*, Nature 406, 752 (2000).
- [2] H. N. Chapman *et al.*, Nature Phys. 2, 839 (2006).
- [3] T. Kimura *et al.*, Nature Commun. 5, 3052 (2014).
- [4] R. Iida *et al.*, Langmuir 31, 4054 (2015).
- [5] J. Wei *et al.*, J. Am. Chem. Soc. 138, 3274 (2016).

IMAGING ANTI-FERROMAGNETIC A-TYPE DOMAINS IN STRONGLY CORRELATED LASR2MN2O7

M.García-Fernández^{1,2}, S.B. Wilkins², Ming Lu³, Quing'an Li⁴, K.E. Gray⁴, H. Zheng⁴, J.F. Mitchell⁴, and Daniel Khomskii⁵.

¹Condensed Matter Physics and Materials Science Department, Brookhaven National Laboratory, Upton, New York 11973, USA,

²Diamond Light Source Ltd, Harwell Science and Innovation Campus, Didcot OX110DE, UK,

³Center for Functional Nanomaterials, Brookhaven National Laboratory, Upton, New York 11973, USA

⁴Materials Sciences Division, Argonne National Laboratory, Argonne, Illinois 60439, USA

⁵Physikalisches Institut, Universität zu Köln, Zùlpicher Str. 77, D-50937 Köln, Germany

Abstract

We report a soft x-ray nanodiffraction study of antiferromagnetic domains in the strongly correlated bilayer manganite $\text{La}_{0.96}\text{Sr}_{2.04}\text{Mn}_2\text{O}_7$. We find that the antiferromagnetic domains form a unique domain pattern with each domain having an intrinsic memory of its spin direction. This can be explained by the presence of crystallographic or magnetic imperfections locked in during the crystal growth process which pin the antiferromagnetic domains. The antiferromagnetic domain pattern shows two distinct types of domains. One of the domain types was observed to contain a periodic ripple in the manganese spin direction with a period of approximately $4 \mu\text{m}$.

Strongly correlated electron systems display a wide range of potentially useful properties. In these systems the correlation of electrons results in very rich phase diagrams with different and interesting ground states. As a consequence of the competition between different phases, very interesting properties like superconductivity and colossal magnetoresistance can occur. This competition between phases leads to electronic domains and inhomogeneities over a range of real-space length scales, from nanometers to hundreds of microns. Understanding the role that these domains play in defining the properties of strongly correlated electron systems appears as a mandatory requirement in order to achieve a full understanding of these systems. Among one of the most challenging properties to be studied in these materials is the antiferromagnetic order, one of the most ubiquitous ground states. The absence of any net magnetic moment from antiferromagnetic domains prohibits the use of most magnetic imaging techniques. Here we present results from a new imaging technique, soft x-ray resonant nano-diffraction. Reciprocal-space resolved soft x-ray diffraction, sensitive to long range electronic ordering, with a nano sized x-ray probe, focused by a Fresnel zone plate is used to study A-type antiferromagnetic (AFM) domains in $\text{La}_{0.96}\text{Sr}_{2.04}\text{Mn}_2\text{O}_7$.

The existence of two different A-type AFM regions in the sample is demonstrated. These regions have the same magnetic \mathbf{Q} -vector, but differing orientations of the ordered moment, at 90 degrees to one another. The two regions have an unequal population, and when studied in retail, they are found not to be symmetry related. Further, we found that one of the regions exhibits a type of fine structure that is absent in the other region. A possible explanation for this "ripple" state will be presented based on a Dzyaloshinskii-Moriya type interaction due to the loss of inversion symmetry within each bilayer. By temperature cycling we observe that both, the domain pattern and spin directions, are quenched and the material exhibits a kind of 'memory'.

Acknowledgements

This research was funded by the Department of Energy, Office of Basic Energy Sciences, under Contract No. DE-AC02-98CH10886 at Brookhaven National Laboratory and DE-AC02-06CH11357 at Argonne National Laboratory.

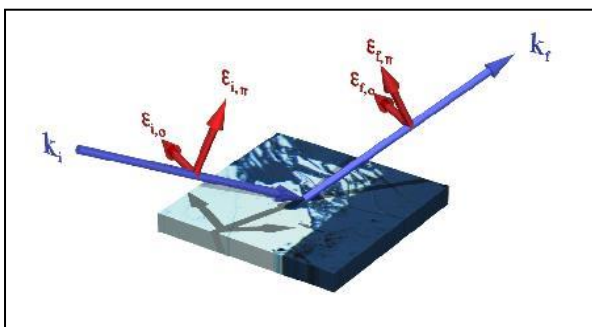


Figure 1: Sketch of experimental setup.

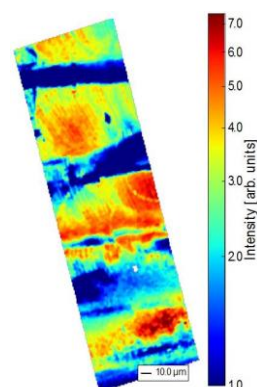
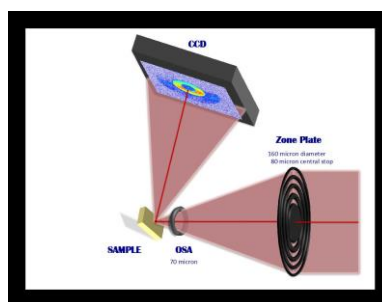


Figure 2: Map of the antiferromagnetic (001) reflection with a beam size of less than 300 nm and a step size of $2 \mu\text{m}$ for the azimuthal angle $\psi = 20^\circ$.

References

- [1] Mirian Garcia-Fernandez et al., *Phys. Rev. B: Condens. Matter*, **88**(7), 075134 (2013).

USING AN OPAQUE BEAMSTOP FOR LOW-BACKGROUND HARD X-RAY PTYCHOGRAPHY TO IMAGE WEAK OBJECTS

J. Reinhardt¹, R. Hoppe², C. G. Schroer¹

¹Deutsches Elektronen-Synchrotron (DESY), D-22607 Hamburg, Germany

²Institute of Structural Physics, TU Dresden, D-01062 Dresden, Germany

Abstract

Ptychography – a scanning coherent imaging technique – provides high spatial resolution and also element sensitivity [1]. The resolution and sensitivity of this technique are limited by the sample's scattering signal that is detected over noise and over background scattering in high angles in the diffraction patterns. Whereas spatial resolution of less than 10 nm has been reported for strongly scattering samples also in the hard X-ray regime [2], imaging of weak objects is still challenging. For instance, catalytic nanoparticles in the range of 10 nm and smaller scatter 3 to 5 orders of magnitude less than the smallest features of a typical testpattern, cf. Fig. 1.

In order to yield more signal for weak objects the fluence on the sample could be increased by orders of magnitude for enhanced statistics and a clearer signal over noise. Usually, this is done by longer exposure or lowered requirements on coherence, that might lead to diminished reconstruction quality due to instabilities etc. Moreover, background scattering from air molecules, other components such as windows or the detector material itself will increase concomitantly, especially if a flight tube is not available. An alternative option is to suppress background scattering by implementing an opaque beamstop blocking the central beam downstream of the sample. In this way, the strongest source of parasitic scattering – the incoherent interaction of the intense central beam with matter – is eliminated. Consequently, the background is considerably reduced and the weak sample signal emerges clearly up to high angles in the diffraction patterns.

Here, we present a dual-exposure scheme in the hard X-ray regime together with simultaneous ptychographic reconstruction of two datasets with and without an opaque beamstop. Our approach successfully results in a quantitative image of a weakly scattering sample with high resolution and so far unprecedented sensitivity to less than 10^5 atoms[3].

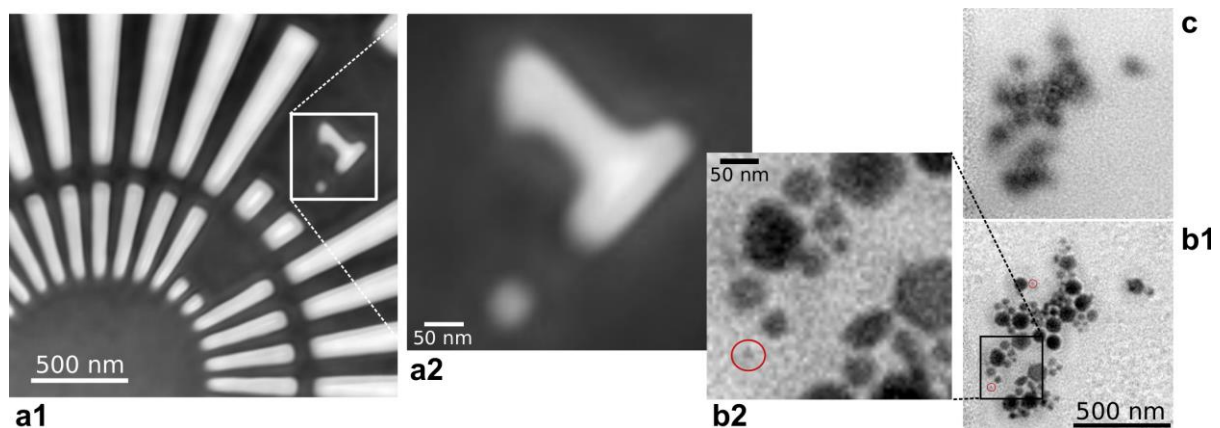


Figure 1: a1) shows a phase reconstruction of a testpattern (NTT-AT) with the smallest feature enlarged in a2). In comparison, b1) shows a phase reconstruction of nanoparticles with the red circles depicting particles as small as 15 nm in diameter, which are enlarged in b2). The 15 nm sphere in b2) scatters 4000 times less than the dot in a2). c) shows the phase reconstruction in conventional ptychography mode without a beamstop dominated by noise and without detailed features.

References

- [1] R. Hoppe, J. Reinhardt et al., *Appl. Phys. Lett.* 100 (25), (2012).
- [2] A. Schropp et al., *Applied Physics Letters* 100 (25), (2012).
- [3] J. Reinhardt et al., (submitted, 2016)

X-RAY GRATING-BASED PHASE TOMOGRAPHY USING ANGULAR SIGNAL RADIOGRAPHY WITHOUT MECHANICAL PHASE STEPPING

Chenxi Wei, Yuan Bao, Faiz Wali, Yangchao Tian

National Synchrotron Radiation Laboratory, University of Science and Technology of China, Hefei, Anhui, People's Republic of China

Abstract

The x-ray grating interferometer, which is sensitive to the deviation angle of the incoming x-rays, has attracted significant attention in the past years due to its capability in achieving x-ray phase contrast imaging with low brilliance source. However, the conventional information extraction method (phase stepping technology) prolongs the time needed for data acquisition by several times compared with conventional x-ray absorption image acquisitions.

An improved information extraction method was developed by combining the stair grating [1] and angular signal radiography [2]. The stair grating was fabricated such that the linear grating structures were shifted from one detector row to the next, and the amount of the lateral shift was equal to a fraction of the period of the self-imaging of the phase grating (G1). Meanwhile, the angular signal radiography has the advantages such as simplified phase retrieval algorithm, reduced overall radiation dose and improved image acquisition speed.

Our proposed method can be used in computed tomography and spatial resolution loss in the direction parallel to the linear grating structures is reduced as compared to the current research results [1]. Furthermore, it could be able to extract the scattering signal due to visibility reduction, which improves the capability of extraction information with reverse projection method [3]. In addition, this method avoids the strict requirements on system stability.

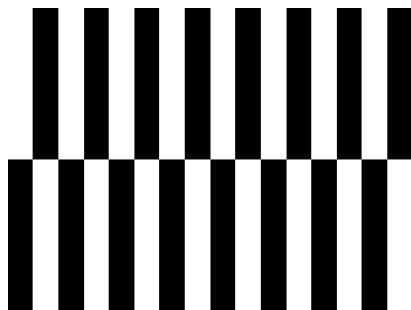


Figure 1: the structure of the stair grating



Figure 2: reconstruction of absorption



Figure 3: reconstruction of refraction



Figure 4: reconstruction of scattering

References

- [1] Y. Ge, K. Li, John Garrett and Guang-Hong Chen. *Opt Express*, 2014. 22(12): p. 14246-52
- [2] P. Li, K. Zhang, Y. Bao and P. P. Zhu, *Optics Express*, 2016. 24(6): p. 5829-5845.
- [3] P. P. Zhu, K. Zhang, Z. Wang et al., *Proc. of the National Academy of Sciences of the United States of America*, 2010. 107(31): p. 13576-13581.

Effect of carbon implantation on the magnetic properties of nano-architectural ZnO

Y. F. Wang¹, J. W. Chiou², W. F. Pong¹, T. Ohigashi³, N. Kosugi³

¹ Department of Physics, Tamkang University, No. 151, Yingzhuang Rd., Tamsui Dist., New Taipei, Taiwan

² Department of Applied Physics, National University of Kaohsiung, No. 700, Kaohsiung University Rd., Nanzih Dist., Kaohsiung, Taiwan

³ UVSOR Facility, Institute for Molecular Science, No. 38, Nishigo-Naka, Myodaiji, Okazaki, Japan

Abstract

Efforts have been made to elucidate the C implantation effects in the room temperature ferromagnetism of ZnO nanowires (NWs) and C implanted nanowires (C:NWs) using X-ray based microscopic and spectroscopic techniques. The photoluminescence spectra and magnetic hysteresis loops reveal that the reduction of intrinsic defects population and the increase of dislocations/interstitial population via C implantation can strongly enhance the saturated magnetization at room temperature. Experimental results of C K-edge X-ray-absorption near-edge structure (XANES), core-level X-ray photoelectron spectroscopy and X-ray magnetic circular dichroism demonstrate that the high density of implanted C are bonding with O in the surface of ZnO C:NWs which strongly bond with nearest-neighbor (NN) O around Zn vacancy (V_{Zn}) sites and quench the magnetic moments in the O sites. The valence-band photoemission spectroscopy, O K-edge scanning transmission X-ray microscopy and the corresponding XANES spectroscopy demonstrate that the majority C defect in the bulk level differs from the surface and the decrease in unoccupied (occupied) density of states at/above (at/below) the conduction-band minimum (valence-band maximum) or the Fermi level is related to the population of implanted C which bond with NN O around the V_{Zn} sites in the impurity region/surface, as revealed by comparing the ZnO C:NWs to the NWs. Results of Fourier-transformed spectra of Zn K-edge extended X-ray absorption fine structure and phase related analysis on Zn-O bond distances suggest that interstitial C are the majority defect in the bulk level of ZnO C:NWs.

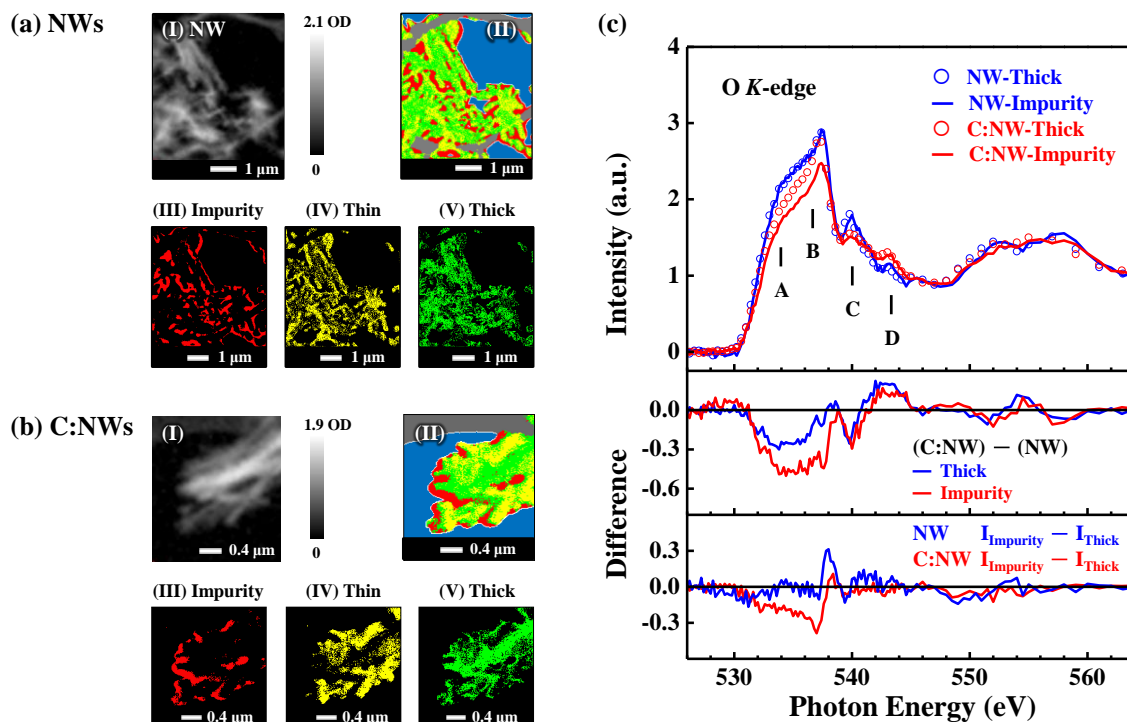


Figure 1: (a) and (b) represent the optical density image (I), O K-edge STXM stack mapping (II) and decomposed STXM mapping (III-V) of randomly selected sample regions of ZnO NWs and C:NWs, respectively. (c) represents O K-edge STXM-XANES and difference spectra of ZnO NWs and C:NWs.

INTERFACIAL CHEMICAL REDOX AT A MESOSCOPIC NIO/PEROVSKITE HETEROJUNCTION FOR EFFICIENT SOLAR CELL BY SCANNING TRANSMISSION X-RAY MICROSCOPE

Ming-Wei Lin¹, Kuo-Chin Wang², Ming-Hsien Li², Yu-Ling Lai¹, Jeng-Han Wang³, Takuji Ohigashi⁴, Nobuhiro Kosugi⁴, Peter Chen², Der-Hsin Wei¹, Tzung-Fang Guo², , and Yao-Jane Hsu*¹

1 National Synchrotron Radiation Research Center, Hsinchu, 30076, Taiwan

2 National Cheng Kung University, Tainan, 70101, Taiwan

3 Department of Chemistry, National Taiwan Normal University, Taipei, 10610, Taiwan

4 Institute for Molecular Science, 38 Nishigo-Naka, Myodaiji, Okazaki, 444-8585, Japan

Abstract

The integration of NiO-perovskite solar cells exhibits high power conversion efficiencies (PCE) when incorporated into mesoscopic NiO hole-transport layers. Herein we studied the origin of such highly efficiencies in terms of chemical structure and electronic properties at a NiO-perovskite heterojunction by X-ray photoelectron spectra (XPS), near-edge X-ray absorption fine structure (NEXAFS) spectra, a scanning transmission X-ray microscope (STXM) and DFT calculations. We found a pronounced chemical redox reaction at a NiO-perovskite heterojunction that produced a hole-dopant interfacial layer at the heterojunction which plays a significant role to facilitate the carrier transport, and thus enhances the photovoltaic efficiencies.

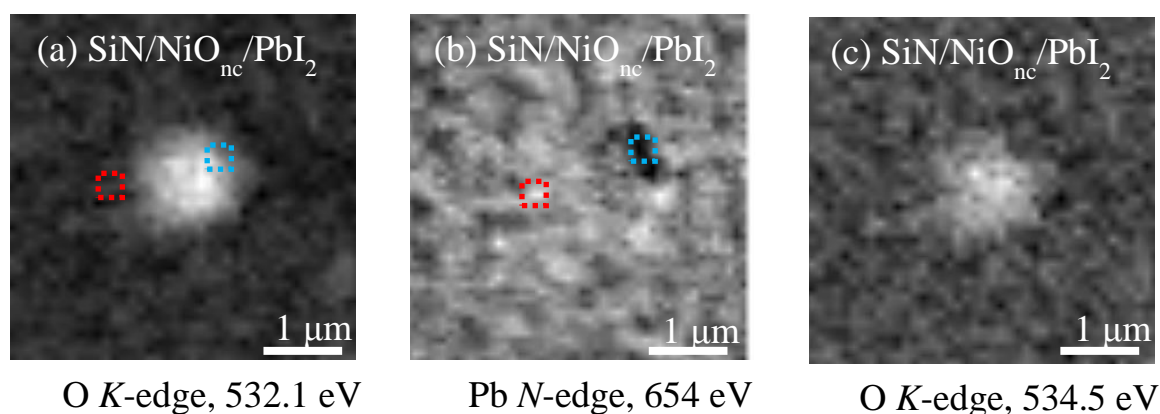


Figure 1: The STXM images of (a) O K-edge at 532.1 eV, (b) Pb N-edge at 654 eV, and (c) O K-edge at 534.5 eV for SiN/NiO/PbI₂.

References

- [1] Ming-Wei Lin and Y.-J. Hsu, et. al., "Interfacial Chemical Redox Reaction at a Mesoscopic NiO/CH₃NH₃PbI₃ Heterojunction for Efficient Photovoltaic Cells", (submitted).
- [2] J.-Y. Jeng, K.-C. Chen, T.-Y. Chiang, P.-Y. Lin, T.-D. Tsai, Y.-C. Chang, T.-F. Guo, P. Chen, T.-C. Wen, Y.-J. Hsu, *Adv. Mater.* 26, 4107 (2014).
- [3] K.-C. Wang, J.-Y. Jeng, P.-S. Shen, Y.-C. Chang, E. W.-G. Diau, C.-H. Tsai, T.-Y. Chao, H.-C. Hsu, P.-Y. Lin, P. Chen, T.-F. Guo, T.-C. Wen, *Sci. Rep.* 2014, 4, 4756.

INVESTIGATION OF L X-RAY PARAMETERS OF HIGH Z ELEMENTS

Harsh Mohan

Department of Physics, M.L.N. College, Yamuna Nagar, 135 001, India

Abstract

X-ray fluorescence microscopic analytical techniques require the knowledge of X-ray parameters. In current years extensive attention has been given to its application in biology, in particular for its capability to map high Z trace elements in presence of low Z elements [1,2]. The components of soft tissue are cells and extracellular matrices that are accountable for biological tasks. In order to envisage soft tissue efficiently, we should label the structure of interest with a probe suitable for the observation method. X-ray visualization of the microstructures of soft tissues can be performed by specifically labeling of each biological constituent with a high Z element probe. For achieving this devour, the precise understanding of X-ray parameters is one of the essential perquisite [3]. The equations for the modified Fluorescence (ω_s) and Coster-Kronig yields (f_s) are given by

$$\omega_s = \frac{\omega_s^0}{1 - (Z_1^2/2 \beta v^2)[1 - (\beta / 4v^2)](1 - \omega_s^0)}$$

and

$$f_s = f_s^0 [1 - Z_1^2(1 - \beta/4v^2)/2\beta v^2]^2$$

where, ω_s^0 is the single hole Fluorescence yield; Z_1 is the atomic number of the projectile; f_s^0 is the single hole Coster-Kronig yield; β is a parameter fixed from electron binding energies. It takes the value 0.9 for the L-shell and v is the projectile ion velocity. The values of these parameters for high Z is shown in Figure 1.

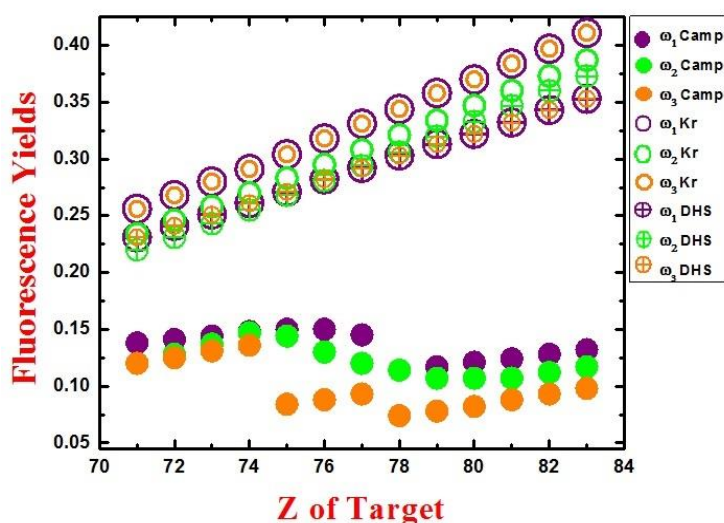


Figure1: Fluorescence yields versus Z of target.

Their behavior of these parameters in understanding this phenomenon and existing developments will be highlighted. Necessities and opportunities for supplementary endeavor will also be discussed.

References

- [1] C. Lechene, R. R.werner, *Microbeam Analysis in Biology* (Academic, New York, 1979).
- [2] A. Gianoncelli, B. Kaulich, R. Alberti, T. Klatka, A. Longoni, A. de Marco, A. Marcello, M. Kiskinova, *Nucl. Instr. Meth. Phys. Res. A* 608, 195 (2009).
- [3] R. Mizutani, Y. Suzuki, *Micron* 43, 104 (2012).

EFFECT OF IMPURITIES IN NICKEL OXIDE POWDER ON THE MICROSTRUCTURE AND ELECTRICAL PROPERTY OF A NICKEL-YTTRIA-STABILIZED ZIRCONIA ANODE

Yong Guan, Jianhong Liu

National Synchrotron Radiation Laboratory, University of Science and Technology of China, #42, hezuohua south road, Hefei, China

Abstract

Understanding the impact of raw materials for use as electrodes on their microstructures is important for improving the electrical performance of fuel cells. In this study, two types of NiO that have a similar appearance but different types of impurities were used to prepare an anode support for Ni-yttria-stabilized zirconia (Ni-YSZ) anodes, which are referred to as anode-1 and -2, respectively. The Nano-CT technique was used to reconstruct the microstructure of the anode support and AFL and calculate multiple parameters, such as triple phase boundary, size of Ni, YSZ and pores. In addition, the electrical properties of the entire cell with anode-1 and -2 were investigated and compared with each other. The microstructure and electrical performance of anode-1 was better than that of anode-2. Further investigations indicated that the difference in the microstructures and electrical properties between anode-1 and -2 was primarily due to an over-sintering phenomenon occurring in anode-2. This phenomenon resulted from a decreased sintering temperature due to MgO impurities introduced by the raw materials in anode-2. When the sintering temperature of anode-2 was decreased, an anode with a microstructure similar to that of anode-1 was obtained.

LATTICE BOLTZMANN MODELING OF GAS TRANSPORT WITH ELECTROCHEMICAL REACTION IN NI-YSZ ANODES USING RECONSTRUCTED MICROSTRUCTURE FROM NANO-CT

Yangchao Tian, Pengfei Guo

National Synchrotron Radiation Laboratory, University of Science and Technology of China, #42, hezuohua south road, Hefei, China

Abstract

In order to further understand impact of the microstructure of nickel-yttria-stabilized zirconia (Ni-YSZ) on the performance of solid oxide fuel cell (SOFC), X-ray nano computed tomography (nano-CT) used to obtain three-dimensional (3D) model of Ni-YSZ composite anode samples subjected to different thermal cycles. Some key parameters, such as phase connectivity and triple phase boundary (TPB) density, have been calculated using 3D reconstructions (Figure 1). The electrochemical reaction occurring at active-TPB has been added into Lattice Boltzmann Method for the simulation of multi-component mass transfer in porous anodes. With the help of actual TPB distributions measured by nano-CT the effect of different electrode geometries on the mass transfer and the electrochemical reaction in anodes subjected to different thermal cycles are investigated. The results demonstrate that based on nano-CT data the simulation for gas transport with electrochemical reaction in nickel-yttria-stabilized zirconia anode using Lattice Boltzmann method can help us to further understand the relationship between microstructure of electrode and its performance.

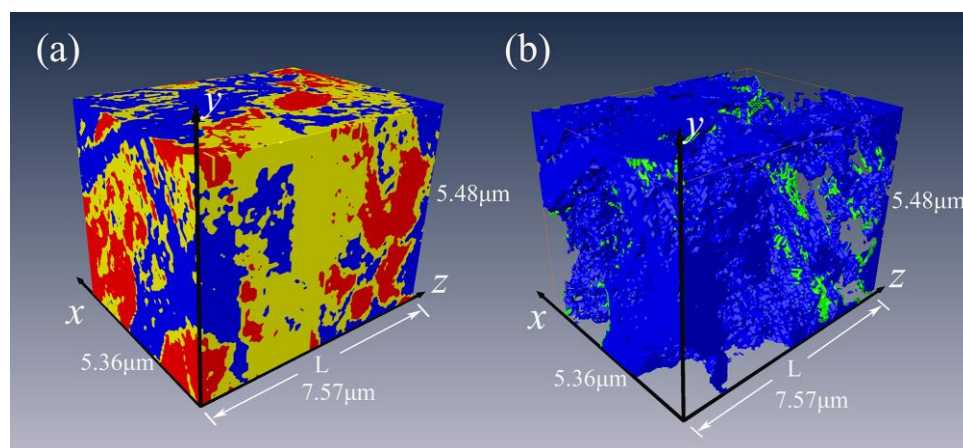


Figure 1 (a) 3D rendering of an anode sample with Ni shown in red, YSZ shown in yellow, pore shown in blue; (b) Corresponding 3D distribution of TPB sites (green) and pore (blue).

NONDESTRUCTIVE MATERIALS CHARACTERIZATION IN 3D BY LABORATORY DIFFRACTION CONTRAST TOMOGRAPHY

C. Holzner¹, E. M. Lauridsen², H. Bale¹, A. Lykegaard², P. Reischig², A. Merkle¹, L. Lavery¹, M. Feser³

¹ Carl Zeiss X-ray Microscopy, Inc., Pleasanton, CA USA

² Xnovo Technology ApS, Køge, Denmark

³ Lyncean Technologies, Fremont, CA USA

Abstract

The ability to characterise the crystallographic microstructure of polycrystalline samples, such as metals and ceramics, non-destructively and in three-dimensions, is a powerful tool for understanding many facets of materials performance.

The introduction of diffraction contrast tomography as an additional imaging modality on the ZEISS Xradia Versa laboratory X-ray microscope has opened up a whole new range of possibilities for studies of the effect of 3D crystallography. The non-destructive 3D crystallographic imaging capabilities of the laboratory diffraction contrast tomography technique (LabDCT) [1, 2], complements the structural data obtained by traditional absorption-based tomography and together they provide an unprecedented insight into materials structure [3].

Here we will present a selection of results of LabDCT with particularly emphasis on its non-destructive operation, demonstrated through 4D evolutionary studies obtained by repeating the imaging procedure numerous times on the same sample. We will discuss the boundary conditions of the current implementation, point to the future of the technique and discuss ways in which this can be correlatively coupled to related techniques for a better understanding of materials structure evolution in 3D.

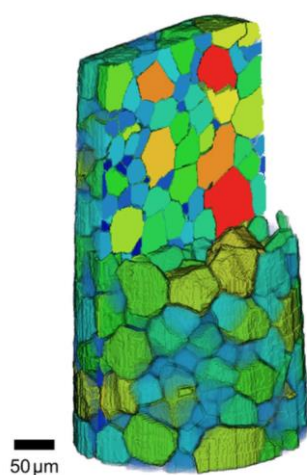


Figure 1: Non-destructive representation of grain morphology by a virtual slice through the sample volume of a Ti-alloy.

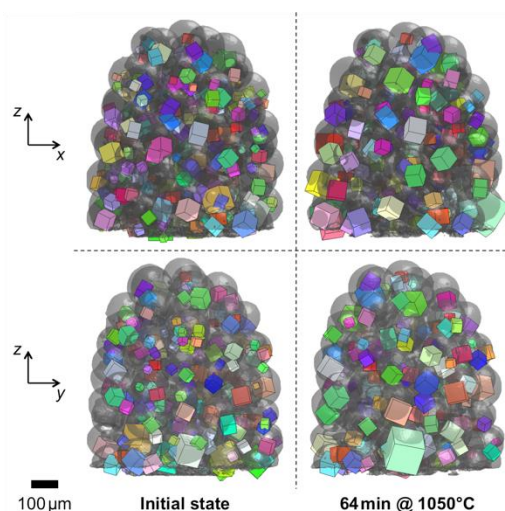


Figure 2: Different views of reconstructed grain maps from two different time steps of a sintering experiment with Cu.

References

- [1] A McDonald, S.A. et al., Scientific Reports **5**, 14665 (2015).
- [2] Feser, M., Holzner, C. and Lauridsen, E.M. US Patent 9,110,004 (2012).
- [3] Technology Note, *Contrast with Submicron 3D X-ray Imaging for Difficult to Image Materials* (Pleasanton, CA: Carl Zeiss X-ray Microscopy [2015]) http://pages.zeiss.com/rs/270-LXH-014/images/TechNote_Contrast_digital.pdf

TOWARD IN-OPERANDO NANO-TOMOGRAPHY OF GREEN ENERGY AND NANO-MATERIAL REVEALED BY NANO-TXM

Yen-Fang Song¹, Chun-Chieh Wang¹, Nai-Lih Wu², Jian-Qiang Wang³, Michael H. Huang⁴

¹ National Synchrotron Radiation Research Center, Hsinchu 30076, Taiwan, R.O.C.

² Department of Chemical Engineering, National Taiwan University Taipei 106, Taiwan, R.O.C.

³ Shanghai Institute of Applied Physics, Chinese Academy of Sciences, Shanghai 201800, PR China

⁴ Department of Chemistry, National Tsing Hua University, Hsinchu 30013, Taiwan, R.O.C

Abstract

Global warming and climate change caused by the environmental pollution as well as lack of energy resource are extremely serious problems. The nano-transmission X-ray microscopy (TXM) at beamline BL01B of the Taiwan Light Source (TLS) has carried out successfully the researches of energy resources, especially green energy, nano-materials and porous materials. For example, working energy storage Li-ion battery [1], solid oxide fuel cell [2], shale gas [3], nanomaterials formation process [4,5], 3D integrated circuit, earthquake fault gauge, evolution and function of dinosaur teeth [6]. This beamline provides full-field imaging at an energy of 8 keV with a spatial resolution of 50 nm, 15 μm field of view, and the Zernike-phase contrast. In order to provide new insights into these significant researches, a new full-field TXM beamline at Taiwan Photon Source (TPS) has been designed and will be constructed in near future. This new beamline will provide 37 nm spatial resolution, 38 μm field of view, in-operando tomography with 15 min exposure time, 1.5×10^{-4} energy resolution for chemical mapping and Zernike-phase contrast at the energy range of 4.5-15 keV.

In this presentation, I will present (1) in-operando and tomographic study on the interior microstructures of working Li-ion batteries (Fig. 1 and Fig. 2) [1]. (2) Cr deposition and poisoning phenomenon at $(\text{La}_{0.6}\text{Sr}_{0.4})(\text{Co}_{0.2}\text{Fe}_{0.8})\text{O}_{3-\delta}$ electrode of solid oxide fuel cells [2] (3) In-operando observation of the sulfidation process of Cu_2O nano-particle for the growth of Cu_2S nanocages [4]. (4) Formation of polyhedral gold supercrystals [5]. Moreover, I will introduce the new TXM beamline design for in-operando nano-tomography at TPS.

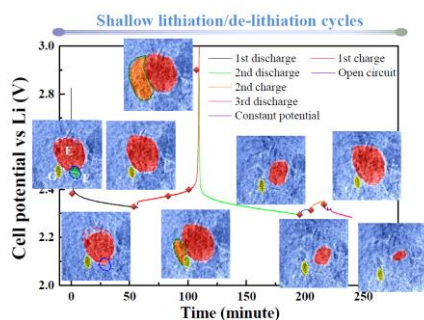


Figure 1: Dynamics of polysulfide dissolution and re-deposition in working Li-S battery by In-operando TXM. The image size is $15 \times 15 \mu\text{m}^2$.

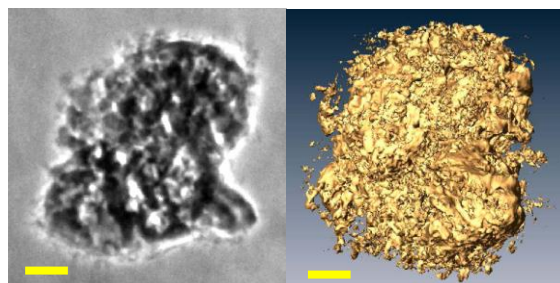


Figure 2: TXM 2D image (left) and tomography (right) of porous Sn particle in lithium ion battery. The scale bar is $2 \mu\text{m}$.

References

- [1] S-C Chao, Y-F Song, C-C Wang, H-S Sheu, H-C Wu and N-L Wu, *J. Phys. Chem. C* **115**, 22040 (2011). W-C Chen, Y-F Song, C-C Wang, Y Liu, D T Morris, P A Pianetta, J. C. Andrews, H-C Wu and N-L Wu, *J. Mater. Chem. A* **1**, 10847 (2013). C-N Lin, W-C Chen, Y-F Song, C-C Wang, L-D Tsai and N-L Wu, *J. of Power Sources* **263**, 98 (2014).
- [2] X Chen, C Jin, L Zhao, L Zhang, C Guan, L Wang, Y-F Song, C-C Wang, J-Q Wang, S P Jiang, *Intern. J. Hydro. Ener.* **39**, 15728 (2014).
- [3] Y Wang, J Pu, L Wang, J-Q Wang, Z Jiang, Y-F Song, C-C Wang, Y Wang, C Jin, *Fuel* **170** (84–91) (2016).
- [4] C-H Kuo, Y-T Chu, Y-F Song, and M H. Huang, *Adv. Funct. Mater.* **21**, 792 (2011)
- [5] C-W Liao, Y-S Lin, K Chanda, Y-F Song, and M H. Huang, *J. Am. Chem. Soc.* **135**, 2684 (2013)
- [6] C-C Wang, Y-F Song, S-R Song, Q Ji, C Chiang, Q Meng, H Li, K Hsiao, Y Lu, B Shew, T Huang, and R Reisz, *Scientific Report* **5**:15202, 1-11 (2015).

DARK-FIELD IMAGING OF WATER MIGRATION IN LAYERED CEMENTITIOUS MATERIALS

Abstract

Internal water movement in porous materials is strongly entangled with the material's structural features. In concrete, a deep understanding of the water movement driven by the hydration-related microstructural change, and by the environmental conditions, is strictly necessary to design better concrete curing methods [1]. For example, in the application of repair materials for concrete, the pore structural features in the top repair layer affect the water transport to the bottom concrete substrate and thus the efficiency of this technology.

In this work, we aimed at investigating internal displacements of pure water due to spatial micro- and meso-structural heterogeneities in porous materials by dark-field X-ray imaging, based on exploiting the small-angle X-ray scattering arising from the structure at sub-spatial resolution scale. We performed time-lapsed radiography measurement with Talbot-Lau interferometer (TLI) [2] during hydration of a layered system made of cementitious materials, i.e., two types of mortars with different water-to-cement (w/c) ratio, which was subjected to drying from the top, and two reference mortar samples. The results show the capability of dark-field X-ray imaging by TLI at laboratory scale to visualize the water migration from the higher w/c bottom mortar to the lower w/c top mortar, driven by the capillary forces originated by the smaller pores at lower w/c layer than in the other one. The qualitative analysis on dark-field images in figure 1 confirms this water displacement by the time-resolved pixel-wise scattering signal change in the regions of two mortar layers, after extracting with the signal created by hydration and drying from reference samples [3]. Compared to the traditional attenuation-based X-ray imaging applied in previous studies [4], our approach, with the advantage of high temporal resolution, high image contrast at low spatial resolution, offers the feasibility of investigating the couplings of water transport dynamics and material's structure. In absence of any contrast agents, it could be applied to study different pure water transport related dynamic processes and in other types of porous (cementitious) materials.

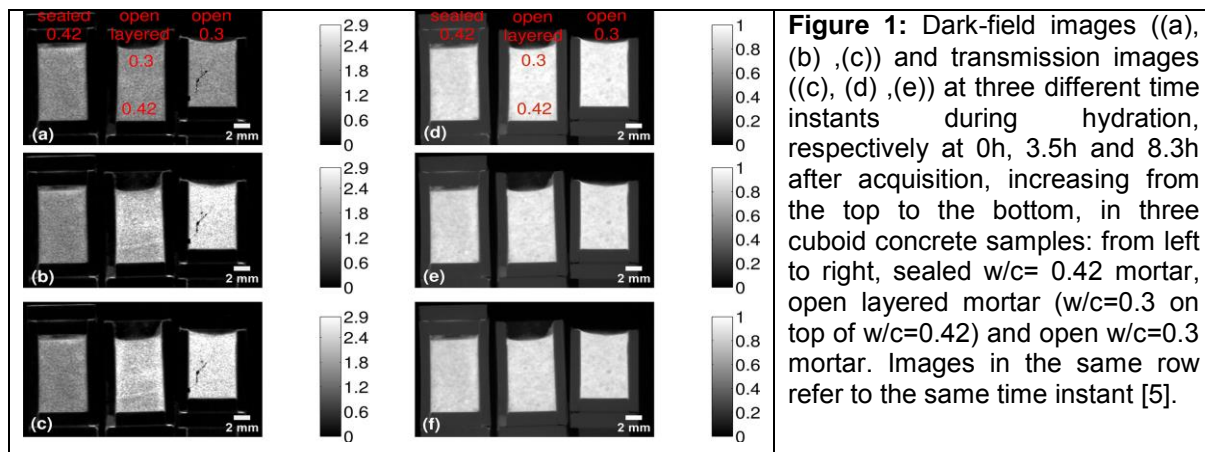


Figure 1: Dark-field images ((a), (b), (c)) and transmission images ((d), (e), (f)) at three different time instants during hydration, respectively at 0h, 3.5h and 8.3h after acquisition, increasing from the top to the bottom, in three cuboid concrete samples: from left to right, sealed $w/c=0.42$ mortar, open layered mortar ($w/c=0.3$ on top of $w/c=0.42$) and open $w/c=0.3$ mortar. Images in the same row refer to the same time instant [5].

References

- [1] Cement, Concrete and Aggregates Australia (CCAA), 2006, "Curing of Concrete".
- [2] F. Pfeiffer, M. Bech et al., *Nat. Mater.* 7 (2008) 134-137.
- [3] F. Prade, M. Chabior et al., *Concr. Res.* 74 (2015) 19-25.
- [4] D. P. Bentz, K. K. Hansen, *Cem. Concr. Res.* 30 (2000) 1157-1168.
- [5] Manuscript to be submitted to *Cem. Concr. Res.*

X-RAY MICROSCOPY STUDIES OF VITRIFIED NUCLEAR WASTE FORM

Z. Cai¹ and M. Tang²

¹Argonne National Laboratory, 9700 S. Cass Ave., Argonne, IL 60439, USA
²Los Alamos National Laboratory, P.O. Box 1663, Los Alamos, NM 87545, USA

Abstract

Over the past five decades, US nuclear industry and defense related programs have produced huge amount of used nuclear fuel and high-level nuclear waste that are expected to remain radioactive for more than hundreds of thousand years. These nuclear wastes are currently stored either on site in spent fuel pools or in waste storage tanks that is only meant to contain the waste for perhaps decades, not centuries. It has been determined that these wastes will eventually be immobilized by vitrification [1], a process by which the wastes will ultimately be transformed and confined into a stable glass or glass-ceramic matrix, for permanent disposal. Fission products yielded from thermal neutron fission of most fissionable actinides exist in *4p* and *5p* nonmetals, *5s* and *6s* alkalis and alkaline earths, *4d* transition metals, and most lanthanides [2]. Vitrification leads to a multi-element and multi-phase glass/glass-ceramic waste form of combined fission products [3], a probably most complex materials system exist on earth. X-ray microscopy techniques including micro-fluorescence, micro-diffraction, and micro-spectroscopy were used to study dissolution of elemental species in glass matrix, phase separation, interaction between glass and separated phases, and secondary phase separation in glass waste forms for fundamental understanding their structural complexity spatially, compositionally, and hierarchically. These studies provide a base for further evaluation of the thermodynamic stability of glass waste form, concurrent structural evolution of material due to radioactive species decay, leach rate performance in a repository environment, and waste form's decay heat and radiation durability.

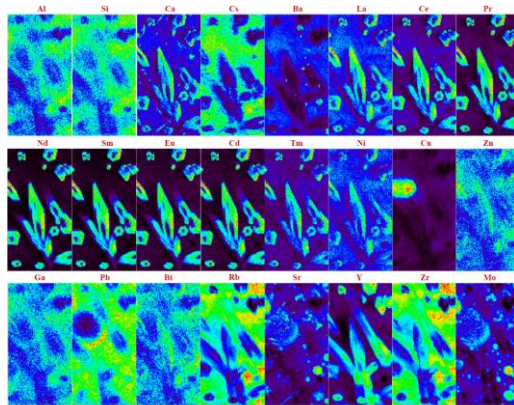


Figure 1: X-ray fluorescence maps of a specimen prepared from a simulated glass waste form. The measurement was performed using 20-keV X-rays.

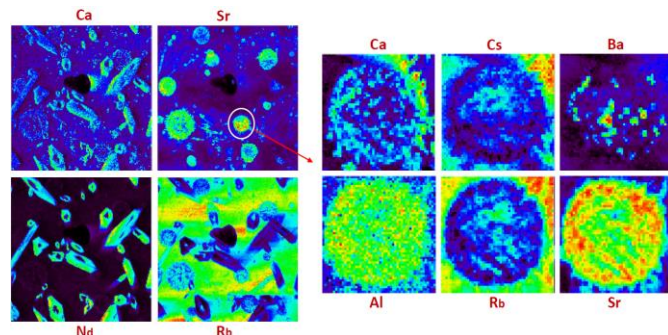


Figure 2: X-ray fluorescence maps of a glass waste form indicating a secondary phase separation within a primarily phase separated feature. The maps on right side have a dimension of 40 µm x 40 µm.

References

- [1] J. D. Vienna, "Nuclear Waste Vitrification in the United States: Recent Developments and Future Options," *International Journal of Applied Glass Science* 1 309 (2010).
- [2] B. C. Purkayastha, and G. R. Martin, *Canadian Journal of Chemistry* 34 293 (1956).
- [3] J. Crum, L. Turo, B. Riley, M. Tang, and A. Kossoy, *J. Am. Ceram. Soc.*, 95 1297 (2012).

2D AND 3D SOFT X-RAY SPECTRO-MICROSCOPY AND SPECTRO-PTYCHOGRAPHY OF FUEL CELL CATHODES

A.P. Hitchcock¹, J. Wu¹, X.H. Zhu¹, L. G. de A. Melo,¹ D.A. Shapiro², T. Tyliszczak², V. Berejnov³, D. Susac³ and J. Stumper³

¹ Brockhouse Institute for Materials Research, McMaster University, Hamilton, Canada

² Advanced Light Source, Berkeley Lab, Berkeley, USA

³ AFCC Automotive Fuel Cell Cooperation Corp. Burnaby, Canada

Abstract

Polymer electrolyte membrane (PEM-FC) fuel cells are being introduced as an alternative to CO₂ producing internal combustion engines for consumer automobiles. The key component of PEM-FC is the membrane-electrode-assembly (MEA) which consists of a special, catalyst impregnated coating applied to both sides of a proton conducting separator/solid electrolyte (perfluorosulfonic acid, usually Nafion[®]). The rate limiting reaction is oxygen reduction at the cathode. A critical component of the cathode is a proton conductor (ionomer), needed to ensure protons can migrate to all catalytic sites. We are using soft X-ray Scanning Transmission X-ray Microscopy (STXM) and Ptychography to map ionomer distributions in cathode layers in both 2D and 3D. Ptychography is well known to give an exceptional improvement in spatial resolution relative to conventional STXM [1] and this is observed in our measurements (**Fig 1**). However the PEM-FC cathode has highly crystalline regions (graphitic carbon support and Pt catalyst) which will scatter very well, surrounded by the non- or low-crystalline ionomeric polymer, which is expected to be a very poor X-ray scatterer. By measuring the difference of images below and above the F 1s edge, we use the chemically unique nature of the ionomer to enhance its signal since it is the only F-containing species in the cathode. Once the higher spatial resolution of ptychography is discounted there is good agreement in the fluorine distributions determined by STXM and ptychography (Fig. 1). Only signal from the F-containing ionomer contributes to the difference signal, since the energies used are far away from absorption edges of C or Pt. Radiation damage is a major concern; the long exposure times (200 ms at each point) used for the 5.3.2.1 NS measurements (Fig. 1) caused significant F loss. At the 11.0.2 STXM we were able to record high quality ptychography images with only 20 ms dwell, greatly reducing the exposure and thus damage. The short dwell time allowed a much larger area to be measured (**Fig. 2**) with similar morphology and F distributions as in Fig. 1. [2]

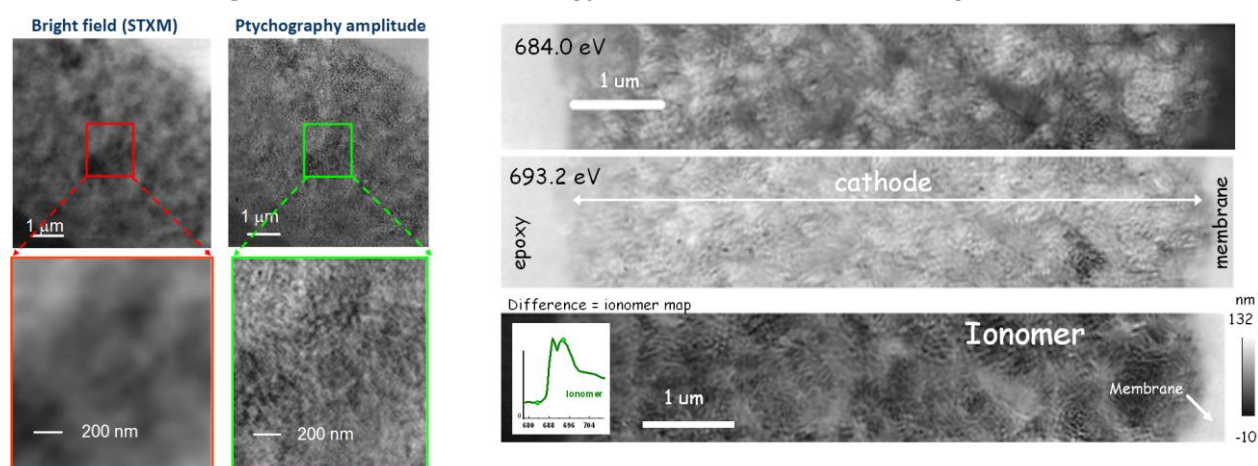


Figure 1: Comparison of STXM and ptycho. $OD_{693}-OD_{684}$ F maps of the same area (5.3.2.1, NS-I, June 2015)

Figure 2: Ptychography images over full width of a PEM-FC cathode at 684 and 693 eV, and the difference. Estimated spatial resolution is 10 nm. (11.0.2 Apr 2015)

References

- [1] D.A. Shapiro et al., Nature Photonics 8 (2014) 765
- [2] Measurements performed at ALS, LBNL, supported by DoE BES.

UNDERSTANDING TRANSPORT PHENOMENA IN ELECTROCHEMICAL ENERGY DEVICES: A CORRELATIVE APPROACH

B. Tjaden, Donal P. Finegan, Dan J.L. Brett, Paul R. Shearing

The Electrochemical Innovation Laboratory, Department of Chemical Engineering, University College London, WC1E 7JE, UK

Electrochemical energy devices have the potential to revolutionize distributed low-carbon power supply. However, in order to accelerate their commercialization across a range of applications, a much improved understanding of the underlying material microstructure is required. In particular, the rate capability of batteries, oxygen transport membranes (OTMs) and fuel cells is limited by mass transport in porous media which, in turn, is a function of microstructural characteristics such as tortuosity, porosity and mean pore diameter. However, unlike the latter two parameters, tortuosity is notoriously difficult to quantify which is why a variety of methods has been developed for this purpose. These differ considerably from each other in terms of calculation approach and data preparation techniques.

Here, we utilise X-ray nano CT to reveal the complex microstructure and resolve geometric features affecting mass transport of tubular porous support layers of OTMs. It is only because of high resolution tomography, that we can examine the relationship between the pore structure and mass transport via image and simulation based tortuosity calculation methods (**Figure 1**). In turn, this has been validated using diffusion cell experiments to evaluate the bulk transport properties of the same samples for different binary gas mixtures at different temperatures [1].

We conclude, that image and simulation based methodologies arrive at lower tortuosity values in comparison to diffusion cell experiments (**Figure 2**). Even the widely used Bruggeman [2] and Maxwell relations prove to be unfit to estimate tortuosity values in the analysed microstructure. The observed difference may stem from Knudsen diffusion effects which are not accounted for in the entirety of tomography based modelling techniques. Secondly, tortuosity values extracted via diffusion cell experiments are a function of gas mixture, temperature and microstructural characteristics rather than a constant value. Consequently, care must be taken in applying purely continuum interpretations of diffusion in these complex porous media.

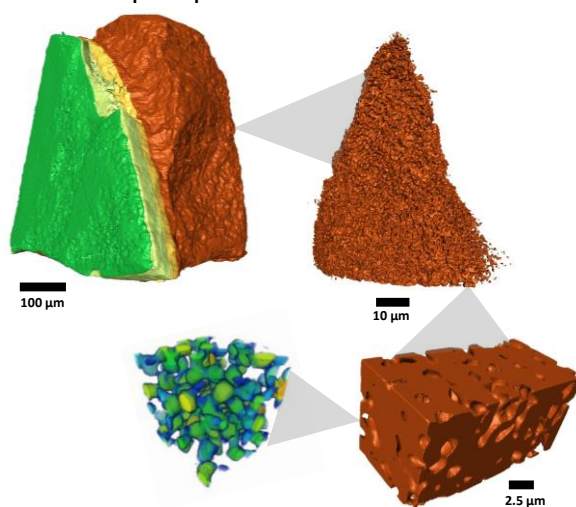


Figure 1: X-ray nano CT of porous support layer of OTM for diffusion simulation

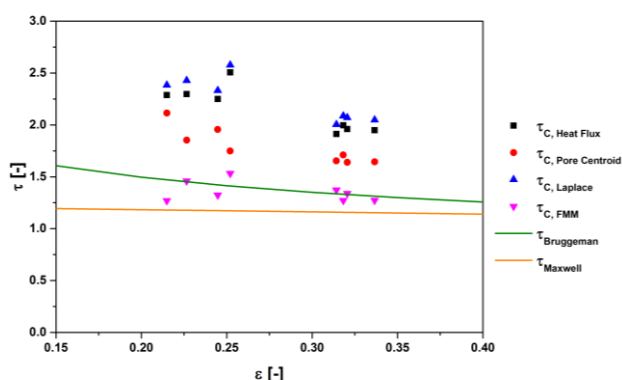


Figure 2: Comparison of tortuosity calculated via different image and simulation based methods

References

- [1] B. Tjaden *et al.*, *Solid State Ionics*, 2016.
- [2] B. Tjaden *et al.*, *Curr. Opin. Chem. Eng.*, 2016.

IN-SITU X-RAY NANO-CT/XAFS SYSTEM FOR POLYMER ELECTROLYTE FUEL CELLS UNDER OPERATING CONDITIONS

O. Sekizawa¹, T. Uruga^{1,2}, N. Ishiguro³, H. Matsui⁴, K. Higashi¹, Y. Iwasawa¹, M. Tada^{3,4}

¹ The University of Electro-Communications, 1-5-1 Chofugaoka, Chofu, Tokyo 182-8585, Japan

² Japan Synchrotron Radiation Research Institute, 1-1-1 Kouto, Sayo, Hyogo 679-5198 Japan

³ RIKEN Harima Branch, 1-1-1 Kouto, Sayo, Hyogo 679-5148 Japan

⁴ Nagoya University, Furo-cho, Chikusa-ku, Nagoya, Aichi 464-8602, Japan

Abstract

Crucial issue for developing next generation polymer electrolyte fuel cells (PEFCs) is spatiotemporal information on active factor and reaction mechanism, especially the degradation factor and mechanism in PEFC cathode catalysts. PEFC has multi-layered structures consisting of a membrane electrode assembly (MEA) with a cathode catalyst layer, gas diffusion layer (GDL) and so on. The electrochemical reactions occur spatially inhomogeneously under potential-operating conditions. To visualize the oxygen reduction reaction and degradation mechanisms for the electrocatalysis, in-situ non-destructive 3D imaging of the internal structures and chemical states of MEA in PEFC under the operating conditions is required. We succeeded in conducting 3D imaging of the chemical state distribution of electrode catalysts in an MEA by X-ray computed laminography (XCL) XAFS technique [1, 2]. The XCL is a suitable 3D imaging technique for laterally extended planar objects, such as PEFCs. The geometric restriction of XCL measurement, however, imposed a specific design on the PEFC, which made it difficult to maintain the operating conditions of the PEFC. Therefore, we developed two types of in-situ X-ray computed tomography (XCT) systems consisting of a newly designed PEFC based on a Japan Automobile Research Institute (JARI) standard cell [3]. One is a wide-field transmission CT system (field of view: 500 μm , spatial resolution: 1 μm) and the other is a high-resolution imaging CT system using a Fresnel zone plate (FZP) objective (field of view: 50 μm , spatial resolution: 50 nm).

Figure 1 shows a reconstructed image of PEFC measured using the transmission CT system. Figure 2 shows a reconstructed cross-sectional image of an MEA measured using the imaging CT system. 3D imaging of the PEFC MEA was successfully conducted under the operating conditions (supplied gases: H_2 and N_2 , temperature: 80 $^\circ\text{C}$). The rotation angle of the PEFC was restricted from -80 to $+80$ $^\circ$ due to its design. A rotary joint and slip ring was used to rotate the PEFC sample smoothly connected with gas tubes and heater cables. The X-ray images were measured using a 2D image detector, which consists of a scintillator crystal, objective lens, and a sCMOS camera.

This work was partly supported by the Polymer Electrolyte Fuel Cell Program of the New Energy and Industrial Technology Development Organization (NEDO) of Japan.

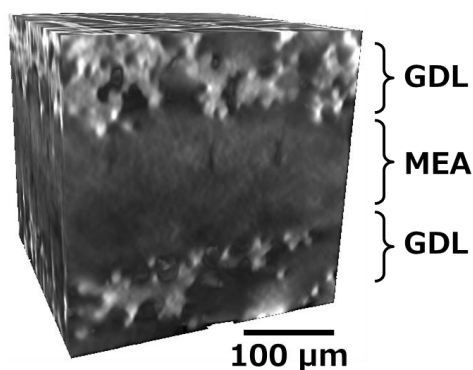


Figure 1: Reconstructed image of PEFC.

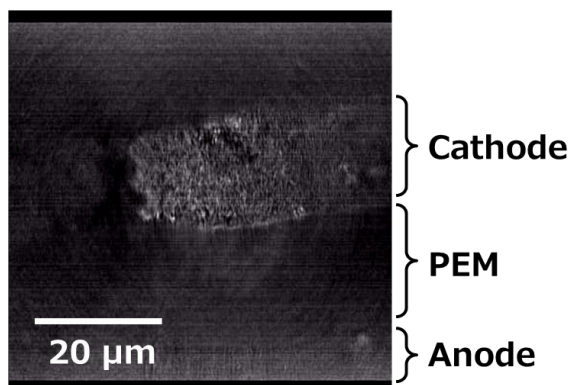


Figure 2: Cross-sectional image of MEA.

References

- [1] T. Saida, *et al.*, *Angew. Chem. Int. Ed.* **51**, 10311 (2012).
- [2] O. Sekizawa, *et al.*, (accepted to *J. Phys.: Conf. Ser.*).
- [3] Y. Hashimasa, *et al.*, *J. Power sources*, **155**, 182 (2006).

METAL POISONING OF CATALYST PARTICLES AS STUDIED BY X-RAY IMAGING AT MULTIPLE LENGTH SCALES

F. Meirer¹, S. Kalirai¹, Y. Liu², J. Nelson Weker², A. Wise², S. Webb², C.M. Krest², M. Farmand³, D. A. Shapiro³, U. Boesenberg⁴, G. Falkenberg⁴, and B.M. Weckhuysen¹

¹ Inorganic Chemistry and Catalysis, Utrecht University, 3584 CG Utrecht, The Netherlands

² Stanford Synchrotron Radiation Lightsource, Stanford University, Menlo Park, CA 94025, USA

³ Advanced Light Source, Lawrence Berkeley National Laboratory, Berkeley, CA 94720, USA

⁴ Deutsches Elektronen-Synchrotron DESY, 22607 Hamburg, Germany

Abstract

Modern X-ray imaging techniques allow for the combination of high spatial resolution, a large field of view, short dwell times, and the capability to obtain spectroscopic information. This has opened the door to high-resolution studies correlating chemistry and morphology of, for example, whole catalyst particles used in fluid catalytic cracking (FCC).

FCC is an important process in the petrochemical industry, accounting for 40-45% of worldwide gasoline production. In FCC, catalyst particles are employed to crack large hydrocarbon fractions into more valuable materials, such as gasoline and propylene [1]. During operation FCC catalyst particles accumulate metals such as Fe, Ni, V, Ca, and Na that have been related to catalyst deactivation. However, detailed knowledge about metal deposition mechanisms as well as the deposition's effects on particle morphology and chemistry is limited.

In this presentation I will summarize our recent studies of individual FCC catalyst particles using synchrotron based hard X-ray full field transmission X-ray microscopy [2,3], hard X-ray fluorescence tomography [4], and soft X-ray ptychographic imaging [5].

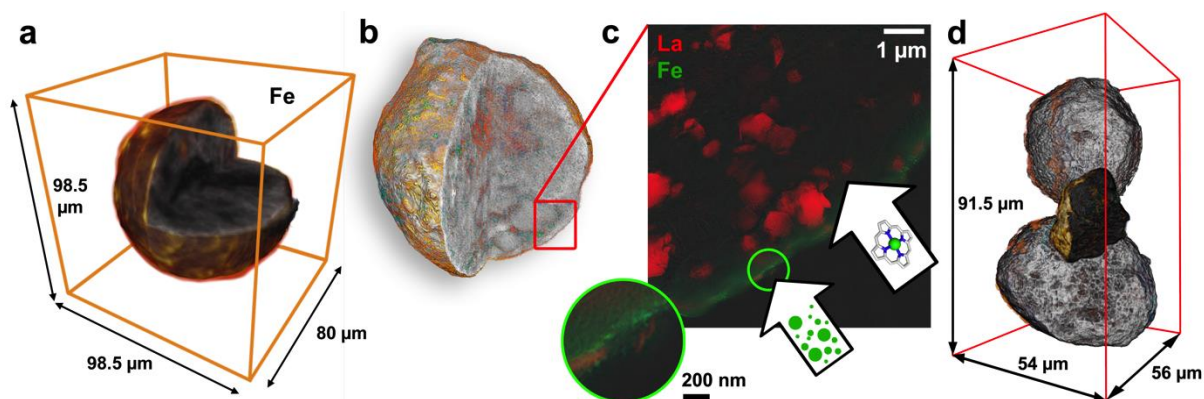


Figure 1: X-ray imaging of a whole FCC particle showing (a) particle morphology and 3D distribution of multiple elements (shown is Fe) mapped by hard X-ray fluorescence tomography (a) and the 3D distribution of specific metals (Fe and Ni) as mapped by hard X-ray nanotomography (b). In (c) a selected surface region of a particle cross-section as imaged by soft X-ray ptychography is displayed, visualizing the effects of two different Fe deposition mechanisms. The effect of Fe deposition at the surface of FCC catalyst particles could be responsible for particle agglutination as observed by hard X-ray nanotomography (d).

References

- [1] E.T.C. Vogt, B.M. Weckhuysen, *Chem. Soc. Rev.* 44, 7342-7370 (2015).
- [2] F. Meirer, D. T. Morris, S. Kalirai, Y. Liu, J. C. Andrews, B. M. Weckhuysen, *J. Am. Chem. Soc.* 137, 102-105 (2015).
- [3] F. Meirer, S. Kalirai, J. Nelson Weker, Y. Liu, J. C. Andrews, B. M. Weckhuysen, *Chem. Commun.* 51, 8097-8100 (2015).
- [4] S. Kalirai, U. Boesenberg, G. Falkenberg, F. Meirer, B.M. Weckhuysen, *ChemCatChem* 7, 3674-3682 (2015).
- [5] A. M. Wise, J. Nelson Weker, S. Kalirai, M. Farmand, D. A. Shapiro, F. Meirer, B. M. Weckhuysen, *ACS Catal.* 6, 2178-2181 (2016).

MULTI-SCALE X-RAY MICROSCOPIC IMAGING OF HETEROGENOUS REDUCTION OF IRON-ORE SINTERS

M. Kimura^{1,2}, Y. Takeichi^{1,2}, Y. Niwa¹, H. Nitani^{1,2}, R. Murao³, Y. Liu⁴

1 Photon Factory, Institute of Materials Structure Science, High Energy Accelerator Research Organization (KEK), Tsukuba, Ibaraki 305-0801, Japan

2 Department of Materials Structure Science, School of High Energy Accelerator Science, SOKENDAI (The Graduate University for Advanced Studies), Tsukuba, Ibaraki 305-0801, Japan

3 Advanced Technology Research Laboratories, Nippon Steel & Sumitomo Metal Co., Futtsu, Chiba 293-8511, Japan

4 Stanford Synchrotron Radiation Lightsource (SSRL), Menlo Park, CA 94025, USA

Abstract

Iron-ore sinters constitute the major component of the iron-bearing burden in blast furnaces, and the mechanism of their reduction and their change of mechanical properties is one of the most important factors to be considered in iron making. The heterogeneous reduction of iron-ore sinters [1] was investigated by multi-scale X-ray microscopic imaging: in-house X-CT, the two-dimensional XAFS mapping using a semi-micro beam (ca. 20 μ m) at PF BL-15A1 [2], and TXM (XAFS-CT) using the zone-plate system at SSRL BL6-2 [3].

The heterogeneous change in chemical states of iron: Fe^{III}, Fe^{II}, and Fe⁰ was clearly observed in multi-scales from tens of nm to mm. Figure 1 shows an image obtained by TXM (XAFS-CT) measured at X-ray energies near Fe *K*-edge for a sinter in the middle of reduction. The reduction progresses near domain boundaries of different chemical states such as Fe^{III} and Fe^{II}. In a macroscopic scale, the progress of reduction is affected by the difference of chemical compositions (the Fe/Ca ratio) as well as the domain boundaries of different chemical states. The different progress of reduction causes the stress field, resulting in the initiation of micro cracks. Multi-scale X-ray microscopic imaging successfully showed that domain boundaries of different chemical states initiate crack formation during the reduction process.

The approach of multi-scale X-ray microscopic imaging is to be applied to various structural materials in order to understand the fracture mechanism in terms of chemical states as well as microstructures. Some results such as steel (Fe-Fe₃C) and Ni₃Al will be presented.

A part of this work was supported by Cross-ministerial Strategic Innovation Promotion Program (SIP, unit D66) operated by the cabinet office.

Experiments at the PF were performed under the approval of the PF Program Advisory Committee (Proposal No. 2014G707 and 2015S2-002). The TXM at SSRL has been carried out under the approval of SSRL (LOI and Proposal No. 4468, 2016).

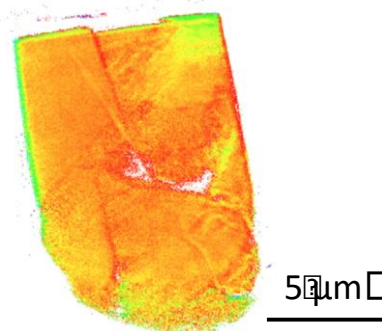


Figure 1: TXM image: Fe *K*-edge shift for a sinter in the middle of reduction.

References

- [1] M. Kimura, et al., J. Phys.: Conf. Ser. (in print, 2016).
- [2] N. Igarashi, et al., J. Phys.: Conf. Ser. 072016, 425 (2013).
- [3] Y. Liu, et al., Anal. Bioanal. Chem. 1297, 404.5 (2012).

X-RAY BEAM INDUCED CURRENT FOR NANOSCALE ENGINEERING OF ELECTRONIC DEVICES

M. Stuckelberger¹, B. West¹, B. Lai², J. Maser², V. Rose², D. P. Fenning³, M. I. Bertoni¹

¹School of Electrical, Computer and Energy Engineering, Arizona State University, Tempe, AZ, USA

²Advanced Photon Source, Argonne National Laboratory, Argonne, IL, USA

³Department of Nanoengineering, University of California San Diego, La Jolla, CA, USA

Abstract

X-ray beam induced current (XBIC) is a powerful technique to probe charge collection efficiency of fully operational electronic devices with high spatial resolution. The potential for correlative measurements of electronic status with composition via x-ray fluorescence (XRF/XBIC) and/or structure via diffraction (XRD/XBIC) provide tremendous potential for studying electronic materials in solar cells and other devices *in-situ* and *operando*.

While conducting XBIC measurements is relatively straight forward, the data quantification and interpretation is much more complicated. Factors such as the penetration depth of x-rays and the resulting depth-dependent charge carrier generation that defines the interaction volume need to be taken into account. This leads to a 3D problem if spatial non-uniformity of surface and interface topology is taken into account. Hence, we need to correct the XBIC signal in 3D for beam attenuation of passive and active layers. For time-dependent measurements—either actively driven as part of *in-situ* XBIC or due to specimen changes over time, e.g. due to beam-induced device damage—even 4D data need to be taken into account. We will discuss fundamental and experimental aspects involved in the conversion from XBIC to charge collection efficiency, including electrons and photons leaving the sample, the problematics of precise beam intensity measurements, signal amplification, and the extraction of the number of charge carriers generated per incident photon.

In our presentation, we will discuss the opportunities and challenges of XBIC drawing from experience (see Fig. 1) at different beam lines at APS and CLS, along with Monte Carlo simulations (see Fig. 2) to support the findings. On this base, taking into account practical and theoretical considerations of beam energy and spotsize, we compare XBIC to other techniques such as electron and laser-beam induced current, and Kelvin probe.

Finally, we will present an outlook for future *in-situ* and *operando* XBIC measurements to enable further insight into the working principle and limitations of electronic devices in general and solar cells in particular.

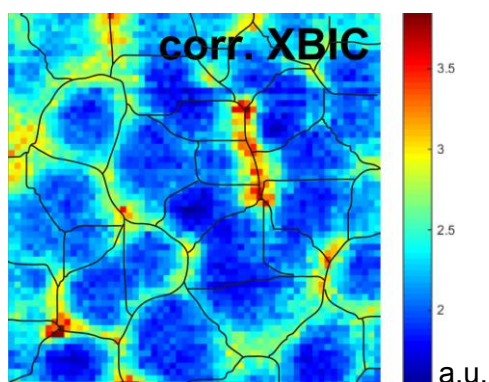


Figure 1: Corrected XBIC map of a high-efficiency metal-halide perovskite solar cell (semitransparent architecture with mesoscopic TiO₂ scaffold). The black lines were obtained from a watershed analysis of the simultaneous XRF measurement indicating the perovskite morphology. The scan is 8x8 μm² with 50 nm step size and 1 s dwell, measured at APS nanoprobe beamline 26-ID-C. The corrections allow for the interpretation of the XBIC as charge collection efficiency.

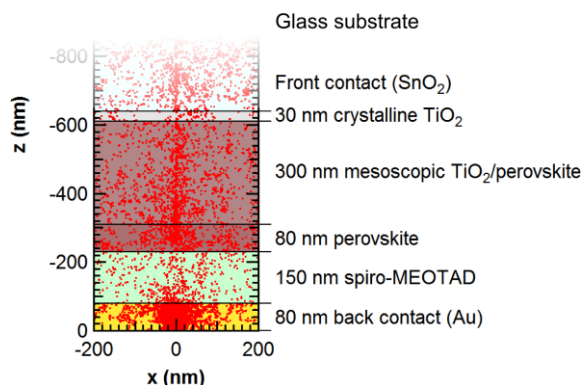


Figure 2: Layer stack of a metal halide perovskite solar cell measured at APS nanoprobe beamline 26-ID-C. Each red dot indicates the end-of-trajectory of one electron. At these places, the electrons tend to recombine, hence, the sensitivity of XBIC measurements critically depends on the distribution of the end-of-trajectories. For actual distribution simulations, we use larger data sets but show here only the result from 10⁴ incident photons for better visibility.

STXM Study of Pd@TiO₂ and NH₃ doped Pd@TiO₂ Nanoparticles

H. Lee¹, T. X. Tung², T. H. Yoon²

*1 Department of Chemistry, Sookmyung Women's University, Seoul 140-742, Republic of Korea
2 Department of Chemistry, Hanyang University, 222 Wangsimniro, Seoul 133-791, Republic of Korea*

Abstract

The correlation between the defect structures of hydrothermally grown TiO₂ nanorods (TNR) and their photocatalytic activity has been investigated by using various surface spectroscopic analysis techniques including scanning transmission X-ray microscopy (STXM). Defect states related to Ti³⁺ and oxygen vacancies in TNR were observed when the growth time was over 90 minutes (i.e. those over 500 nm in height), and these TNR samples showed photocatalytic oxidation activity with respect to the molecules. In addition, ammonia was predominantly doped around PdO nanostructure. Particularly, we prove that photocatalytic activity in effective nitrogen doped surface area is far higher than in undoped area of Pd@TiO₂ nanoparticles

INFRARED SHIELDING MATERIALS---MOLYBDENUM-CONTAINING TUNGSTEN BRONZES

Ruixing Li

School of Materials Science and Engineering, Beihang University, Beijing 100191, China

Abstract

There has been great demand to control the Near-Infrared Radiation (NIR, wavelength of 780 to 2500 nm) (heat rays) by employing transparent coating on the windows of automobile and building. Such transparent coating with infrared filtering property will reduce energy consumption for the air conditioning and thereby decrease the emission of carbon dioxide from the housing and automobile. Consequently, a remarkable absorption of near infrared together with high visible light transmittance is required for solar control filter. Typical materials are indium oxide antimony (ATO), indium tin oxide (ITO), rare earth six boride, *etc.* The new members are tungsten bronzes.

A series of molybdenum-containing tungsten bronzes was synthesized by a solvothermal process at 200 °C using ethylene glycol, acetic acid, tungstate and molybdate as starting materials. All the diffraction peaks of XRD for the samples synthesized with starting Mo/W (mol.) = 0 - 0.2 could be rough indexed as tungsten bronzes, which accompanied with a shift of main peaks after introduction of molybdenum and a split peak for starting Mo/W (mol.) = 0.1. Content of nitrogen, based on both the thermogravimetry and X-ray photoelectron spectroscopy, rose with the increase of molybdenum content. Optical property was evaluated using the Fourier transform infrared spectrometer, which proved that the molybdenum-containing tungsten bronzes could shield infrared rays better than the samples without molybdenum. And the shield efficiency was related with the content of molybdenum.

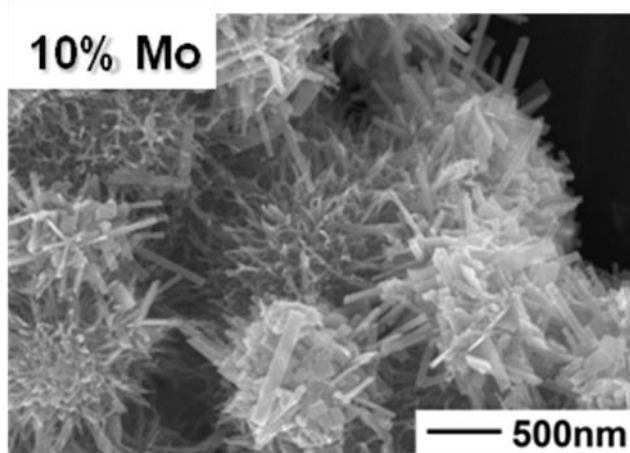


Figure 1: Molybdenum-containing ammonium tungsten bronze.

References

- [1] T. Wang, Y. Li, J. Li, Z. Feng, D. Sun, B. Zhao, Y. Xu, R. Li, H. Cai, *RSC Adv.*, 4, 43366 (2014).

MULTI-SCALE IMAGE-BASED MODELING OF MASS TRANSPORTATION IN A NOVEL-FABRICATED POROUS SOLID OXIDE FUEL CELL ANODE

Xuekun Lu¹, Tao Li², Josh Bailey¹, Thomas Heenan¹, Kang Li², Dan J.L. Brett¹, Paul R. Shearing¹

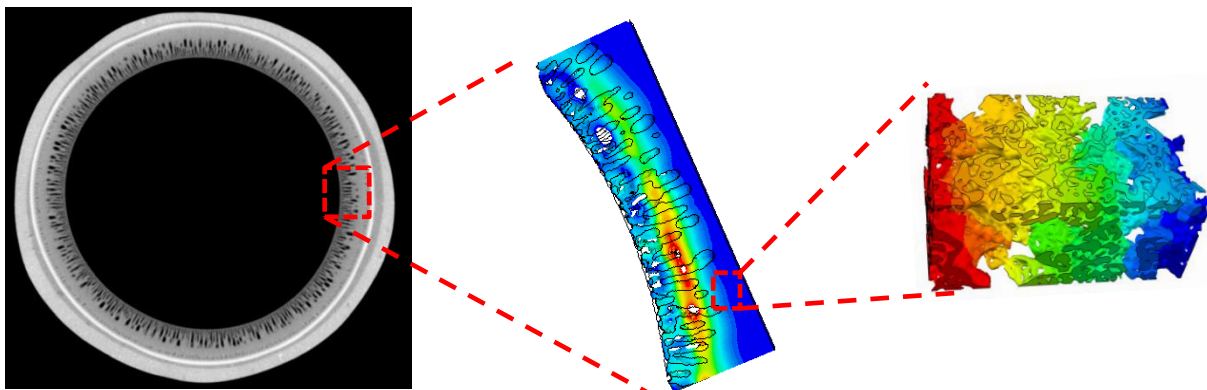
Department of Chemical Engineering, University College London, Torrington Place, London, WC1E 6BT, UK

Department of Chemical Engineering, Imperial College London, SW7 2AZ

Abstract

Solid Oxide Fuel Cells (SOFC) are promising electrochemical devices for future energy systems since they are energy efficient and environmental-friendly. Great efforts have been made in the past years to optimise their micro-structure for better electrochemical performance. Mass transportation of the reactants and products significantly determines the efficiency of the electrochemical energy conversion, because of which most of the cathodes and anodes are fabricated with high porosity. However, few studies have been reported to measure the diffusion coefficient in the electrode because of the tiny feature size.

X-ray computed tomography is a widely used technique for non-destructively 3D characterisation of the microstructure. The improvement of the resolution makes it possible to inspect the whole electrode in hierarchical resolution. In present study, the gas diffusion phenomenon was simulated in a novel fabricated tubular SOFC anode[2] based on multi-scale imaging technique. The tortuosity, effective diffusion coefficient and flow resistance in spongy region of the anode were extracted via the image-based simulation using Zeiss Xradia Ultra 810 system at the resolution of 32 nm. These information were then incorporated into the total diffusion coefficient simulation based on a larger scale anode data collected from Zeiss Xradia Versa 520 system at the resolution of 400 μm . It is the first time to study the gas diffusion phenomenon in SOFC electrode consists of features with distinct length scales.



[1]M. Lee et. Al, Formation of micro-channels in ceramic membranes - Spatial structure, simulation, and potential use in water treatment. Journal of Mebrane Science, 483 (2015) 1-14.

MULTI-SCALE ADVANCED CHARACTERISATION OF THE DEGRADATION AND FAILURE OF ELECTROCHEMICAL ENERGY DEVICES

K.M. Kareh¹, F. Tariq^{1,2}, V. Yufit^{1,2}, E. Ruiz-Trejo¹, D. Eastwood^{3,4}, M. Biton¹, Kathrin Freedman⁵, Emanuel Peled⁵, Peter D. Lee^{3,4}, Diana Golodnitsky⁵, N. Brandon¹

¹Department of Earth Science and Engineering, Imperial College London, Prince Consort Road, London SW7 2AZ

²IQM Elements Ltd, Quantitative Imaging Division, 88-90 (Office 36) Hatton Garden Holborn, London EC1N 8PG

³School of Materials, University of Manchester, Manchester M13 9PL

⁴Research Complex at Harwell, Harwell, Oxford, Didcot, Oxfordshire OX11 0FA

⁵Research School of Chemistry, Tel Aviv University, Tel Aviv 4300

Abstract

Electrochemical conversion devices such as solid oxide fuel cells (SOFCs) and batteries can provide power and store energy such as electricity or heat in a clean and efficient manner [1]. For these technologies to be widely available for electrified road transport and other large scale applications, better performance and number of cycles to failure must be achieved. In both SOFCs and batteries, device performance is intimately tied with electrode micro- and nano-microstructure, while the degradation in electrochemical performance remains poorly linked with the degradation at the microstructural scale.

In this work, we first explore the degradation behaviour of a 50% porous Ni-ScSZ (nickel-scandia stabilized zirconia) anode via characterisation of parameters such as the triple-phase boundary (TPB) density, tortuosity and phase connectivity using a combination of X-ray tomography and high-resolution focused ion beam scanning electron tomography. Secondly, we implement an in-operando laboratory X-ray radiography of a Si-Li (silicon-lithium) battery anode to study induced failure mechanisms in two and three-dimensions [2]. Both aspects of this work allow for a better understanding of the reasons behind electrode degradation and failure as well as link microstructural changes to decrease in electrochemical performance.

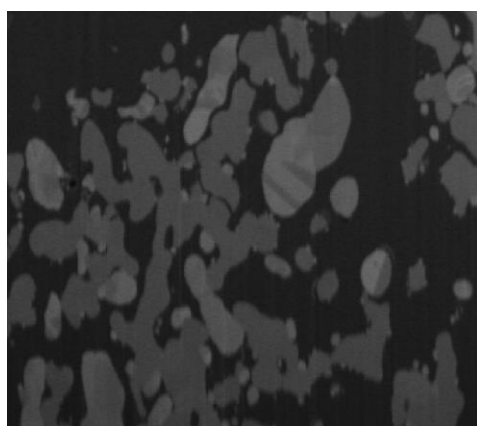


Figure 1: FIB-SEM (xz) slice of a 50% porous Ni-ScSZ anode after cycling and before further processing.

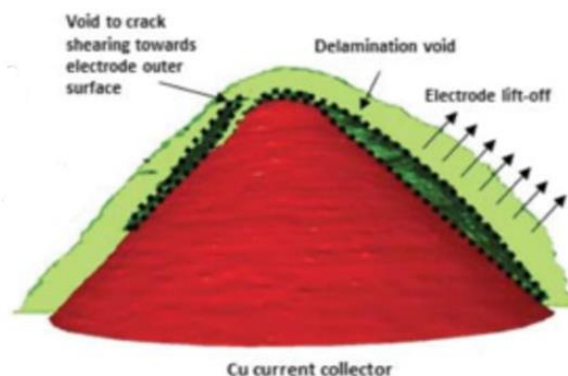


Figure 2: 3D reconstruction of the Si-based anode after anode failure via delamination [2].

References

- [1] S. Singhal, K. Kendall, High-Temperature Solid Oxide Fuel Cells: Fundamentals, Design and Applications. Elsevier Advanced Technology, Oxford, UK, 2003.
- [2] F. Tariq *et al.*, ECS Electrochemistry Letters **3** (7) A76-A78 (2014).

MAPPING ELECTRONIC STRUCTURE INHOMOGENIETIES IN INDIVIDUAL $\text{Li}_x\text{V}_2\text{O}_5$ NANOWIRES

Luis R. De Jesus¹, Gregory A. Horrocks¹, Abhishek Parija¹, Yufeng Liang², David Prendergast², and Sarbajit Banerjee¹

¹Department of Chemistry and Department of Materials Science and Engineering, Texas A&M University, College Station, TX 77845-3012

²Molecular Foundry, Lawrence Berkeley National Laboratory, Berkeley, CA 94720

Abstract

The limitations of Li-ion batteries have emerged as a key constraint in the further development of cellphones, portable laptops, and electric vehicles. These limitations of Li-ion batteries can be in part attributed to challenges with the identification of optimal cathode chemistries and architectures. I will discuss some fundamental challenges involved in designing cathode materials starting from an atomistic perspective and elaborating to single-particle and cathode levels using vanadium pentoxide (V_2O_5) as a model system.

V_2O_5 is a layered structure proposed as a cathode material for batteries due to its available sites that can accommodate Na^+ , Li^+ , and Mg^{2+} -ions and the strong enthalpic driving force for insertion of these ions. Unfortunately, V_2O_5 suffers from poor high rate performance and loss of capacity after cycling over prolonged times. My research focuses on using X-ray microscopy in tandem with first principles density functional theory calculations to evaluate the effects of ion insertion on the electronic structure of V_2O_5 in order to examine the mechanisms that are involved in discharging/charging of the cathode. Preliminary results depict several phases nucleating simultaneously in V_2O_5 after lithiation, mainly due the formation of small polarons in the structure, which profoundly affect the movement of Li-ions within the V_2O_5 lattice. V_2O_5 and other layered compounds that suffer from such polaronic effects would greatly benefit from smart architecture of quasi-amorphous or highly porous structures where charge is not required to travel large distances.

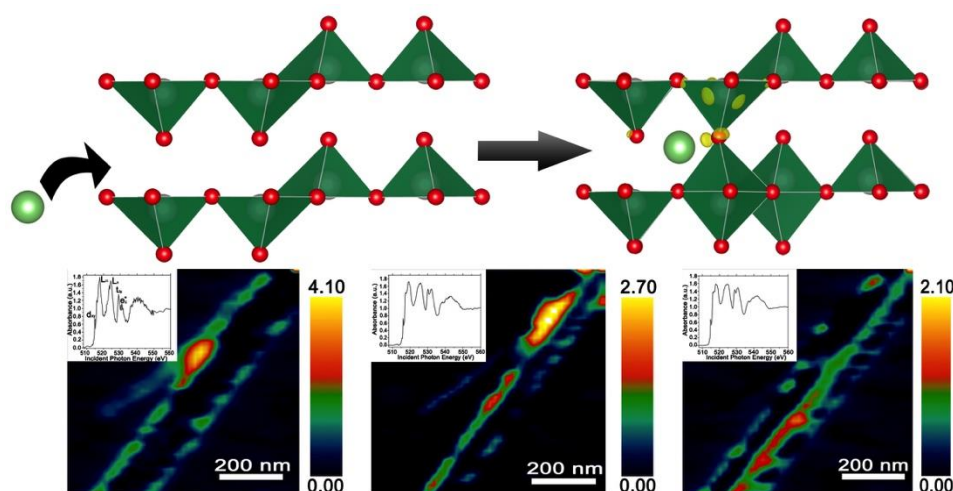


Figure 1: Examining the geometric and electronic structure perturbations and small polaron formation in V_2O_5 . Schematic drawing depicting an ion intercalation unto the crystal structure of V_2O_5 forming a small polaron; the electron charge localization on discrete V-atom can be seen in yellow. (Top) Phase nucleation can be distinguished in a single V_2O_5 nanowire caused by inhomogeneous lithiation. Insets show the corresponding spectra respectively. (Bottom)

X-RAY PTYCHOGRAPHY OF ENERGY STORAGE MATERIALS

A.M. Wise¹, V.S.C Kuppili², S. Sala^{2,3,4}, S. Andrews¹, C. Rau^{3,5,6}, P. Thibault⁴, J. Nelson Weker¹

*1Stanford Synchrotron Radiation Lightsource, SLAC National Accelerator Laboratory,
2575 Sand Hill Road, Menlo Park, California 94025, United States of America*

*2Department of Physics & Astronomy, University College London, Gower St., London WC1E 6BT,
United Kingdom*

3Diamond Light Source, Harwell Science & Innovation Campus, Didcot OX11 0QX, United Kingdom

4University of Southampton, Highfield, Southampton SO17 1BJ, United Kingdom

5School of Materials, University of Manchester, Grosvenor St., Manchester M1 7HS, United Kingdom.

*6Department of Otolaryngology, Northwestern University, Feinberg School of Medicine, Chicago,
Illinois 60611, United States of America*

Abstract

Understanding the structural and chemical transformations which occur in energy storage materials as a result of battery operation is critical for device optimisation, with X-ray imaging techniques proving to be highly valuable in these efforts.[1] In particular, X-ray ptychography holds great potential for unravelling the operation and failure mechanisms occurring in these complex materials. We have employed ptychography in both the hard and soft X-ray energy regimes to investigate the behavior of anode and cathode materials for Li-ion batteries. Hard X-ray ptychography benefits from the high penetration of X-rays at these energies, enabling the investigation of samples in a realistic electrode configuration. Soft X-ray ptychography has demonstrated resolutions 10 nm and better, with high sensitivity to changes in the chemical state of the material. Here we will present the use of ptychography to study the morphology of high capacity Si anodes and $\text{LiNi}_{0.33}\text{Mn}_{0.33}\text{Co}_{0.33}\text{O}_2$ cathodes (Figure 1) using hard X-rays, taking advantage of the phase and absorption information intrinsic to this technique, and the chemical changes occurring in transition metal oxide cathode materials during operation as determined using soft X-ray ptychography.

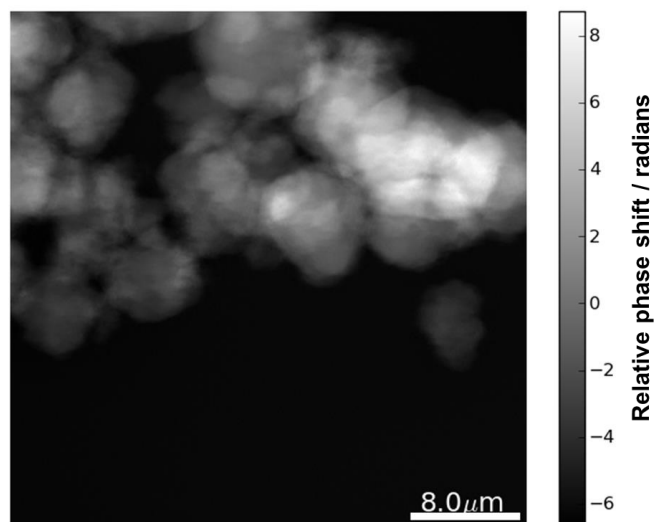


Figure 1: Phase contrast image of $\text{LiNi}_{0.33}\text{Mn}_{0.33}\text{Co}_{0.33}\text{O}_2$ particles reconstructed from ptychography data collected at beamline I13-1, Diamond Light Source.

References

- [1] J. Nelson Weker, M. F. Toney, *Adv. Funct. Mater.* 25, 1622 (2015)

IN-OPERANDO SPECTROSCOPY IMAGING STUDY OF HIGH VOLTAGE SPINEL CATHODE USING HARD X-RAY FULL FIELD MICROSCOPY WITH NM RESOLUTION

Sondes Bauer^{1*}, Lea de Biasi², Holger Geßwein², Tilo Baumbach¹

1 Synchrotron Facility ANKA, Karlsruhe Institute of Technology KIT,

*2 Institute for Applied Materials, Material Process Technology, Karlsruhe Institute of Technology KIT,
Hermann-von-Helmholtz-Platz 1, 76344 Eggenstein-Leopoldshafen, Germany*

Abstract

LiNi_{0.5}Mn_{1.5}O₄ spinel cathode was found to be an attractive cathode due to the presence of simultaneous high rate capability and high energy density caused by 3D Li⁺ diffusion and high operating voltage, relevant for the next generation lithium-ion batteries. In order to improve the electrochemical properties, there are various approaches, such as substituting Ni and / or Mn by doping elements such as Fe, Co, Cu, Cr or a coating of the cathode material and the optimization of the microstructure by suitable thermal treatments.

The work will be concentrated on doped high-voltage spinels which will be specially examined with a defined granular structure. In the foreground, the influence of various doping elements and the granular texture (crystallite size, porosity) on the cycling behavior will be studied by devoting a combination of complementary methods such X-ray absorption near edge spectroscopy (XANES), micro-X-ray fluorescence XRF, X-ray diffraction and voltage/specific capacity profiles measurement. The investigation of spinel cathode using spectroscopic imaging method in full field transmission microscopy mode in operando is a novel approach, used recently to understand the electrochemical reaction of the Li-ion battery and the lithiation mechanism with nm up to μm local resolution. Locally resolved in-Situ XANES and in-Situ XRF at the synchrotron facility ANKA using the full field and the scanning microscopy imaging methods were recently applied at the NANO beamline to the Fe-doped spinel cathode to get insight into the evolution of the oxidation states as well as into elemental distribution changes during the charging and discharging.